CFD MODELLING AND PERFORMANCE EVALUATION OF A FORCED CONVECTION MIXED-MODE SOLAR GRAIN DRYER WITH A PREHEATER

By

Angula, Johannes Penda (B.Sc. Eng)

210546069

Supervisor: **Prof. Freddie L. Inambao**

Dissertation submitted in fulfilment of the requirements for the degree of
MASTER'S OF SCIENCE IN ENGINEERING (M. Sc Eng)
(MECHANICAL ENGINEERING)
College of Agriculture, Engineering and Science, University of KwaZulu-Natal,
Durban, South Africa

03 June 2021

As the candidate's supervisor, I agree to the submission of this dissertation.

Name of Supervisor: **Prof. Freddie L. Inambao**

Signature: _____   Date: 03 June 2021

Declaration 1 -Plagiarism

I, **Johannes Penda Angula** declare that:

1. The research reported in this thesis, except where otherwise indicated is my original research.
2. This thesis has not been submitted for any degree or examination at any other university.
3. This thesis does not contain other persons' data, pictures, graphs or other information, unless specifically acknowledged as being sourced from other persons.
4. This thesis does not contain other persons' writing, unless specifically acknowledged as being sourced from other researchers. Where other written sources have been quoted, then:
    a) Their words have been re-written but the general information attributed to them has been referenced
    b) Where their exact words have been used, then their writing has been placed in italics and inside quotation marks, and referenced.
5. This thesis does not contain text, graphics or tables copied and pasted from the internet, unless specifically acknowledged, and the source being detailed in the thesis and in the References sections.

Signed: …………   ……………………   Date: 03 June 2021

Declaration 2 -Publications

This section presents the articles that form part and/or include the research presented in this dissertation.

ISI/SCOPUS/DoHET Accredited Journals

1. **Johannes P. Angula** and Freddie Inambao, Review of Solar Grain Drying. *International Journal of Mechanical Engineering and Technology,* 10(11), 2019, pp. 275-296.
   http://www.iaeme.com/ijmet/issues.asp?JType=IJMET&VType=10&IType=11   (Published)

2. **Johannes P. Angula** and Freddie Inambao, Computational Fluid Dynamics in Solar Drying. *International Journal of Mechanical Engineering and Technology,* 10(11), 2019, pp. 259-274.
   http://www.iaeme.com/ijmet/issues.asp?JType=IJMET&VType=10&IType=11   (Published)

3. **Johannes P. Angula** and Freddie L. Inambao, Optimization of Solar Dryers through Thermal Energy Storage: Two Concepts, *International Journal of Mechanical Engineering and Technology* (IJERT), 13(10), 2020, pp. 2803-2813.
   https://dx.doi.org/10.37624/IJERT/13.10.2020.2803-2813   (Published)

4. Johannes P. Angula and Freddie Inambao, Modelling and CFD Simulation of Temperature and Airflow Distribution Inside a Forced Convection Mixed-Mode Solar Grain Dryer with a Preheater. *International Journal of Innovative Technology and Exploring Engineering* (IJITEE), 10(4), 2021, pp. 33-40.
   DOI: 10.35940/ijitee.B8283.0210421   (Published)

5. Johannes P. Angula and Freddie Inambao, Performance Evaluation of a Forced Convection Mixed-mode Solar Grain Dryer with a Preheater, *International Journal of Innovative Technology and Exploring Engineering* (IJITEE), 10(4), 2021, pp. 41-51.
   DOI: 10.35940/ijitee.D8443.0210421   (Published)

The candidate is the main author for all the publications while Prof. Freddie L. Inambao is the supervisor.

Signed: ………   …………………………   Date: 03 June 2021

Dedication

This work is dedicated to the highest God, the sustenance of my existence. And to my family for their love, understanding, and for standing by me through thick and thin.

Acknowledgments

I would like to express my utmost gratitude firstly to my supervisor Professor Freddie L. Inambao for his guidance and positive support throughout the study. His research vision, technical expertise, dynamism and motivation has always inspired me to conduct research and professionally present the findings to peers in the engineering spectrum. It has been a humbling and learning experience to work with you, Professor. I would also like to express my sincere gratitude to my editor Dr Richard Steele for his professionalism and personal effort to edit this dissertation. Not to forget Dr Santiago Stringel for his technical expertise in solar drying, and the assistance rendered with some of the equipment used in the experiment is very much appreciated. Furthermore, my appreciations of gratitude are also given to the LAN manager Mr Shaun Savvy for providing me with a computer packed with the necessary software to conduct the research comfortably. Last but not least, I am very thankful to the UKZN fraternity for the enabling environment and to the large extent, my fellow post-graduate students in the Green Energy Solutions Group (UKZN) who rendered their support throughout my study.

Abstract

Solar drying of agricultural food products as an art of food preservation has been in existence since the 17th century. In most tropical and subtropical countries, the drying process of harvested agricultural products such as grains is mainly carried out using the method of open-air drying or sun drying to preserve the harvest. With the advances of technology over time, new solar drying methods such as indirect and mixed-mode solar drying are evolving. Mixed-mode solar dryers are among the most efficient solar drying methods for improving the harvest and storage of grains. One of the advances in the development of solar dryers is the use of computational fluid dynamics (CFD) and computer-aided design (CAD) codes to model, simulate, and analyze dryer systems' performance.

This study was conducted in two phases. The first phase entailed the use of CAD and CFD codes to model and simulates a forced convection mixed-mode solar grain dryer integrated with a preheater. A 3D model was developed with great accuracy using SolidWorks code and, the CFD simulation was carried out using ANSYS Fluent code. In the second phase, an experiment was conducted using an existing indirect solar dryer which was modified and converted to a mixed-mode solar dryer suitable for the study. The modeling and simulation results were validated against experimental results to evaluate the dryer system' performance. The study was conducted at various airflow speed and preheater temperatures ranging from 0.5 m/s to 2 m/s and 30 °C to 40 °C, respectively. The type of grains used in the experiment were corn grains whereby 72 freshly harvested maize ears/cobs were dried. The study was conducted under the weather conditions of Durban, South Africa, at the University of KwaZulu-Natal.

This study aimed to investigate solar drying technologies towards performance enhancement of a forced convection mixed-mode solar grain dryer that incorporated a preheater through modeling and optimization. This approach was followed in order to develop a better understanding of the effects of forced convection and air preheating on airflow distribution and temperature distribution within a solar dryer. The results from both the CFD modeling and experiment were satisfactory, resulting in a correlation with a maximum relative error of 16.3 %. The dryer system's performance results indicated a maximum thermal efficiency of 58.8 % with a corresponding drying rate of 0.0438 kg/hr. The minimum thermal efficiency for the dryer system was 47.7 %, with a corresponding drying rate of 0.0356 kg/hr. The fastest drying time of maize ears was achieved in 4 hours and 34 minutes from an initial moisture content of 24.7 % wb to 12.5 % wb. At the same time, open-sun drying yielded the slowest drying time of 15 hours from an initial moisture content of 27.3 % wb to 12.7 % wb. There was a significant improvement in the dryer system's performance, whose initial efficiency was 36 % when operating as an indirect solar dryer. These results are a clear indication that using a solar dryer system

in mixed-mode operation with forced convection and the assistance of a preheater or backup heater can significantly improve drying processes and increase food preservation. The study further presents design concepts of incorporating cost-effective solar thermal energy storage systems that can be implemented to optimize solar dryers. In this case, solar energy can be harvested and stored during peak sunshine hours and made available for usage during off-peak sunshine hours.

Table of Contents

List of Figures

List of Tables

CHAPTER 1

1. INTRODUCTION

1.1 Background

Accessible renewable energy sources include solar energy, wind energy, and geothermal energy. Compared to other renewable energy sources, solar energy has great potential and better reliability for drying technologies in relation to agricultural food preservation. In most tropical and subtropical countries food losses after harvest are very significant, estimated to be of the order of 40% but can increase to about 80% in adverse conditions due to improper drying [1]. In these countries, the drying process of harvested agricultural products such as grains is mainly carried out by open-air sun drying as a way of preserving the harvest for the longer term [2]. Such an approach involves exposing the grains directly to the sun's rays whereby the absorbed sun radiation is converted to thermal energy, increasing the grain temperature and resulting in the evaporation of moisture from the grain. Based on the principles underlying the drying process, theories indicate that at 25 °C room temperature and 1 bar atmospheric pressure, the water which is removed in the form of moisture requires a minimum latent heat of vaporization of 2442 kJ/kg [10].

Grains contain vital nutrients such as carbohydrates, minerals and vitamins which form part of the overall healthy diet of a human being. In addition, they provide the dietary fiber which helps in lowering the risk of being affected by heart disease [1]. In many parts of the world, particularly in developing countries, traditional methods of open-air sun drying of grains are still practiced, even for large-scale production [10]. This is because this method is cheap and easily available. This method, however, has various limitations that negatively affect the quality of the products, which sometimes can lead to inedible products [2]. Food products dried using the traditional method of open-air sun drying are also susceptible to damage due to birds, insects, rain, dirt or fungi due to the uneven drying process [3]. The problems associated with open-air sun drying can be eliminated with the use of appropriate solar dryer technologies. Using solar dyers to dry the harvested food products can minimize food wastage and production cost. Solar dryers can be a beneficial tool to small-scale farmers, particularly those in rural areas where conventional sun drying of crops such as maize is carried out.

As technology evolves, new advanced techniques and strategies of food drying are being discovered. There are mainly three ways in which the process of solar drying can be carried out. The drying process can be carried out using either a direct, indirect or a mixed-mode solar dryer [3,10]. All three methods have

different advantages and disadvantages, and can employ natural air convection or forced air convection processes. Solar drying of food is widely practiced throughout the world and is seen as a green energy solution to food preservation. It is a cheaper and more effective method of food drying in comparison to freeze drying and oven drying. The principles and methods of solar drying are discussed in more detail in Chapter 2. The quality of grain serves as an important factor in determining its market and nutritional value. Grain that is obtained through improper and unhygienic drying methods can result in poor quality grains that can have adverse economic effects on both domestic and international markets. A proposal based on current research indicates that drying processes need to be carried out in closed and hygienic environments such as inside a solar or industrial dryer [4]. In this way, the quality of dried food products is enhanced and enough food can be made available to cater for the population needing it. Grains can be safely preserved through drying to avoid huge wastage and so that they can be available during off-seasons at remunerative prices [4].

The technology of solar thermal energy is rapidly gaining acceptance as an energy saving measure in agricultural applications [11]. The great benefits of solar energy such as plentiful, unlimited energy, and environmentally-friendliness makes it widely preferred over other forms of alternative energy for many industrial applications including solar drying [5]. Research has shown that the drying process has many variables and it is almost impossible to control all the variables and achieve a uniform drying of the final product [5,6]. The process of drying is largely dependent on factors such as air temperature and velocity, product type, layer thickness, moisture content, method of drying, drying kiln structure, moisture diffusivity, crop porosity and ambient air humidity. Food items such as grains contain two types of water; chemically bound water and physically held water which is normally removed during the drying process.

The most important reasons for the popularity of dried products are increased shelf life, product diversity and a substantial reduction in volume which results in less storage space. Sharma et al. [6] stated that the short wavelength solar radiation which is partly reflected and partly absorbed will determine the color of the crops. The absorbed radiation will increase the temperature of the crop which results in moisture diffusion and evaporation of moisture from the crop surface due to the surrounding air movement. There are many different types of grains that are consumed in many parts of the world and form part of their staple food. The most popular grains are maize corn, rice, wheat, oats, millet, sorghum, and barley. In many parts of Africa, maize is considered as a staple food and more popular than other types of grains such as rice which is widely consumed in countries such as India, China, and Indonesia.

Research on the use of computational fluid dynamics (CFD) tools to design, analyze and optimize solar drying systems have been conducted by numerous research studies. Computational Fluid Dynamics is considered to be a cost-effective and an accurate measure of predicting the drying kinetics of a solar dryer. As discussed in more detail in Chapter 3, there are many CFD codes or software programs that can be used to model and simulate the drying process of products in a solar dryer. Using a CFD code, one can run multiple simulations and analyze data as often as desired without running many experimental trials [7]. One of the great benefits in modeling and simulating the drying process is that there is no cost involved in setting up and running the model. Hence, it also serves as a selection tool in obtaining a suitable design for the desired drying system. Despite modeling the complex phenomena of drying, the use of CFD codes helps researchers and food scientists to gain a better understanding of the dynamics and physics of food processing operations [8]. Research studies show that the accuracy of different CFD codes varies and that simulation results mainly depend on the knowledge and understanding of the user in using the software [12].

Although solar energy is freely available and inexhaustible, its applications are limited by the availability of using it. Solar energy is weather dependent, hence, applications that require solar energy such as solar drying will only function if there is sufficient solar irradiance available. This problem affects the production of many farmers who rely on solar drying. Over the past decades, numerous research studies have been conducted to identify ways of harvesting and storing solar thermal energy for later usage [11]. The stored thermal energy can be used for applications such as extending drying processes, hot water for household applications, heating, and other industrial applications. Researchers have conducted experiments on various materials and their capabilities on storing solar thermal energy [11]. In general, thermal energy can be stored in the form of sensible heat, latent heat or thermochemical heat energy. Different forms of heat storage utilize different materials such as rocks, gravel, water, paraffin wax, and metals to store the energy. The heat storage capacity of a thermal energy storage system is mostly dependant on the thermal properties of the material and the design of the storage system. As an ongoing improvement on existing solar drying technologies, a study incorporating a thermal energy storage system in order to improve the drying process of solar dryers is presented in Chapter 7.

In this study the term maize ear and maize cob will be used interchangeably although both of these terms refer to the same meaning.

1.2 Statement of the Problem

Nowadays researchers seek sustainable development through the utilization of energy sources that have little or no adverse impact on the environment. In most rural areas of South Africa, maize (*Zea mays L.)* is the most important grain crop which is cultivated, consumed directly and serves as a staple diet for the majority of the population. Drying of maize ears in rural areas is still practiced in an open direct sun drying method which leads to major losses and poor maize quality. This is due to the lack of technical solutions to dry the harvested food and preserve it. A substantial amount of research work has been conducted on drying grain using solar energy by means of natural and forced convection but there is still rooms for improving performance. Many researchers have developed protypes to assess the performance of the solar dryers, but they have not conducted any modeling of the driers to predict the end results and evaluate them for performance improvement. Research studies show that a mixed-mode solar dryer using forced convection offers better drying compared to other types of solar dryer [4,5,10]. This calls for further research on solar grain drying, particularly drying of maize, using a mixed-mode solar dryer.

Solar dryers with enhanced performance can lead to desirable properties of dried food such as the right moisture content, less damaged grain, low mold count, and high nutritive value. The use of software presents an efficient and reliable way to model and simulate real world problems in order to optimize design systems. Simulation modeling studies are therefore needed for the efficient design and operation of solar dryers. They allow for the prediction of airflow, temperature effect, radiative effect, flow behavior and humidity inside the dryer. The research works that are presented in this study are based on a solar dryer developed for a previous project by the Department of Mechanical Engineering at the University of KwaZulu-Natal, South Africa [9]. Initially, this solar dryer prototype was designed as an indirect solar dryer and its thermal efficiency was found to be 36%. The prototype was used to dry synthetic fecal sludge. Findings of the experiment were that the dryer was able to dry synthetic fecal sludge in 12 hours from an initial moisture content of 70 % wb to 20 % wb [9]. In order to improve the thermal performance and drying process of this indirect solar dryer system it was necessary to change its operation to mixed-mode operation with forced convection, and incorporate a preheater to aid the solar collector. Hence, in this study the solar dryer was adapted for modeling and experimental validation to compare results of mixed-mode operations with forced convection preheated air in which maize ear/maize cobs were dried.

1.3 Research Aim

The aim of this study was to investigate solar drying technologies in terms of performance enhancement of a forced convection mixed-mode solar grain dryer that incorporated a preheater through modeling and optimization. An experiment was undertaken to gain a better understanding of the effects of forced convection and air preheating on airflow and temperature distribution in a solar dryer and whether this improves drying time.

1.4 Research Objectives

To realize the previously mentioned aim, the research focused on the following objectives:

- Create and evaluate a simulation model in ANSYS Fluent CFD code. The model was conducted at various environmental conditions to predict and simulate the operational parameters of an actual solar grain dryer using maize ears as the drying product.

- Compare the simulation model by means of an on-site experiment to provide ways of improving solar drying for sustainable farming.

- Investigate the behavior of the drying fluid inside the dryer through modeling and simulation using the CFD code.

- Establish the effect of a preheater on the performance of an experimental forced convection mixed-mode solar dryer.

1.5 Research Questions

This research work aimed to answer the following questions:
- Is the simulated model consistent with the on-site experimental results?
- How does forced convection and air preheating affect the performance of a solar dryer system?
- What is the optimal combination of drying parameters that can maximize drying efficiency of the solar dryer system?
- Is the drying time improved?

1.6 Scope of Study and Limitations

The scope of this research focuses on the use of a forced convection solar grain dryer with a preheater, operating as a mixed-mode dryer. In this operation, the drying air is heated in two stages whereby in the first stage an electrical air heater is used to raise the temperature of air, and a solar collector is used in the second stage to further increase the air temperature. The process of two stage air heating was introduced in this study to facilitate the reduction of humidity level of the drying air and enhance moisture removal rate during the drying process. In this study, maize ear/maize cobs were used for the experiment to investigate solar drying of grains. The modeling and simulation of the solar dryer system and of the fluid flow and heat transfer within the solar dyer system was carried out using a 3-dimensional computer-aided drawing (CAD) code (SolidWorks) and a CFD code (ANSYS Fluent), respectively. The simulation results were validated against experimental results. To facilitate force convection drying during the experiment, the solar dryer used compressed air whose pressure and air flow was regulated through a filter-pressure regulator and needle flow control valve, respectively. The preheating of air was limited to a maximum of 40 °C and the air flow velocity was varied from 0.5 m/s to as high as 2 m/s.

1.7 Chapter Outline

This research work conducted on the study of a forced convection mixed-mode solar grain dryer with a preheater is structured in chapters. Some of the chapters such as Chapters 2, 3, 5, 6, and 7 have been written as research papers that were published in various journals. This dissertation is structured as follows:

Chapter 1 – Introduction: This chapter presents the introduction of solar thermal energy technology in relation to solar drying of agricultural products but mainly focusing on grains. It also introduces the importance of using CFD codes in analyzing solar dryer systems. Furthermore, it highlights the relevance of the research work carried out in this dissertation including research aim, objectives and research questions.

Chapter 2 – Review of Solar Grain Drying: This chapter presents a review of literature pertaining to solar drying technologies. It seeks to identify gaps that are of interest for further research on solar drying. It also presents principles and theory of food drying.

Chapter 3 – Computational Fluid Dynamics in Solar Drying: This chapter presents research work that has been published on the theory, principles, and applications of CFD in solar drying. It emphasizes the importance of CFD in designing, analyzing and enhancing the performance of solar dryer systems.

Chapter 4 – Methodology: In this chapter, a methodological approach to this research work is presented. It details the materials and methods taken in order to realize the stipulated objectives of the study. The methodology is presented in two parts. The first part presents the methodology of modeling and simulation using the CFD code while the second part presents the methodology of the experimental approach.

Chapter 5 – Results and Discussion – CFD Modeling and Simulation: This chapter presents the results and discussion of the research work pertaining to CFD modeling and simulation. A thorough analysis of the temperature and airflow distribution within the mixed-mode solar dryer system is presented and discussed.

Chapter 6 – Results and Discussion – Experimentation: This chapter presents the results and discussion of the research work pertaining to the performance of the forced convection mixed-mode solar grain dryer with a preheater. It also presents an evaluation of different drying parameters that can be used to improve the solar dryer efficiency. The work improves understanding of the effects of preheating the drying air and the inclusion of forced convection on mixed-mode solar dryer systems.

Chapter 7 – Optimization of Solar Dryers Through Thermal Energy Storage: Two Concepts: This chapter presents a concept paper that was published on the use of thermal energy storage materials to store solar energy. It aims at identifying cost-effective solar thermal energy storage systems that can be implemented to optimize solar dryers. Conceptual designs of the proposed solar thermal energy storage systems are presented and discussed. The goal is to effectively harvest and store solar energy as heat during peak sunshine hours and use it during off-peak sunshine hours in order to extend drying processes.

Chapter 8 – Comparison of Results, Overall Conclusion, and Recommendations for future works: This chapter present a comparison between experimental results and, CFD modeling and simulation results. It further presents an overall conclusion for the thesis, and the recommendations for future works.

1.8 References

1. Salunkhe, D. K. and Kadam, S. S. Handbook of Fruit Science and Technology. New York: Marcel-Dekker, 1995.

2. Sontakke, M.S. and Salve, S.P. Solar Drying Technologies: A review. *International Refereed Journal of Engineering and Science*, 4(4), 2015, pp. 29-35. http://www.irjes.com/pages/v4i4.html.

3. Tiwari, A. A Review on Solar Drying of Agricultural Produce. *Journal of Food Processing & Technology*, **7**(623), 2016. doi: 10.4172/2157-7110.1000623.

4. Parakash, S., Jha, S. K. and Datta, N. Performance Evaluation of Blanched Carrots Dried by Three Different Dryers. *Journal of Food Engineering*, 62, 2004, pp. 305-313. https://doi.org/10.1016/S0260-8774(03)00244-9.

5. Akinola, A. O. and Fapetu, O. P. Exergetic Analysis of a Mixed-Mode Solar Dryer. *Journal of Engineering* and *Applied* Sciences, 1, 2006, pp. 205-10.

6. Sharma, A., Chen, C. R. and Vu Lan, N. Solar-Drying Systems: A Review. *Renewable and Sustainable Energy Reviews*, 13(6-7), 2009, pp. 1185-1210. https://doi.org/10.1016/j.rser.2008.08.015.

7. Janjai, S., Lamlert, N., Intawee, P., Mahayothee, B., Bala, B. K., Nagle, M. and Muller, J. Experimental and Simulated performance of a PV-Ventilated Solar Greenhouse Dryer for Drying of Peeled Longan and Banana. *Solar Energy,* 83(9), 2009, pp. 1550-1565. DOI: 10.1016/j.solener.2009.05.003.

8. Ambesange, A.I. and Kusekar, S.K. Analysis of Flow Through Solar Dryer Duct Using CFD. *International Journal of Engineering Development and Research*, 5(1), 2017, pp. 534-552. http://www.ijedr.org/papers/IJEDR1701082.pdf.

9. F. L. Inambo, and S.S. Stringel. Development of a Solar dryer. *Green Energy Solution Research Group*. Department of Mechanical Engineering. University of KwaZulu-Natal, Durban, South Africa.

10. Ekechukwu, O. V. and Norton B. Review of Solar-Energy Drying Systems II: An Overview of Solar Drying Technology. *Energy Conversion Management*, **40** (6), 1999, pp. 615-655. DOI: 10.1016/S0196-8904(98)00093-4. https://doi.org/10.1016/S0196-8904(98)00093-4

11. K. Kant, A. Shukla, A. Sharma, A. Kumar, and A. Jain. "Thermal energy storage based solar drying systems: A review," Innovative Food Sci. Emerg. Technol., vol. 34, pp. 86-99, 2016,. https://doi.org/10.1016/j.ifset.2016.01.007.

12. Bin, X. and Sun, E.D. Applications of Computational Fluid Dynamics (CFD) in the Food Industry: A Review. *Computers and Electronics in Agriculture,* **34**(1), 2002, pp. 5-24. DOI: 10.1016/S0168-1699(01)00177-6.

CHAPTER 2

2.   REVIEW OF SOLAR GRAIN DRYING

This chapter presents work that was published under the title "Review of Solar Grain Drying" in the *International Journal of Mechanical Engineering and Technology* (IJMET), a journal accredited by the Department of High Education and Training (DHET) of South Africa.

To cite this article: Johannes P. Angula and Freddie Inambao, Review of Solar Grain Drying. *International Journal of Mechanical Engineering and Technology,* 10(11), 2019, pp. 275-296.

The link to this article:

http://www.iaeme.com/IJMET/issues.asp?JType=IJMET&VType=10&IType=11

REVIEW OF SOLAR GRAIN DRYING

Johannes P. Angula and Freddie Inambao*

Department of Mechanical Engineering,
University of KwaZulu-Natal, Durban, South Africa
https://orcid.org/0000-0001-9922-5434

*Corresponding Author Email: inambaof@ukzn.ac.za

ABSTRACT

Solar energy is one of the renewable energy sources which is abundant and pollution free. Over the years it has grown rapidly in the field of agriculture for the purpose of food preservation. The use of solar energy to dry agricultural products can be achieved using three techniques, namely, direct solar drying, indirect solar drying, and mixed-mode solar drying. Drying of agricultural products is usually modelled as either thin layer or deep bed layer. Various researchers have conducted numerous experiments and simulations to study and model the performance output of solar dryers in terms of the outlet temperature, type of heat collector, drying air velocity, drying period, and moisture removal rate. In this paper a review is presented on the different techniques used in solar drying, different aspects of solar drying, and modelling of thin layer and deep bed. In addition, principles of operation of solar drying systems and practical examples of some of the available solar dryer systems are presented. The main objective of this review is to identify areas of improvement in solar grain drying systems that need to be addressed for performance enhancement and quality assurance of the relevant solar drying technologies.

Keywords: Design, Grain, Solar Collectors, Solar Drying, Costs, Performance, Energy, Storage, Economic Feasibility

Cite this Article: Johannes P. Angula and Freddie Inambao, Review of Solar Grain Drying. *International Journal of Mechanical Engineering and Technology* 10(11), 2019, pp. 275-296.
http://www.iaeme.com/IJMET/issues.asp?JType=IJMET&VType=10&IType=11

1. INTRODUCTION

In most tropical and subtropical countries, the drying process of harvested agricultural products such as grain is mainly carried out by means of open-air drying or sun drying for the purpose of preserving the harvest. Grains are widely consumed daily by majority of people either directly or indirectly. They serve as an important source of carbohydrates, minerals, and vitamins that our body need as part of an overall healthy diet. In addition, they provide dietary fiber which helps in the reduction of bad cholesterol level in our blood in order to minimize the risk of heart diseases [1]. Traditional method of drying grains that is widely practiced in many countries involve direct sun drying. This method has been practiced for centuries by

many subsistence and commercial farmers due to some benefits associated with it. However, it is indicated that this method has various disadvantages according to [2], such as:

- The direct exposure to solar radiation reduces the grains quality

- Damage due to birds, pests, rodents

- Damage due to dew or rain

- The issue of uneven drying can lead to the presence of insects and possible growth of microorganisms

- The issue of open drying can cause dirt or debris to contaminate the grains

- The method is labor and time intensive since the grains must be protected from possible animals' invasion and covered from bad weather

Poor quality grains resulting from poor and unhygienic drying methods can have bad effects on local consumption and as well affect the economy in international markets. To avoid unwanted situations like that, the method of drying need to be carried out in a closed and hygienic environment such as in a commercial dryer or an improved solar dryer to that ensures the quality of the grains are not compromised. With such methods in place, grains can be preserved for longer period to avoid unwanted wastage and ensure enough availability during the off-peak seasons for own consumption and at good selling prices [3]. The technology of using solar energy has drawn attention of many people and is widely accepted in many parts of the world as a green energy that can be used in agricultural applications for several good reasons [4]. Although there are many types of renewable energy sources such wind energy, solar thermal energy offers great advantages over other type of renewable energy sources due to its availability and costs [4]. In general, grains, like all other food items contain two types of water that one should understand when drying. The first type of water is the bound water which is the water molecules that are chemically bound to the body tissues of the grains, and the other type of water is physically held inside the grain structure. The physically held water is the water which is normally removed during drying processes. Research has shown that the consumption of dried product has increased over the years because of some associated benefits such as the ability to be preserved for longer periods and occupies less storage area as in comparison to fresh products. In a case study by Sharma et al. [5] it is indicated that the amount of solar radiation that is absorbed and reflected can negatively affects the color of the crop which is in direct contact with the solar radiation wavelength. In contrary, the amount of radiation energy absorbed by the crop contributes to moisture evaporation from the crop surface as a result of temperature increase. The evaporation of moisture on the crop surface is aided by natural or forced convection of the surrounding air.

2. OVERVIEW OF SOLAR DRYING

Solar energy is a green form of energy and most plentiful type of renewable energy source. Research shows its technology is growing rapidly in agriculture applications thereby reducing conventional energy consumption [6]. Solar drying of crops involves using solar energy to remove moisture in the crops being dried to a moisture level that is desirable for healthy preservation of the crops. Various researches have shown that solar drying technology is very beneficial for countries such as South Africa which receive sufficient sunshine per year in many parts of the country. The following sections aim to provide a brief overview of the drying principles of agricultural products. In general, the principles apply to mechanical conventional drying but in this review the concern is with solar drying with an emphasis on drying grains.

2.1. Safe Storage of Grains

Grains are important sources of dietary fiber and carbohydrates, and therefore contribute to a healthy lifestyle. Therefore, drying and storage of grains are essential for human wellbeing [7]. According to Kenneth et al. [8], the storage temperature of grains and the amount of moisture present in the grains can determine its maximum storage time without compromising on its quality. There are two ways to determine the moisture content of grains; direct method or indirect method. The direct method is carried out by heating the grains in an oven so that the moisture can evaporate. The sample is normally weighed before heating and then weigh it after heating to determine the loss in sample mass. The process is carried out until there is no difference in mass. The indirect method involves the use of moisture meters. The moisture meter works on the principles of electrical conductance or capacitance to determine the level of moisture content present in the grain structure. The discussion of both methods to measure moisture content is however beyond the scope of this paper. Figure 1 shows the correlation between safe storage time and grain moisture at different temperatures.
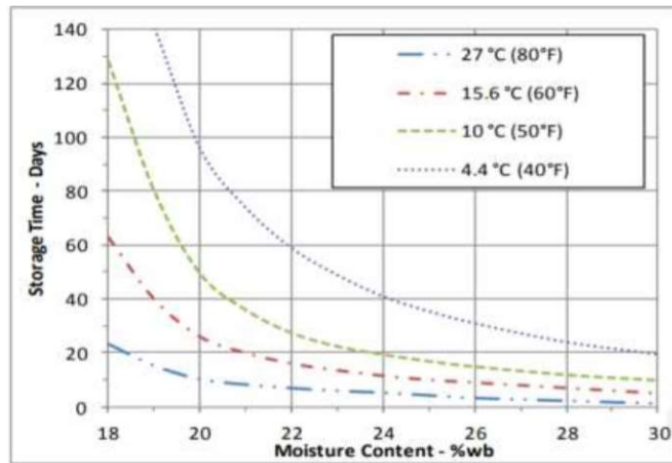
Figure 1 Maximum storage time for corns [10].

Research shows that a good combination of low moisture content and low temperature discourages the growth of unwanted bacteria, hence allowing the grains to be stored for longer periods. As shown in Figure 1, grains with a moisture content as low as 18 % wb and a temperature of about 10 °C can be safely stored for about 140 days. However, if the conditions of grains are recorded to be 30 % wb moisture content and a temperature of 27 °C, spoilage can occur in less than 10 days. According to research, most fungi develop under 70 % relative humidity. Grains have the ability to retain moisture during storage and the amount of moisture depends on the conditions in which they are stored [11]. Table 1 shows an allowable safety margin on the level of moisture of various grains required for a year storage period at 70 % relative humidity and 27 °C storage temperature [11].

Table 1. Recommended moisture content for a year storage [11].

Grains type	Maximum moisture content
Maize	13.5 %
Paddy rice	15.0 %
Unhusk rice	13.0 %
Sorghum	13.5 %
Beans	13.5 %

There is a threshold limit on the amount of humidity that grains need to hold when being stored, as shown for different types of grains in Table 1. The limit sets a boundary for the grains to undergo any chemical or physical changes while being stored. Grains like many other food types have tendency to retain water into their structure depending on the storage conditions. However, some of the concluded results from researches show that maize grains can be safely stored if the moisture content is kept below 13.5 % with the surrounding air temperature ranging between 25 °C and 30 °C and a relative humidity of 70 % [11]. This implies that if the moisture content of maize rises above 13.5 % deterioration of the maize corns can be expected. The moisture content shown in Table 1 is in close relation to the recommended moisture contents for different grains as given in the review of Kenneth et al. [8]. According to this review, the allowable storage moisture content for corns is recommended not to be more than 12 %. This is in good correlation with the required moisture content given in table 1. Table 2 shows the recommended moisture contents of different selected grains to be stored for less than 6 months in winter and as well for a period of more than 6 months in summer.

Table 2. Storage moisture contents of different selected grains [8].

Grains type	Under 6 months	More than 6 months
Barley	14%	12%
Corn	15.5%	13%
Edible Beans	16%	13%
Oats	14%	12%
Sorghum	13.5%	13%
Soybeans	13%	11%

2.2. Description of the Principles of Drying

Theories on the principles that govern the drying process of food is discussed as obtained from reviews I and II by Ekechukwu [12] and Ekechukwu et al. [13] respectively. The principles of drying are generally the same for different drying methods but in this review solar drying is discussed. Findings from [13] indicate that for drying to take place, the process requires at least 2258 kJ/kg of energy to convert liquid water into water vapor at standard atmospheric pressure. Furthermore, research shows that the rate of drying of a food product is dependent to the forms in which water is held within a food product body structure. A material with free or unbound water is regarded as non-hygroscopic and the material with bound moisture is referred to as hygroscopic. According to Belessiotis et al. [14], moisture content can be expressed on a wet (W) basis as shown by equation 1:

$$W = \frac{m_w}{m_w + m_d} \text{ , and} \tag{1}$$

Alternatively, moisture content can be expressed on a dry (X) basis as given by equation 2 from the review of Belessiotis et al [14]:

$$X = \frac{m_w}{m_d} \tag{2}$$

2.2.1. Drying Rate

Drying rate is an important aspect of drying which helps in the achievement of a good quality dried product. There are various factors that affects the drying rate both on the side of the food product and the side of drying air. On the side of the product, research findings indicate that temperature and moisture content of the product have an impact on the drying rate. While on the side of the drying air, its current conditions such as its temperature, relative humidity, and its velocity will also influence the drying rate. According to Beuchat [15], agricultural products such as grains retain water through sorption forces and thus, they are hygroscopic.

The drying rate process has two phases as shown in Figure 2: the constant rate, and the falling rate. Grains is one of the types of cereals food and, the drying process of cereals usually occurs in the falling rate period [16].
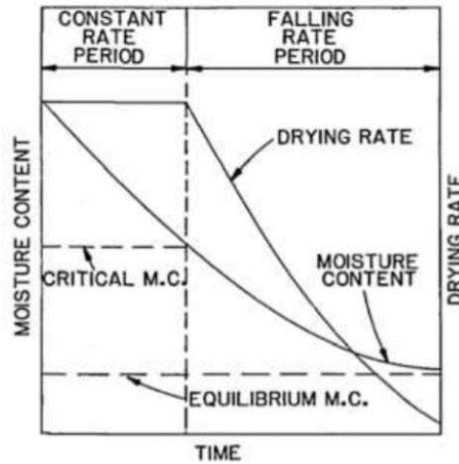
Figure 2. Drying rate phases of high moisture grains [10]

Phase 1 (constant rate): during this phase, there is no noticeable change in the drying rate because initially the surface of the product is saturated or full of with water vapor and consequently evaporation will only take place on the surface until a point of unsaturation is reached were drying rate begins to change[14]. Essentially water molecules diffuse from the product saturated surface through a porous membrane into the environment. The temperature on the surface of the product remain constant provided there is a balance between mass transfer rate of water vapor and the heat transfer rate. Due to the effectiveness of radiation in transferring heat, the constant rate is increased by supplementing the heat transfer by convection and raising the surface temperature above the wet bulb temperature [18]. Further research shows that the scale of the constant rate is affected by the coefficient of heat transfer or mass transfer, the exposed drying area, and the temperature or humidity gradient existing between the drying air and the product surface.

Phase 2 (falling rate): As shown in Figure 2, this period begins at the point when the constant rate period ends. This is the point when water molecules inside the product begins to migrate to the surface due to mass and energy difference. Phase 2 is represented by two zones: (i) the zone that indicates that the surface of the product is not saturated with water molecules, and (ii) the zone where internal movements of molecules controls the moisture removal rate at the surface. During this phase the drying rate continues to fall because the surface of the product remains unsaturated. This is because water vapor diffusion is constantly controlled by internal movement of liquid while the surface of the food product is continuously depleted with water molecules [14, 18].

2.2.2. The Water Activity

The water activity (α_w) of a food product is described as the ratio between the vapor pressure of the product when in equilibrium with the ambient air, and the vapor pressure of pure water, at the same temperature [19]. Water activity is very crucial in food drying industries because it is used as a measure to predict the possibility of microorganism growth on food products

[14]. It should be noted that water activity is not the same as moisture content although the two show similarities. The water activity is given by equation 1 below:

$$\alpha_w = \frac{p_w}{p_w^*} \approx \varphi \tag{3}$$

Where p_w is the partial pressure of a water solution and p_w^* is the partial pressure of pure water, at identical conditions. The water activity is shown to be approximately equal to the equilibrium relative humidity φ of the product at the same atmospheric condition. Every agricultural product has a water activity limit which marks the boundary for microorganisms to stop growing on the product. According to Beuchat [15], most bacteria begins to develop on the surface of the product when a water activity level of about 0.85 is reached, while mold and yeast generally start growing on the product when a water activity level of about 0.61 is reached. Further findings anticipate most fungi to start forming when a water activity level of about 0.70 is reached. To combat problems associated with water activity of food products, measures are put in place to reduce or control the water activity level such as the removal of liquid water or adding solutes. Drying is one of the method or process to remove water so that the water activity is lowered. Despite reducing water activity of products, solutes are also known to enhance the functional and sensory properties of foods. Water activity of a food product can be predicted from its freezing point or it can be measure either using the equilibrium sorption rate method, the vapor pressure measurement method, or the hygrometric instrument method. [20].

2.2.3. Desorption

The efficiency of drying a food product is dependent on how water is held inside it. Food products such as grains are hygroscopic and thus they retain water through sorption forces, namely, absorption or adsorption. Bound water is generally considered to be absorbed by the cell wall material by hydrogen bonding hydroxyl groups [21]. Absorption integrates water in liquid form into the solid structure of the grain while adsorption is defined as the adherence or the binding force between grain and water surfaces [10].

In processes of drying food products such as grains, the amount of water inside the grain needs to be lowered to the desired level by desorbing moisture. The desorption process occurs when the force that pushes water outside the grain exceeds the sorption forces (absorption and adsorption). Research shows that the sorption and desorption forces in drying grains with air depends on various factors such as temperature, air pressure, grain structure, moisture content, air relative humidity, and air velocity [9, 22, 23].

2.2.4. Equilibrium Moisture

Equilibrium moisture occurs when the grain moisture remains constant as a result of the balance between sorption forces and desorption forces. This implies that the rate of moisture desorption to the surrounding environment equals its rate of absorption of moisture from the surrounding. Research shows that the equilibrium moisture of a product is significantly affected by properties that affects its chemical compositions [12].

Brooker et al. [16] found that crops with high oil content usually have a high tendency to absorb less moisture from their surroundings as compared to starchy crops. Many researchers have failed to develop theoretical models of equilibrium moisture content that can accurately predict the equilibrium moisture content of a wide variety of agricultural products in different environment. This is attributed to oversimplification of equations by many assumptions in the model development, although doing so would promote a better understanding of the drying kinetics [13]. Moisture absorption in food products is based on capillary condensation within the pores of the product to be dried and it can be modelled by Kelvin's equation (4). This

equation shows the relationship between the vapor pressure and the saturated vapor pressure of liquid in capillaries at the same temperature conditions [24]. However, Kelvin's equation (4) will not provide accurate information at a very high relative humidity ($\geq$ 95 %) where most condensation occurs.

$$ln\left(\frac{P_v}{P_{vs}}\right) = \frac{2\sigma V cos\,\alpha}{r'R_oT} \tag{4}$$

Langmuir came up with an equation (5) that models the isothermal moisture equilibrium based on the kinetic model of evaporation and condensation rates of vapor for a single layer of water vapor molecules on the inner surface of the product [25]. This equation predicts the volume of water that is absorbed isothermally at a vapor pressure, but the model only applies to single layer, hence it does not account for multilayer absorption and the relation between absorbed molecules.

$$V_v = V_m \left[\frac{bP_v}{(1+bP_v)}\right] \tag{5}$$

Further research shows that Brunauer et al. [26] came up with a modified Langmuir equation (6) that does not only account for single layer but also model the multilayer absorption. In their model, they assumed that the material has inner surfaces that are made of a collection of absorption sites.

$$\frac{P_v}{V_v(P_{vs}-P_v)} = \frac{1}{V_m c} + \left(\frac{c-1}{V_m c}\right)\left(\frac{P_v}{P_{vs}}\right) \tag{6}$$

Although several equations have been developed to model isotherms, most of them change depending on the temperature range with different constants. Equation 7 shows the modified Henderson's equation of isotherms for corn that does not change the equation's constant for different temperature range (Thompson et al 1968 cited in [10]). This equation was validated with lab test results obtained by Samapundo et al. [9] with the constants used by Lopes et al. [27] as shown in Figure 3.

$$M_e = 0.01 \left[\frac{\ln(1-RH)}{-8.65\times10^{-5}(T+49.81)}\right]^{\frac{1}{1.8634}} \tag{7}$$
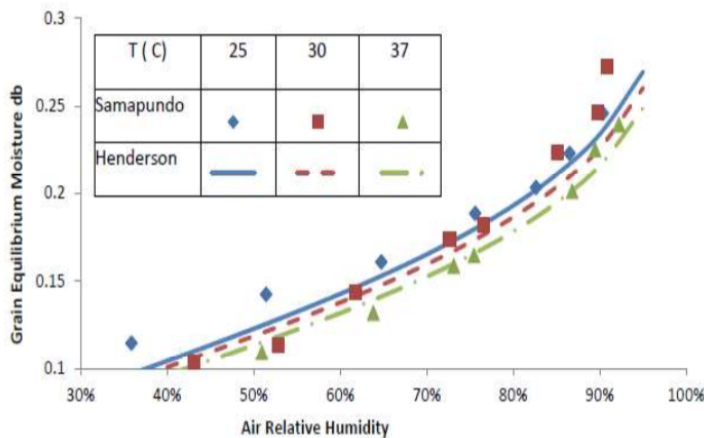

Figure 3. Comparison of Samapundo et al.'s [9] data with modified Henderson's equation data cited in [10].

17

2.2.5. Diffusion and Vapor Pressure Deficit

Water is distributed and stored inside the grain structure, and it needs to reach the grain surface in order to be removed by the air [10]. Diffusion is a movement process of molecules from a high concentration area to low concentration area due to partial pressure differences. This process in the capillaries of moist solids is dependent on the nature of the material, moisture content, and moisture bonding [22]. Vapor Pressure Deficit (VPD) is defined as the difference between the vapor pressure of air at saturation point and its actual vapor pressure. VPD is directly related to transpiration while the saturation vapor pressure (vp_{sat}) given by equation 8 is temperature dependent [10].

$$vp_{sat} = \frac{77.3450 + 0.0057(T + 273.15) - \frac{7235}{(T + 273.15)}}{8200(T + 237.15)} \tag{8}$$

Although the actual vapor pressure of air is an important factor in drying grains, it is generally not taken into consideration during grain drying. It is a function of temperature and relative humidity and can be obtained from psychometric charts. An important application of VDP is to evaluate the potential of condensation of a greenhouse crop and identify when it is likely to happen [28]. According to Prenger et al. [29], "VPD is the difference between the amount of moisture in the air and how much moisture the air can hold when it is saturated".

2.3. Solar Drying Methods

There are two main types of solar dryer technologies that are in practice: active and passive solar drying technology. Within these two technologies, drying process can be carried using either indirect, direct or mixed solar dryers. In an active solar drying method, forced convection is employed in the system whereby the heated air is circulated by a fan, or by similar devices. Therefore, the presence of a fan or similar device to cause air circulation means the possibility of an additional energy source to power the fan need to be considered. In a passive solar drying method, the use of forced convection is prohibited because this method only relies on natural convection heat transfer phenomena to circulate the air. This method might be advantageous compared to active solar drying method because it does not require an extra source of energy to power it.

According to the Department of Energy of South Africa [30], most areas in the country average more than 2500 hours of sunshine per year, and an average solar-radiation levels range between 4.0 kWh/m^2 and 9.0 kWh/m^2 in one day as shown in Figure 4. The annual global average solar radiation per day is about 220 W/m^2 for South Africa compared with a much lower average solar irradiation of many countries [30]. With enough sunshine in Africa (particularly in South Africa) one could make use of the opportunity to utilize the solar energy which is abundant and inexhaustible. Figure 4 shows the average annual solar radiation falling one square meter surface of African countries. The lowest intensity is denoted with a light green color measuring as low as 1461 kWh/m^2 and the highest intensity denoted with a faint pink color measuring as high as 3287 kWh/m^2 annually.
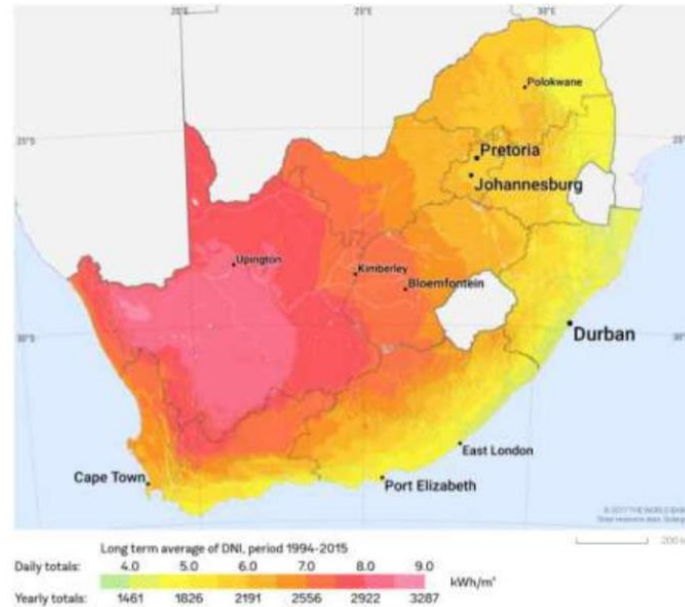
Figure 4. Direct average normal solar irradiation over South Africa from 1994-2015 [31].

Grain seeds normally retain about 10 % of the moisture from their surroundings, which makes it almost impossible for them to achieve total dryness. However, they can be reliably stored containing at such a humidity amount. It should be noted that whichever drying method is used on grains, it is important to have total control of the drying temperature. High drying temperature will cause physical damage to the seeds. The drying temperature selected will depend upon on the end use of the grains [11]. The next section gives an in-depth understanding of the different solar drying methods that are commonly in practice, and practical examples thereof.

2.3.1. Direct Solar Drying

In this method, the products are directly exposed to solar radiation as briefly discussed in the previous sections. Direct solar drying is generally composed of an insulated drying chamber which has a glass or plastic transparent cover, high absorptivity surface, and drilled holes to allow the drying air to enter and exit the drying chamber. The transparent cover transmits part of the solar radiation and get absorbed inside the chamber. The absorbed radiation energy results in an increase in temperature on the surface which heats up the passing air drawn inside the chamber due to natural convection (in passive solar dryers) or by forced convection (in active solar dryers) [5]. In this process, part of the solar radiation is lost to the atmosphere by reflection of the transparent cover. Part of the transmitted radiation is reflected from the product surface, but the rest is absorbed by it. The absorbed radiation energy and hot air circulating causes the temperature of the product to increases allowing it to reduce its moisture content by evaporation [32]. Figure 5 shows a typical example of a direct solar dryer. Although direct solar drying is simple to implement, it presents several limitations as indicated below [5]:

- It can only be used for small scale production due to its capacity.

- Direct exposure of products to solar radiation can lead to chemical reactions such as discoloration.

- The drying process results in moisture condensates on the glass.

- The drying process can be difficult if there is low absorbed energy.
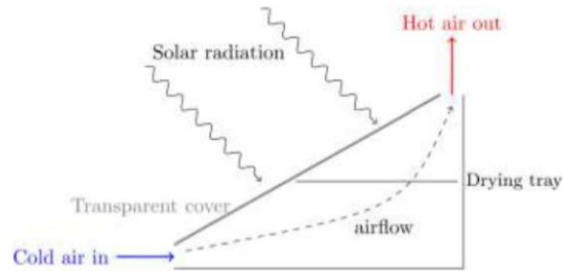
Figure 5. Typical design of a solar dryer [13].

According to Belessoitis et al. [14], further research indicates that this method has many disadvantages which may disqualify it for industrial implementation such as:

- Limited or no control quality of the final product.
- There are no technical measures developed to keep track of the drying process during long period of drying.
- The process very slow in drying especially in bad weather.
- High exposure of the drying product to bad weather can negatively affect the quality of the final product. It can also lead to bacteria growth on the product.
- The process can lead to significant losses due to dirt, dusts, or attacks by insects, rodents, and others.

Shown in Figure 6 is another type of direct solar drying whereby the drying material (grapes) is not directly exposed to the sun's ray but is dried partially in the shade. According to Belessoitis et al. [14], the grapes are hung on wires to form shelves in scaffoldings open to all sides except the roof. This allows the grapes to be dried by natural free convection of air circulating and by indirect solar energy.

Figure 6. Preliminary drying of seedless grapes in the shade [14]

According to further information provided by Belessoitis et al. [14], direct solar drying is generally based on estimates related to experience because it is proven that scientific control
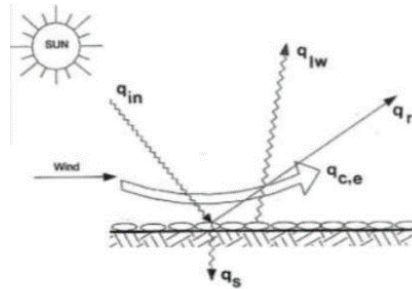
of final moisture content is not possible. Figure 7 shows the principle of open-air solar drying of crops. According to Jain et al. [33] an energy balance for direct solar drying can be expressed by equation 9 below:

$$I = \dot{q}_{in} = \dot{q}_{dr} + \dot{q}_s + \dot{q}_L \tag{9}$$

Whereby $\dot{q}_L$ is the sum of solar heat losses, given by this formula:

$$\dot{q}_L = \dot{q}_{lw} + \dot{q}_r + \dot{q}_{c,c} \tag{10}$$

Figure 7. Principle of direct solar drying [33].

As shown in Figure 7, In direct solar drying, only a portion of the total solar radiation is absorbed by the product and the rest is lost to the atmosphere by reflection. Research shows that the color of the product being dried has significant effect on the absorptivity of the product. Therefore, products with a high absorptivity coefficient such as dark color materials (as shown in Table 3 below) will absorb more solar radiation and reflect less energy back to atmosphere.

Table 3. Absorptivity coefficient for different material color [14].

Material color	Absorptivity coefficient
Dark color material	0.90
Grey, red, or green color substances	0.70
Light color substances	0.50

2.3.2. Indirect Solar Drying

This method uses solar radiation energy that is absorbed by the solar collector to heat the oncoming air. In this method the food product is not directly exposed to solar radiation as in the case of direct solar drying method. Therefore, chemical reactions in a product that could possibly lead to discoloration and vitamins degradation are prevented. An indirect solar dryer is typically composed of three components:

- A solar collector,
- A drying chamber, and
- A funnel or air exist channel.

As depicted in Figure 8, ambient cold air enters into the collector by natural convection or forced convection in which the absorbed radiation heats up the air molecules. The heated air is then caused to circulate around the product by natural or forced convection inside the drying chamber. Since the temperature of the heated air is significantly higher than the product, there is heat transfer by convection which leads to evaporation of moisture and consequently resulting into dried product.
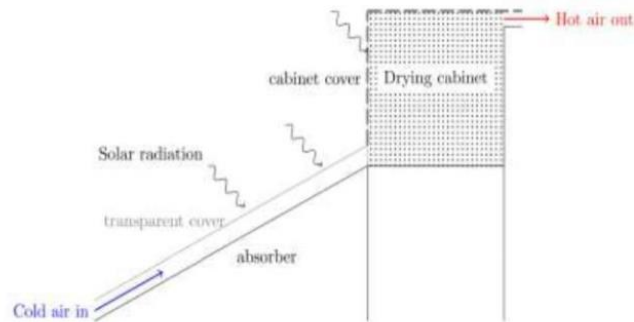
Figure 8. Working principle of indirect solar dryer [13].

An experiment with a solar dryer using a forced convection system integrated with gravel as heat storage material for chili drying was conducted by Mohanraj et al. [34] at Pollachi, India. Essentially the system consisted of a flat plate solar air heater connected to a drying chamber. The blower is connected on one side of the solar collector and sand mixed with aluminum scrap was used to store the heat. Their results indicated that after a day of drying the moisture content was reduced from 72.8 % to about 9.1 % at the bottom tray and 9.8 % at the top tray. The gravel in the solar dryer conducted heat for 8 hours during peak sunshine hours and the chilies continued to dry for 4 hours after sunset. Evaluation of the results collected from drying copra grains in a forced convection solar dryer compared to the results of sun drying in a study by the same researchers [35] indicated that indirect forced convection solar dryer caused a reduction in moisture content (wet basis) from 52 % to 7.8 % in 66 hours, with a system pickup efficiency ranging between 13 % and 45 %. The sun drying results indicated that moisture content was reduced from about 52.3 % (wet basis) to about 9.2 % in 7 days, with a thermal efficiency estimated to be around 21 % [35].
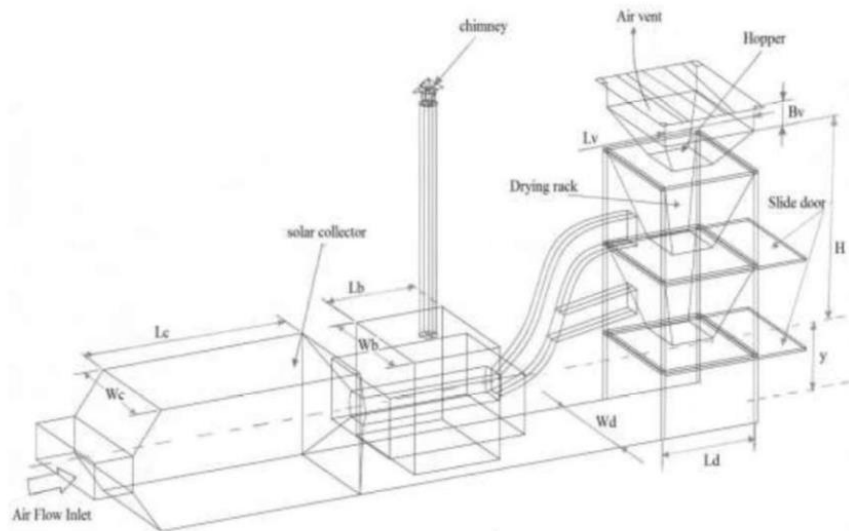
Figure 9. Schematic view of an indirect solar dryer with a back-up heater [36].

A study by Tonui et al. [36] was conducted on the development of a solar grain dryer that incorporate a biomass burner as a back-up heater, as shown by the schematic diagram in

Figure 9. The dryer is composed of the solar collector, drying chamber, biomass burner and forced convection air flow system. Their test was conducted in an environment whose air temperature and relative humidity were 26 °C and 72 %, respectively. The average daily global solar radiation incident on a horizontal surface was around 21.6 MJ/m^2/day. Based on the results obtained, the prototype was able to reduce the moisture content of 100 kg maize from 21 % to 13 % (wet basis), and a thermal efficiency of 57.7 %.

In a study conducted Ferreira et al. [37], they developed and investigated an indirect hybrid solar-electrical dryer which is composed of a solar heating chamber and a drying chamber as shown in Figure 10. Their work indicates that apart from solar heating, an auxiliary heating system was incorporated into the design to compliment solar heating. Their dryer was designed with an auxiliary heating system at the bottom of the drying chamber, which is composed of 20 incandescent lamps of 100 W each. Although it was a brilliant idea to have an auxiliary heating system, the performance was very poor because of high thermal losses and uneven drying of the products.

Figure 10. Hybrid solar-electric dryer [37].

In another case study by Mohanraj et al. [34] on the development of an indirect forced convection solar dryer, the designed and constructed their solar dryer which incorporates gravel as a heat storage material for drying chilies. Based on their experiment, the dryer was able to reduce the moisture content of chili from 72.8 % to as low as 9.2 % (wet basis) in 4 hours. The integration of the gravel in the dryer ensured that a consistent air temperature in the dryer was achieved and the resultant thermal efficiency of the dryer was around 21 % with a moisture removal rate estimated to be about 0.87 kg/kWh. This shows that the use of force convection and incorporation of better heat storage capacity material in dryers are ways to improve the performance of solar dryers.

2.3.3. Mixed Solar Drying

A mixed solar dryer combines the operational principles of the direct type solar dryer and the indirect type solar dryer. The combined actions of solar radiation incident directly on the product and pre-heated air provide the necessary heat required for the drying process. The air is generally pre-heated as it traverses the passages in the solar collector before to enters the drying chamber [38]. Figure 11 depicts an example of a hybrid passive solar dryer. Some of the hybrid solar dryers are typical examples of mixed solar dryers. Research shows that hybrid dryers can positively increase the drying rate of products without compromising the product quality as in the case of direct solar drying [32]. These systems are less common in practice due to their complexity in implementing and maintaining them.

The Department of Food Technology at Lund University developed a technology suitable for developing countries in order to preserve fruits, called Solar Assisted Pervaporation (SAP) [40]. Phinney et al. [39] define SAP as the movement of chemical particles from one side of a nonporous semipermeable membrane to another membrane by diffusion. Chaignon et al. [40] conducted a model analysis on two types of solar dryer (direct and indirect) using COMSOL Multiphysics software and SAP pouches as the drying materials. The motive was to produce a simulation and compare with on-site results to gain a better understanding of the different parameters of a dryer such as geometry, ambient conditions, and materials in order to identify parameters to consider in optimizing the design. Several assumptions to simplify the problem were made during the modelling such as the heat and mass transfer equations which were modelled on the base of isothermal properties, assuming a convective heat transfer coefficient, etc. [40].
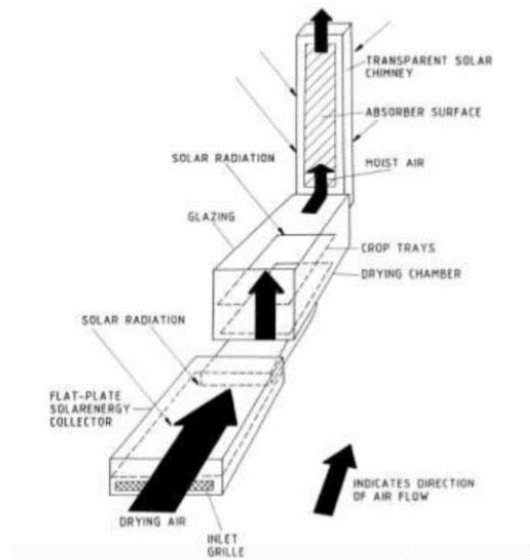
Figure 11. Typical design of a hybrid solar dryer [13].

In a study conducted by Balaji et al. [41], they investigated a mixed mode solar dryer for food preservation. In their design prototype, air is heated in a separate solar collector. The heated air is then allowed to pass through a grain bed inside the dryer and at the same time the drying cabinet absorbs solar energy directly through the transparent walls and roof. Essentially the drying product is heated by both the direct solar energy and heat from the passing air. The results of their experiment showed a drying rate and system efficiency of about 0.62 kg/h and 57.5 %, respectively. Another similar study was conducted by Ayensu et al. [42] on the simulation of a non-mechanical solar dryer with energy storage. In their study they investigated the drying characteristics of the dryer. The results of their experimental simulation indicate that the solar collector could transfer 118 W/m^2 to the drying air at a temperature of 32 °C. Based on the results they obtained, they concluded that:

- For a given storage capacity using 1kg of wheat grain they can reach steady state conditions with or without thermal storage in 2 hours.
- For a given temperature the moisture content of wheat grain is inversely proportional to drying time.

- As the moisture content in the grain decreases, the drying rate also decreases.
- Thermal storage significantly reduces the temperature of wheat grain, thereby enhancing its quality.

Bharadwaz et al. [43] conducted a study on the development of a solar dryer for drying crops. The orthogonal view shown in Figure 12 indicates that the dryer is composed of a separate solar collector, a centrifugal blower, a drying chamber, and an air flow system.
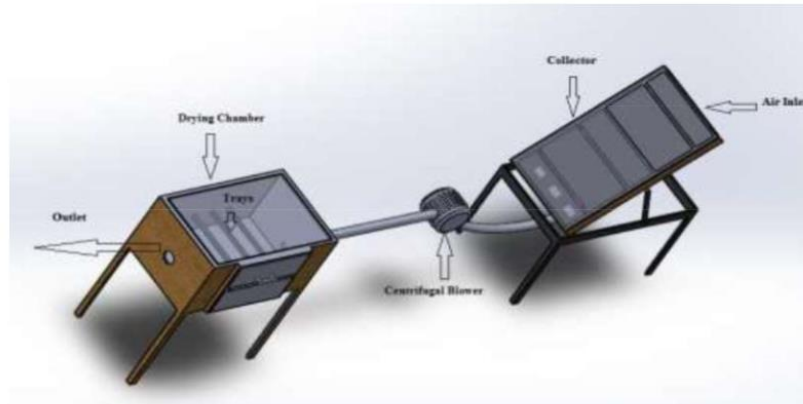
Figure 12. View of the proposed solar dryer by Bharadwaz et al [43].

Their experiment appreciated the use of forced convection that it can significantly reduce the drying time and improves the thermal efficiency of the dryer in comparison to a natural convection dryer. The results from their study indicated an efficiency of the solar collector of 35.33 % and that of the dryer to be 13.8 %. They found that temperatures inside the solar collector and drying chamber were both significantly higher than the ambient temperature during most hours of the day. Which was an indication of effectiveness of their solar dryer. There was also a reduction in relative humidity inside the drying chamber. Although mixed mode solar dryers are more efficient than other types of dryers, they have the disadvantage of exposing the food product to direct solar radiation during drying. However, various enhancement techniques to improve the performance of mixed mode solar driers can still be researched and experimented on to improve their effectiveness and durability.

2.4. Advantages of Solar Drying Systems

According to Ekechukwu et al. [13], there are several advantages associated with drying products using solar energy such as:

- A reasonably higher temperature with low humidity and air movement will results in a higher drying rate.
- Generally, the food products inside the solar dryer are protected against flies, rain and dust that can adversely affect the product quality.
- The quality of the dried product is usually better in terms of its nutrients, hygiene and even color.
- Solar drying permits early harvesting and reduces the field losses of the products.
- It promotes better planning of harvesting season.
- Drastically reduces spoilage in storage.
- Reduces transportation costs of products to the markets and allows farmers to sell their products at better prices during early harvesting season.
- Is environmentally friendly.

2.5. Disadvantages of Solar Drying Systems

Although there are a lot of good advantages of solar drying, the main disadvantages of solar dryers are [13]:

- Limited time of solar insolation during the day
- Drying time is usually longer
- Initial investment costs might be high

2.6. Thin Layer Drying and Deep Bed drying

In the thin layer model of drying grains, all grains are considered as fully exposed to the air at a constant drying temperature, pressure, air flow, and humidity. A grain bed thickness of up to 20 cm is generally considered as a thin layer and most conventional dryers are designed based on thin layer principles. During a thin layer test, the sample weight is normally taken at different times to determine the reduction in moisture content. The results are plotted against time to obtain the drying curves. In some cases, one might be interested in validating the heat and mass transfer equation by taking measurements of the exhausted air [45]. Omid et al [17] states that precise control of drying conditions is very important in conducting a thin layer drying experiment on agricultural products.

Garg et al. 1990 cited in [46] came up with a mathematical model of a mixed mode solar dryer whereby the drying product was modelled as a thin layer. In their model, they consider the radiation absorbed by the product to be directly related to the absorptivity effect of the product, the transmissivity effect of the glass cover, and to solar incidence radiation. Grains generally dry in the falling rate, and several theories have been formulated to describe the mechanisms of moisture movement in solids during drying in the falling rate period. It is considered that moisture movement within a grain kernel takes place by diffusion of liquid and/or vapor [17]. Several researchers have modelled thin layer drying using Fick's law expressed by equation 12 or empirically derived equations [47].

$$\frac{M_t - M_e}{M_0 - M_e} = \frac{8}{\pi^2} \sum_{n-1}^{\infty} \frac{1}{(2n+1)^2} exp\left(-(2n+1)^2 \pi^2 \frac{D_{eff}t}{4H^2}\right) \tag{12}$$

An empirical model (expressed by equation 11) by Thompson was developed to accurately predict the drying time of corns in the temperature range of 60 ℃ to 140 ℃ [12].

$$t = A'ln\left[\frac{M_t - M_e}{M_0 - M_e}\right] + B'\left\{ln\left[\frac{M_t - M_e}{M_0 - M_e}\right]\right\}^2 \tag{11}$$

Where $A' = 1.86178 + 0.004887, B' = 427.2640e^{-0.03301T}$

Osodo et al. [48] stated that there are various statistical methods that can used in selecting the most suitable model that describes the drying behavior of a product under specific drying conditions. These methods provide a means of comparing the experimental data for the drying behavior of the product to the data predicted by the drying model. The statistical tools that are commonly used include the Coefficient of Determination (R^2), which varies between 0 and 1. Another important tool that can be used is the Modelling Efficiency (EF), which also varies between 0 and 1. Results yielding values that are closer to 1 imply a good fit between experimental data and model data. Root Mean Square Deviation/Error (RMSD/E) is another statistical tool that can be used, whose values ranges from 0 to large numbers. Results with values closer to 0 imply minimal error, hence, there is a good fit between experimental and model data. A study was conducted by Mukwangole et al. [49] on modelling maize cobs in a natural convection solar dryer. During their experiment, they compared their results with various drying mathematical models available in literatures using the coefficient of determination. Their motive was to determine which model best describe their drying curves. The experiment yielded results that are best fitting with the Midilli drying model of drying

maize cob with a coefficient of determination R^2 of 0.99912 as compared to other models. Recent approaches to solar drying method include the use of Computational Fluid Dynamics (CFD) software to aid the design processes. The CFD software can be used by researchers to analyze problems and get exact solutions that can be used in optimizing designs and so improving overall system performance [50].

The process of deep bed drying is generally complex in nature and its discussion is not covered in detail in this review as there are many available literatures that has covered it. Deep bed drying process involves a stationary product which is kept in the dryer for a certain time period while the drying air continuously flows over It [18]. According to Ekechukwu (1999) [12] deep bed is composed of layers of thick beds of drying product and the drying air moves from the bottom bed to the top of the product bed. This implies that the lower zone or bottom bed dries much more quickly than the top zone. As the drying air at high temperature and low humidity moves through the drying product mass, it removes moisture from the product. This movement takes place in a depth of the product bed known as the drying zone and creates a temperature gradient between the upper drying and bottom drying zone. At the beginning of drying, the drying zone starts from the bottom bed and progresses upwards in the direction of the drying air as it moves through the drying product mass. Deep bed drying process is generally composed of two drying period rates: the maximum drying rate period, and the decreasing drying rate period. During the maximum drying rate period, drying proceed from the bottom of the bed until it reaches the top of the bed. While the decreasing rate period begins soon after the drying reaches the top of the bed [12]. The major factors affecting deep bed drying include air flow rate, air drying temperature, and the depth of the bed. This implies that efficiency can be achieved by adjusting these parameters without over-drying the crop in the lower bed [18].

2.7. Effect of Drying on Grain Quality

Proper drying procedures are required to maintain the quality of grains during storage period. Good standard drying practices are required to combat the issues associated with bacteria, molds, etc. on grains. If grains are dried at high temperature, discoloration, and other kinds of damages due to heat may occur [51]. Other factors that may be adversely affected by high temperature drying include test weight, milling characteristics, baking characteristics, oil quality, and other nutritional values [52]. During high temperature drying, maize undergoes alterations within the grain structure such as stress cracks and protein denaturation. A common quality problem associated with improper drying and rapid cooling of grain is stress-cracking [53]. Table 4 shows the maximum temperature at which various selected grains for various end uses can be dried safely.

Table 4. Maximum safe drying temperature (℃) of grains [52].

Crop	End Use		
	Seed	Sold for Commercial Use	Animal Feed
Ear corn	43	54	82
Shelled corn	43	54	82
Wheat	43	60	82
Oats	43	60	82
Barley	41	41	82
Sorghum	43	60	82
Soybeans	43	49	-
Rice	43	43	-
Peanuts	32	31	-

Odjo et al. [54], conducted an analysis to investigate the impact of drying and heat treatment on the feeding value of corn. The analysis highlighted two ways to improve the effect of heat

or drying treatment of corn grain and the impact of this on its nutritive value: (1) control of ventilation and drying temperature within the dryer, (2) control of the initial moisture content of the grain. Odjo et al. [54] show that any adverse effects of drying were correlated with higher moisture content in the corn. This means that crucial nutritional aspects such as starch and other polysaccharides in high moisture corn may undergo partial degradation during the pre-drying, increasing the reducing sugar concentration and thus promoting reactions during drying.

3. CONCLUSION

A survey was conducted on the available literatures pertaining to different methods employed in solar drying of agricultural products, particularly grains. It was found that there are a lot of studies that have been conducted on drying grains using solar energy in both natural and forced convection, but there is still room for improving their performance. Many researchers have developed protypes to assess the performance of their solar dryers but they have not conducted any modelling of the dryers to predict the end results and evaluate them for performance improvement. From studies conducted, it is evident that indirect or mixed mode solar dryer using forced convection offers better drying compared to other types of solar dryer but their thermal efficiency needs to be improved. In conclusion, the literature survey has opened doors to the need for further research on improving the performance of solar grain dryers by software modeling and evaluation of the dryers with a preheater. Further research will also allow examination of the behavior of the drying fluid inside the dryer. To ensure better performance is ultimately achieved, software modelling data will be compared with on-site experimental data.

REFERENCES

[1]   Salunkhe, D. K. and Kadam, S. S. Handbook of Fruit Science and Technology. New York: Marcel-Dekker, 1995.

[2]   Tiwari, A. A Review on Solar Drying of Agricultural Produce. *Journal of Food Processing & Technology*, 7(623), 2016. doi: 10.4172/2157-7110.1000623.

[3]   Parakash, S., Jha, S. K. and Datta, N. Performance Evaluation of Blanched Carrots Dried by Three Different Dryers. *Journal of Food Engineering*, 62, 2004, pp. 305-313. https://doi.org/10.1016/S0260-8774(03)00244-9

[4]   Akinola, A. O. and Fapetu, O. P. Exergetic Analysis of a Mixed-Mode Solar Dryer. Journal of *Engineering* and *Applied* Sciences 1, 2006, pp. 205-10.

[5]   Sharma, A., Chen, C. R. and Vu Lan, N. Solar-Drying Systems: A Review. *Renewable and Sustainable Energy Reviews*, 13(6-7), 2009, pp. 1185-1210. https://doi.org/10.1016/j.rser.2008.08.015.

[6]   Upadhyay, N. and Singh, A. Experimental Performance of Solar Greenhouse Dryer for Drying Vegetables & Fruits. *Journal of Emerging Technologies and Innovative Research*, 4, 2017, pp. 153

[7]   Raghavan, V. G. S. and Sosle, V. Grain Drying. In: Mujumdar, A. S. ed., Handbook of Industrial Drying. Milton Park, Abingdon-on-Thames, UK: Taylor & Francis, 2007 pp. 563-573.

[8]   Kenneth, J. and Hellevang, P. E. Recommended Storage Moisture Contents and Estimated Allowable Storage Times. 2013. https://www.ag.ndsu.edu/publications/crops/grain-drying

[9]   Samapundo, S., Devlieghere, F., Meulenaer, B. D., Atukwase, A., Lamboni, Y. and Debevere, J. M. Sorption Isotherms and Isoteric Heats of Sorption of Whole Yellow Dent Corn. *Journal of Food Engineering*, 79(1), 2007, pp. 168-175. Doi: 10.1016/j.jfoodeng.2006.01.040.

[10] Alonso, D. M. J. Modelling of Grain dryers: Thin layers to Deep beds. M.Sc. Dissertation. Bioresource Engineering Department, McGill University, Montreal, 2011.

[11] Drying the Grain. https://www.shareweb.ch/site/Agriculture-and-Food-Security/focusareas/Documents/phm_postcosecha_drying_grain_e.pdf.

[12] Ekechukwu, O. V. Review of Solar Energy Drying Systems I: An Overview of Drying Principles and Theory. *Energy Conversion and Management*, 40(6), 1999, pp. 593-613. DOI: 10.1016/S0196-8904(98)00092-2.

[13] Ekechukwu, O. V. and Norton B. Review of Solar-Energy Drying Systems II: An Overview of Solar Drying Technology. *Energy Conversion Management*, 40 (6), 1999, pp. 615-655. DOI: 10.1016/S0196-8904(98)00093-4. https://doi.org/10.1016/S0196-8904(98)00093-4

[14] Belessiotis, V. and Delyannis, E. Solar Drying. *Review: Solar Energy*, 85(8), 2010, pp. 1665-1691. https://doi.org/10.1016/j.solener.2009.10.001.

[15] Beuchat, L. R. Microbial Stability as Affected by Water Activity [Bacteria, fungi, Spoilage]. *Cereal Foods World*, 26(7), 1981, pp. 346-355.

[16] Brooker, D. B., Bakker-Arkema, F. W. and Hall, C. W. Drying Cereal Grains. *Molecular Nutrition & Food Research*, 20(1), 1976, pp. 95-96. https://doi.org/10.1002/food.19760200143.

[17] Omid, M., Yadollahinia, A. R. and Rafiee, S. A Thin-Layer Drying Model for Paddy Dryer. Proceedings of the International conference on Innovations in Food and Bioprocess Technologies, 12th—14th December, AIT, Pathumthani, Thailand, 2006.

[18] Visavale, G. L. Principles, Classification and Selection of Solar Dryers. In: Hii, C. L., Ong, S. P., Jangam, S. V. and Mujumadar, A. S. eds. Solar Drying: Fundamentals, Applications. Singapore, 2012, pp. 1-50.

[19] Jean-Baptiste, C. and Vassilis, G. Water Activity and its Prediction: A Review. *International Journal of Food Properties*, 4(1), 2001, pp. 35-43. DOI: 10.1081/JFP-100002187

[20] Rahman, M. S. and Labuza, T. P. Chapter 20, Handbook of Food Preservation. CRC Press, Boca Raton, FL. 2007. DOI: 10.1201/9781420017373.

[21] Skaar, C. Handbook of Wood-Water Relations. Berlin: Springer-Verlag, 1988.

[22] Aguerre, R. J. and Suarez, C. Diffusion of Bound Water in Starchy Materials: Application to Drying. *Journal of Food Engineering*, 64(3), 2004, pp. 389-395.

[23] Martinez-Vera, C., Zizearra-Mendoza, M., Galin-Domingo, O. and Ruiz-Martinez, R. Experimental Validation of a Mathematical Model for the Batch Drying of Corn Grains. *Drying Technology*. 13(1-2), 1995, pp. 333-350. DOI: 10.1080/07373939508916956.

[24] Gregg, S. J. and Sing, S. W. Adsorption Surface Area and Porosity. New York: Academic Press, 1967.

[25] Langmuir, I. The Adsorption of Gases on Plane Surfaces of Glass and Mica, and Platinum. Journal of the American Chemical Society, 40(9). 1918. DOI: 10.1021/ja02242a004.

[26] Brunauer, S., Emmett, P. H. and Teller, E. Adsorption in Multi-Molecular Layers. Journal of the American Chemical Society, 60, 1938, pp. 309-319. DOI: 10.1021/ja01269a023.

[27] Lopes, D. D. C., Martins, J. H., Neto, A. J. S. and Filho, A. J. S. Simulation of Drying of Grains with Low Temperatures Using the Hukill Model. A New Approach. *Exact*a - Engenharia de Produção, 3, 2005, pp. 85-93. Doi: 10.5585/exacta.v3i0.636.

[28] Shamshiri, R. R., Jones, J. W., Thorp, K. R., Ahmad, D., Che Man, H. and Taheri, S. Review of Optimum Temperature, Humidity, and Vapour Pressure Deficit for Microclimate Evaluation and Control in Greenhouse Cultivation of Tomato: A Review. *Journal of International Agrophysics,* 32, 2018, pp. 287-302. Doi:10.1515/intag-2017-0005.

29

[29] Prenger, J. J. and Ling, P. P. Greenhouse Condensation Control-Understanding and Using Vapor Pressure Deficit (VPD) fact sheet (series) AEX-800. Columbus, OH: The Ohio State University Extension, 2000.

[30] South Africa. Department of Energy. *Renewable Energy – Solar Power*, 2017. http://www.energy.gov.za/files/esources/renewables/r_solar.html

[31] The World Bank. Solar Resource Maps of South Africa. Solar resource data: Solargis. Available: https://solargis.com/maps-and-gis-data/download/south-africa.

[32] Kumar M., Sansaniwal S. K. and Khatak P. Progress in Solar Dryers for Drying Various Commodities. *Renewable and Sustainable Energy Reviews,* 55, 2016, pp. 346-360. DOI: 10.1016/j.rser.2015.10.158.

[33] Jain, D. and Tiwari, G. N. Thermal Aspects of Open Sun Drying of Various Crops. *Energy,* 28(1), 2003, pp. 37-54. https://doi.org/10.1016/S0360-5442(02)00084-1.

[34] Mohanraj, M. and Chandrasekar, P. Performance of Forced Convection Solar Drier Integrated with Gravel as Heat Storage Material for Chilli Drying. *Journal of Engineering Science and Technology,* 4(3), 2009, pp. 305-314.

[35] Mohanraj, M. and Chandrasekar, P. Drying of Copra in a Forced Convection Solar Drier. *Biosystems Engineering.* 99(4), 2008, pp. 604-607. https://doi.org/10.1016/j.biosystemseng.2007.12.004.

[36] Tonui, K. S., Emmanuel, B. K. M., Mutuli, D. A. and Duncan, O. M. Design and Evaluation of Solar Grain Dryer with a Back-up Heater. *Research Journal of Applied Sciences, Engineering and Technology,* 7(15), 2014, pp. 3036-3043.

[37] Shaikh, T. B. and Kolekar, A. B. Review of Hybrid Solar Dryers. *International Journal of Innovations in Engineering Research and Technology,* 2(8), 2015.

[38] Weiss, W. and Buchinger, J (2001). Solar Drying. Trainings course on the production and sale of solar thermal plants in Zimbabwe. Arbeitsgemeinschaft Erneuerbare Energie (AEE) of the Institute for Sustainable Technologies, Austria.

[39] Phinney, R., Rayner, M., Sjoholm, I., Tivana, L. and Dejmek, P. Solar Assisted Pervaporation (SAP) for Preserving and Utilizing Fruits in Developing Countries. In: Third Southern African Solar Energy Conference, South Africa, 2015.

[40] Chaignon, J. and Henrik, D. Modelling of a Solar Dryer for Food Preservation in Developing Countries. 1-11, 2017. DOI: 10.18086/swc.2017.30.01.

[41] Balaji, B. O. and Olalusi, O. P. Performance Evaluation of a Mixed-Mode Solar Dryer. *AU Journal of Technology,* 11, 2008, pp. 225-231.

[42] Ayensu, A. and Asiedu-Bondzie, V. Solar Drying with Convective Self-Flow and *Energy Storage,* 3, 1986, pp. 273-279.

[43] Bharadwaz, K., Barman, D., Bhowmilk, D. and Ahmed, Z. Design, Fabrication and Performance Evaluation of an Indirect Solar Dryer for Drying Agricultural Products. *International Research Journal of Engineering and Technology,* 4(7), 2017, pp. 1684-1692. DOI:10.13140/RG.2.2.12532.40324

[44] Phadke, P. C. Walke, P. V. and Kriplani, V. M. A Review on Indirect Solar Dryers. *ARPN Journal of Engineering and Applied Science,* 10(8), 2015, pp. 3360-3371.

[45] Farkas, I. and Rendik, Z. Intermittent Thin Layer Corn Drying. *Drying Technology,* 15(6), 1997, pp. 1951-1960. DOI: 10.1080/07373939708917340.

[46] Simate, I. N. Simulation of the Mixed-Mode Natural-Convection Solar Drying of Maize. *Drying Technology,* 19(6), 2001, pp.1137-1155. DOI: 10.1081/DRT-100104810.

[47] Bagheri, H., Arabhosseini, A., Kianmehr, M. H. and Chegini, G. R. Mathematical Modelling of Thin Layer Solar Drying of Tomato Slices. *Agricultural Engineering International,* 15(1), 2013, pp.146-153.

30

[48] Osodo, B. Nyaanga, D. and Muguthu, J. Selection and Verification of a Drying Model for Maize (Zea mays L.) in Forced Convection Solar Grain Dryer. *American Journal of Food Science and Technology,* 5(3), 2017, pp. 93-100. DOI:10.12691/ajfst-5-3-4.

[49] Mukwangole, M. and Simate, I. N. Thin Layer Mathematical Modelling of Cob Maize in a Natural Convection Solar Drier. *Energy and Environment Research,* 7(2), 2017. DOI:10.5539/eer.v7n2p37.

[50] Rajkotia, S., Modi, V. and Chauhan, R. Performance Improvement of Solar Dryer. *International Journal of Scientific Research,* 2(5), 2012, pp. 142-144. DOI: 10.15373/22778179/MAY2013/50.

[51] Akhtaruzzaman, M., Sohany, M., Basunia, M. A., Hossain, M. K. and Sarker, M. S. H. Drying and Quality Features of Selected Maize Varieties Dried in Commercial Processing Complexes. *Agricultural Engineering International,* 19(3), 2017, pp. 148-155.

[52] Jayas, D. S. and Ghosh, P. K. Preserving Quality During Grain Drying and Techniques for Measuring Grain Quality, 2006. https://pdfs.semanticscholar.org/8f0d/219625be0fedde6afc0ad8cc0f50024038d5.pdf.

[53] Gustafson, R. J., Thompson, D. R. and Sokhansanj, S. Temperature and Stress Analysis of Corn Kernel-Finite Element Analysis. *Transactions of ASAE,* 22(4), 1979, pp. 955-960.

[54] Odjo, S. D. P., Malumba, P. K., Beckers, Y. and Bera, F. Impact of Drying and Heat Treatment on the Feeding Value of Corn. A review. *Biotechnology, Agronomy, Society and Environment,* 19(3), 2015, pp. 301-312.

NOMENCLATURE

m_w mass of water [kg]

m_d mass of dry solid [kg]

P_v Water vapor pressure in the product [N.m^{-2}]

P_{vs} Saturation vapor pressure [N.m^{-2}]

σ Surface tension of moisture [N.m^{-1}]

V Volume of liquid moisture [m^3]

$cos\,\alpha$ Angle of contact between moisture and capillary wall in radians

r' cylindrical capillary radius [m]

R_o Universal gas constant [J.mol^{-1}.K^{-1}]

T Drying temperature [$^{\circ}$C]

V_m Volume of water absorbed when internal surfaces are totally covered with monolayer of water molecule [m^3]

V_v Volume of water absorbed by product isothermally at vapor pressure [m^3]

b constant in Eq. (5); dependent on material and its temperature

c constant in Eq. (6); related to heat of absorption of water vapor

RH Relative humidity of air [kg.kg^{-1}]

M_e The equilibrium moisture content [kg.kg^{-1}]

I Total incident solar radiation [W.m^{-2}]

$\dot{q}_{dr}$ Absorbed heat for drying [W.m^{-2}]

$\dot{q}_s$ Heat losses to the soil [W.m^{-2}]

$\dot{q}_{lw}$ Long wave heat losses [W.m^{-2}]

$\dot{q}_r$ Het losses due to reflection [W.m^{-2}]

$\dot{q}_{c,c}$ Convective and evaporative heat losses due to wind movement [W.m^{-2}]

M_t The moisture content at the end of the drying time $[\text{kg.kg}^{-1}]$

M_o The initial moisture content $[\text{kg.kg}^{-1}]$

D_{eff} The effective moisture diffusivity $[\text{m}^2.\text{s}^{-1}]$

t Drying time $[\text{s}]$

H Thickness of the product $[\text{m}]$

n The number of terms taken into consideration (n = 1,2,3,4,….)

CHAPTER 3

3. COMPUTATIONAL FLUID DYNAMICS IN SOLAR DRYING

This chapter presents work that was published under the title "Computational Fluid Dynamics in Solar Drying" in the *International Journal of Mechanical Engineering and Technology* (IJMET), a journal accredited by the Department of High Education and Training (DHET) of South Africa.

To cite this article: Johannes P. Angula and Freddie Inambao, Computational Fluid Dynamics in Solar Drying. *International Journal of Mechanical Engineering and Technology,* 10(11), 2019, pp. 259-274.

The link to this article:

http://www.iaeme.com/IJMET/issues.asp?JType=IJMET&VType=10&IType=11

COMPUTATIONAL FLUID DYNAMICS IN SOLAR DRYING

Johannes P. Angula and Freddie Inambao*

Department of Mechanical Engineering,
University of KwaZulu-Natal, Durban, South Africa
https://orcid.org/0000-0001-9922-5434
*Corresponding Author E mail: inambaof@ukzn.ac.za

ABSTRACT

Computational Fluid Dynamics (CFD) is an exceptional modeling method which is used for accurately predicting and solving complex fluid flow regimes. It is used in many engineering applications including food processing. In food processing CFD can be used in designing, analyzing and improving the performances of solar dryers in order to enhance product quality. An understanding of the drying phenomena is crucial in the dehydration and preservation of food products. With increasing advances in solar drying technologies, modern computers can be equipped with modeling software that conveniently allows drying systems to be improved. The appropriate use of CFD in modeling and simulating solar drying systems has been applied by many researchers and research is ongoing. This paper presents the underlying principles of CFD, the advantages and disadvantages of using CFD, and the recent works that have been carried out. The paper focuses on the application of CFD in solar drying of food products, and identifies potential areas of improvements for further research.

Keywords: CFD, Solar Drying, Modelling, Simulation, Costs, Performance

Cite this Article: Johannes P. Angula and Freddie Inambao, Computational Fluid Dynamics in Solar Drying. *International Journal of Mechanical Engineering and Technology* 10(11), 2019, pp. 259-274.
http://www.iaeme.com/IJMET/issues.asp?JType=IJMET&VType=10&IType=11

1. INTRODUCTION

Drying is one of the most crucial practices in food processing and ensures that food products are safely preserved. It is used for a wide variety of products ranging from low moisture products (e.g. corn), to intermediate moisture products (e.g. coffee), to high moisture products (e.g. fruit) [2, 3]. The use of solar energy has gained popularity in food drying applications due to the ongoing reduction in natural resources, high natural fuel costs, and environment damage [1]. It is also found to be one of the most inexpensive and economical methods of food drying which is pollution free and easy to control [2]. Since at least 1976 different designs of dryers, particularly those incorporating solar energy, have been studied by various researchers to assess their performance [4, 5]. Studies confirm that solar dryer performance is

34

significantly affected by ambient weather conditions. This poses a challenge in assessing important parameters of dryers such as thermal efficiency, drying rate, and drying capacity. One of the technological methods employed in solar drying is the use of Computational Fluid Dynamics (CFD) tools to model and simulate the drying kinetics of agricultural and food products. CFD is a powerful and innovative computational method that uses numerical calculations and algorithms to solve and analyze problems associated with fluid flow in specified regions of interest [7, 8]. According to Ambesange et al. [7], CFD is described as a method which accurately predicts fluid flows using:

- Mathematical modeling (solving partial differential equations of fluid domain),

- Numerical analysis (discretization and solution methods of fluid flow), and

- Software codes (solver, pre-and post-solving functions).

Using a modern tool such as CFD avoids the problem of needing to run multiple experimental drying trials in order to select a suitable design [6]. In addition to the weather effects on drying, performance of solar dryers also depends on crop moisture which because this also affects the drying rate [2]. This implies that for consistency, any comparisons of drying trials need to have products with the same moisture content at the beginning of each trial. This is a difficult parameter to control since agricultural products from the field will not have the same moisture content at the time of harvest. However, with the use of CFD products in a solar dryer can be simulated at the same or different moisture content to account for nonuniformity in drying and enhance performance and product quality. Rosli et al. [9] emphasize that with variable information regarding drying conditions, it is more beneficial and economical to model and simulate the drying process of products than conduct experiments. Jamaleddine et al. [10] indicated that with rapid advancement in technology, CFD is proving to provide an effective solution in predicting drying phenomenon and can be used in optimization, development of equipment and drying strategies for a variety of dryers. Defraeye [18] reviewed advanced computational modelling of drying processes and found that up to 2015 the trend of using CFD methods in the food industry to develop and optimize drying systems grew exponentially (Figure 1).
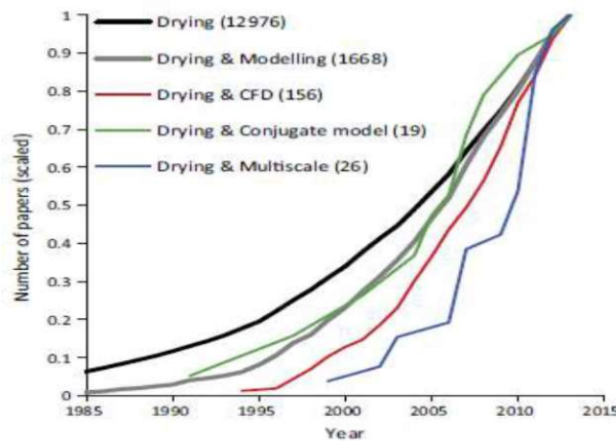
Figure 1. Published peer-reviewed papers on drying technologies and their relation to CFD applications [18]

This exponential growth rate is anticipated to double in the years to come in the food industry due to the reliability and efficiency of CFD. Over decades of technology advancement, several CFD software packages and codes have been developed and are widely used in different process to model and simulate fluid dynamics of different conditions. Commonly used CFD software packages in relation to the food drying process include COMSOL Multiphysics, Star CCM+, ANSYS Fluent, ANSYS CFX, OpenFOAM, FIDAP, CFD 2000, PHOENICS, FEMLAB and FLOW 3D [11, 12, 18]. Other useful software codes that can be used in conjunction with CFD codes are MATLAB, FORTRAN and TRNSYS software. These software codes are used by many researchers in the development of mathematical drying models to simulate the drying behaviour of many food products [44]. In addition, they provide a meaningful way for researchers to test and validate other drying models and select an equation(s) that best describes the drying process of that specific food product.

Multiphysics CFD software is user-friendly and can solve multifaceted 3D conjugate fluid problems so is convenient for users to run models and simulations. The accuracy of the model and simulation mainly depends on the user skills in utilizing the CFD tool to define the problem and apply necessary modeling methods in executing the problem. The ever-increasing utilization of CFD tools in drying technology has led the authors to conduct a study and examine the achievements accomplished in the solar drying field. The aim of this review is to present a study on the utilization and application of CFD methods in solar drying technology of agricultural and food products.

2. OVERVIEW OF CFD IN FOOD DRYING

The conventional drying methods that are commonly used for commercial or industrial purposes are spray drying, fluidized bed drying, solar drying, freeze drying, microwave-assisted drying, infrared drying, and super-heated steam [3, 13]. The following sections are aimed at providing an overview on the fundamental principles of computational fluid dynamics as applied in food drying methods. In general, the principles apply to conventional drying methods but in this paper the emphasis is placed upon solar drying.

2.1 CFD Principles in Drying Processes

An important aspect of CFD methodology is to gain a better understanding of the events happening within the fluid kinetics including the interaction of fluid molecules and solid bodies [14]. Albaali et al. [14] indicated that "these events are connected to the action and interaction phenomena such as heat dissipation, particles diffusion, convection, slip surfaces, boundary layers, and turbulence that are governed by the compressible Navier-Stokes partial differential equations". Navier-Stokes equations (Equation 1 and Equation 2) are used to solve Newtonian fluids. In CFD simulation of food drying, nonlinear partial differential equations (PDEs) are solved so that the mass, momentum, and energy transfer of the physical drying process is determined.

The first equation (Equation 1) is denoted as the continuity equation or conservation of mass law. It indicates a balance between incoming mass flow and outgoing mass flow within a fluid element [15].

$$\rho \frac{\partial u}{\partial x} + \rho \frac{\partial v}{\partial y} + \rho \frac{\partial w}{\partial z} + \frac{\partial \rho}{\partial t} = 0 \qquad (1)$$

Equation 1 is expressed in rectangular coordinates, where ρ is flow density (kg/m^3), t is time (m/s), $u, v,$ and w are fluid velocity components (m/s) in the corresponding rectangular coordinates, and $x, y,$ and z are rectangular coordinates (m). For simplicity, Equation 1 may be written as Equation 1a:

$$\nabla . \rho \vec{V} + \frac{\partial \rho}{\partial t} = 0 \qquad (1a)$$

Whereby ∇ is a vector operator and $\vec{V}$ represents the fluid velocity (m/s) at a given time.

The second equation (Equation 2) is referred to as Newton's second law of motion for fluids or conservation of momentum law. It states that at any given time, the change in momentum of a fluid element is equal to the sum of the external forces acting on that fluid element [3, 15]. Equation 2 can be expanded into a three-dimensional expression as represented by Equation 2a, Equation 2b, and Equation 2c below.

$$\rho \frac{Du}{Dt} = \rho g_x - \frac{\partial p}{\partial x} + \frac{\partial}{\partial x}\left[\mu\left(2\frac{\partial u}{\partial x} - \frac{2}{3}\nabla.\vec{V}\right)\right] + \frac{\partial}{\partial y}\left[\mu\left(\frac{\partial u}{\partial y} + \frac{\partial v}{\partial x}\right)\right] + \frac{\partial}{\partial z}\left[\mu\left(\frac{\partial w}{\partial x} + \frac{\partial u}{\partial z}\right)\right] \quad (2a)$$

$$\rho \frac{Dv}{Dt} = \rho g_y - \frac{\partial p}{\partial y} + \frac{\partial}{\partial y}\left[\mu\left(2\frac{\partial v}{\partial y} - \frac{2}{3}\nabla.\vec{V}\right)\right] + \frac{\partial}{\partial x}\left[\mu\left(\frac{\partial u}{\partial y} + \frac{\partial v}{\partial x}\right)\right] + \frac{\partial}{\partial z}\left[\mu\left(\frac{\partial v}{\partial z} + \frac{\partial w}{\partial y}\right)\right] \quad (2b)$$

$$\rho \frac{Dw}{Dt} = \rho g_z - \frac{\partial p}{\partial z} + \frac{\partial}{\partial z}\left[\mu\left(2\frac{\partial w}{\partial z} - \frac{2}{3}\nabla.\vec{V}\right)\right] + \frac{\partial}{\partial y}\left[\mu\left(\frac{\partial v}{\partial z} + \frac{\partial w}{\partial y}\right)\right] + \frac{\partial}{\partial x}\left[\mu\left(\frac{\partial w}{\partial x} + \frac{\partial u}{\partial z}\right)\right] \quad (2c)$$

These sets of equations are also expressed in rectangular coordinates, whereby g_x, g_y, and g_z are the gravitational acceleration (m/s^2) in the respective coordinates, μ is the fluid dynamic viscosity (kg/m.s) and p is the local thermodynamic pressure. The preceding sets of equations can be written in a combined expression as shown by the simplified Equation 2 [16].

$$\underbrace{\rho\left(\frac{\partial \vec{V}}{\partial t} + \vec{V}.\nabla\vec{V}\right)}_{1} - \underbrace{\nabla p}_{2} + \underbrace{\nabla.\left[\mu\left(\nabla\vec{V} + (\nabla.\vec{V})^T\right) - \frac{2}{3}\mu(\nabla.\vec{V})I\right]}_{3} + \underbrace{F}_{4} \qquad (2)$$

The first term in Equation 2 indicates the inertial forces of the fluid, the second term indicates the thermodynamic pressure forces, the third term indicates the forces due to dynamic viscosity, and the fourth term indicates the external forces applied to the fluid. In solar drying of food products the process involves heat/energy transfer between the drying fluid and product, and the properties of the fluid varies with temperature. This implies that an energy equation needs to be considered to accommodate the heat transfer phenomena. Equation 3 shows the energy equation, which is also referred to as the first law of thermodynamics. It states that at any given time, the change of energy within a fluid element is equal to the sum of the energy added or work done on that fluid element [17].

$$\frac{\partial}{\partial t}(\rho C_a T) + \frac{\partial}{\partial x_j}(\rho u_j C_a T) - \frac{\partial}{\partial x_j}\left(\gamma \frac{\partial T}{\partial x_j}\right) = S_T \qquad (3)$$

In this equation, C_a T represents the temperature of the fluid (K), x_j the fluid element, u_j γ represents the thermal conductivity (W/m.K), while the energy added or work done on the fluid element is represented by the heat sink, S_T. The Navier-Stokes equations coupled with the energy equation applies directly to laminar flows without major modifications. Reynolds number is a dimensionless number which is used for predicting flow conditions. It is essentially used in determining whether the flow will be laminar or turbulent. In general, most if not all flows encountered in engineering applications become unstable (turbulent) for high Reynolds number [15, 19]. In the food drying industry, fluid flow rate is generally high, and the geometry of the drying chamber does not permit laminar flows hence the flows are usually turbulent in nature. Considering the available CFD tools and computational power it is almost impossible to solve turbulent flows computationally using direct Navier-Stokes equations only. Therefore, Navier-Stokes equations coupled with other transport equations are considered to accurately model turbulence in the fluid domain. According to Malekjani et al.

[3], there are two different groups of turbulence models and they are categorized according to the governing equations used in them. The choice of which model group to use lies between:

- Reynolds averaged Navier-Stokes (RANS) models, and

- Large Eddy Simulation (LES) models.

It is of vitally important to choose the correct turbulence model for the simulation as it affects the CFD results and computational time/cost [18]. Apart from the RANS and LES models, there are also other commonly used models for fluid flow such as the Eulerian-Eulerian model and Eulerian-Lagrangian model [10]. These two models are commonly used as multiphase flow models and discrete particle tracking models. In this review, only the RANS and LES models are discussed as commonly applied in solar drying of agricultural foods.

2.1.1. Reynolds Averaged Navier-Stokes Models

Guerrero et al. [19] indicated that the RANS equations are obtained from the decomposition of the fluid flow variables of the governing equations into time-averaged and fluctuating parts, and then obtaining an overall time-averaged equation. This method of time averaging the governing equations results in the removal of the stochastic properties of the turbulent flow which give rise to additional Reynolds stresses [3]. These stresses need to be related to the flow variable by means of turbulence models. RANS models are applicable to most engineering problems and provide sufficiently accurate results. There are five commonly used RANS turbulence models which the user can choose from depending on the given fluid flow problem. Essentially, they form a group of three distinct models, namely: the $k - \varepsilon$, the $k - \omega$, and the RSM models. The RANS turbulence models are identified as:

- Standard $k - \varepsilon$ model,

- Renormalization Group $k - \varepsilon$ model (RNG),

- Realizable $k - \varepsilon$ model,

- Standard $k - \omega$ model, and

- Reynold Stress Model (RSM).

The $k - \varepsilon$ model presents two flow variables which are turbulent kinetic energy, k, and turbulence dissipation rate, ε. The model leads to two transport equations that correspond to the variables that can be computed and provide independent solutions. The two variables correspond to the turbulence velocity of the model as well as to the length scale. In addition to solving the two transport equations, the introduced Reynolds stresses in flow regime can be analyzed by using the Eddy viscosity approach [20]. This model is expanded to include additional effects that account for Reynolds stress anisotropy without actually using the RSM method. According to the review of Sadrehaghighi [21] on turbulence modeling, the $k - \varepsilon$ model is used in many fluid applications because of its convergence rate and comparatively low computational memory requirements. Although it is widely used in many applications, it does not seem to provide sufficiently accurate solutions to flow fields that show adverse pressure gradients and strong curvature to the flow field. The first $k - \omega$ model was developed by Wilcox and includes adjustments that account for the effects of low Reynolds numbers, compressibility, and as well shear flow spreading. It also accounts for solutions of the two transport equations, one for the turbulent kinetic energy, k, and another one for the specific turbulence dissipation rate, ω [22, 23]. The Wilcox model provides a good prediction of the free shear flow spreading rates which makes it a great tool in modeling free shear flows. In the absence of empirical log-wall functions, the $k - \omega$ model has proven to perform better when applied to boundary layers under adverse pressure gradients [24].

According to Sadrehaghighi [21], both the $k - \varepsilon$ model and the $k - \omega$ model assume a linkage of the eddy viscosity to a time and length scale to compute turbulent flow characteristics. Furthermore, the two models are seen to mainly differ in their respective turbulent dissipation rate ε and ω at the boundary wall and how the boundary conditions are specified for the same variables. The RSM also known as the 2nd Order Closures has been proven to provide very accurate predictions of flows in confined space where adverse pressure gradients occur. The RSM model was designed to address the issue of the $k - \varepsilon$ model having difficulty in solving a flow regime that has isotropic modelling of Reynolds stress [21]. According to some literature, RSM requires more computational time and memory to solve the fluid regime, and encounters difficulties in attaining convergence.

In this paper a detailed theory on RANS models is not presented as there are many articles available on the RANS model. A comparison in terms of the advantages and disadvantages of the different RANS models is provided in Table 1 which allows for the selection of suitable model(s) for a given CFD problem.

Table 1. Advantages and disadvantages of the different RANS model [3, 21, 22, 24]

Model type	Advantages	Disadvantages
Standard $k - \varepsilon$ model	Provides better convergence Economical Reasonably accurate for a wide variety of flows with high Reynolds number but without separation Provides satisfactory results for flow field without adverse pressure gradients Suitable for modelling external flows	Insufficient results in some cases due to assumptions and empiricism (such as assuming equilibrium conditions for turbulence) Less accuracy in complex flow regimes and flow with adverse pressure gradients Cannot predict different flows with same sets of constraints
Renormalization Group $k - \varepsilon$ model	Independency from empiricism Accounts for Reynolds stress anisotropy in complex flows Unlike the Standard $k - \varepsilon$ model it is reasonably accurate for flows with low-Reynolds number Enhanced accuracy for swirling flows	Limited results in some cases because it assumes isotropic effects for eddy viscosity Requires more computational time Experiences convergence difficulties
Realizable $k - \varepsilon$ model	Same benefits as for RNG but improved performance in more complex flows Performs better in the main flow Accurately predicts spreading rate of both planar and round jets	Limitations such as it produces eddy viscosities in situations when the domain region contains rotating fluid zones and stationary fluid zones
Standard $k - \omega$ model	Better performance for boundary layers under adverse pressure gradients Suitable for external and internal flows in complex flow regimes Reasonably accurate in modeling drying processes	Difficulty in achieving convergence when compared to the $k - \varepsilon$ models
Reynolds Stress Model	Most complex turbulence model to account for many flow regimes Accurately predicts the Reynolds stresses directional effects Provides very accurate solutions for complex flow regimes such as flows in a confined space under adverse pressure	Very high computational cost and memory required Poor convergence is reported in the literature

gradients

2.1.2. Large Eddy Simulation Model

The previous discussion on RANS models indicates that these models provide mean flow quantities with accuracy at a low cost for different flow regimes. The LES model is an alternative approach that uses a set of Navier-Stokes equations that are filtered to calculate large eddies in time-dependent flow simulations [25]. The LES model is suitable for transient simulations because it always solves three-dimensional (3D) time-dependent turbulent flows. In the LES model, turbulent flows are composed of a large-scale motion and a small-scale motion. The computation of large-scale motion is carried out inside the LES model while the small-scale motion is computed by the Sub-Grid-Scale (SGS) model [17, 21]. Again, in this review the authors have not discussed an in-depth theory on LES model as more information can be found on it in many available articles such as those presented by [17, 25, 26]

Some of the main differences between the LES model and RANS model is the way in which small scales are defined in each model. In the LES model, small scales are assumed to be considerably smaller than the size of mesh elements, while in the RANS models, they are assumed to be smaller than the size of the largest eddy scale [21]. Georgiadis et al. [27] conducted a survey on the use of the LES model and the limitations that require attention. The survey comprised 11 questions which were asked of different members of the LES Working Group to gather ideas on topics related to LES. Some of the conclusive ideas indicated that it is possible to couple both the RANS and LES model (hybrid RANS-LES) in solving a complex flow regime. By doing so, the RANS models can be used in areas such as wall boundary layers where turbulence is normally seen to be in equilibrium, and the coupled LES model in areas such as far from boundary wall where non-equilibrium is expected. In a case study conducted by Kuriakose et al. [28] on the applications of CFD in spray drying of food products, they used the hybrid RANS-LES model to accurately model the spray drying process. Research findings on turbulence theory indicate that the LES model can provide high accuracy in solving complex flow regimes, but it requires costly computational time and memory and consequently is expensive to use. It should also be noted that there is no universal turbulence model which is accepted for specific fluid flow problems. Thus, overall the selection of the most suitable turbulence model for any given flow problem will depend on the complexity and the nature of the fluid flow problem such as the flow physics, computational effort, required accuracy, and simulation time.

2.2. Discretization Methods in CFD

Discretization is the process of representing a solution by a reduced set of data in which partial differential equations (PDEs) are changed into discrete algebraic equations [19, 29]. The governing equations discussed in the preceding sections need to be transformed into a suitable form that enable them to be solved numerically. This is because there are no direct methods to solve PDEs or non-liner ordinal differential equations (ODEs). The method employed in the solution process to change them into solvable forms is achieved by using one of the discretization techniques such as finite volume method (FVM), finite difference method (FDM), or the finite element method (FEM) [10].

An FVM was initially applied by McDonald in a two-dimensional simulation of inviscid flows and later the simulation was expanded to three-dimensional [31]. The FVM is carried out by solving the governing equations on discrete polyhedral control volumes. In addition to governing equations, all forms of equations that describe variables of interest such as turbulence, chemical reactions, radiation, and transport of particles are solved for each control

volume [10]. Essentially the computational domain is divided into smaller domain sets or geometrical volumes that define the region of interest where numerical calculations are computed. In FVM the three-dimensional discretization is computed directly in the physical space. This eliminates the need for coordinates transformation as is the case for FDM. It should be noted that with FVM the quality of the solution is largely dependent on the size, the shape, and the position of the control volume in the domain region. One of the disadvantages of FVM is its sensitivity to distorted control volumes which may lead to wrong calculations or prevent the solution to converge especially if the distorted control volumes are in the critical regions [7]. According to Versteeg et al. [30] as cited in Jamaleddine et al. [10], the boundary conditions at the inlet, outlet, and wall of the region domain also affect the quality of the solution.

The FDM was initially applied by Euler around 1768. Blazek [31] states that "FDM is applied directly to the differential form of the governing equations by introducing a Taylor series expansion for the discretization of the flow variable's derivatives". Further research findings from the literature by Blazek [31] show that the advantage of FDM over other discretization methods is its simplicity and ability to achieve high-order estimates which consequently yield solutions of high accuracy. One of the disadvantages of FDM is its limitation on application because the computational domain is divided into a structured grid. However, FVM is known to be flexible and generally applicable to structured or unstructured grids. According to Zuo [45], in structured grids the number of elements surrounding every node in each region's domain is the same for all nodes, while in unstructured grids the number of elements for each node is not the same for all nodes in the domain. Generally, structured grids are used for simple domains in which accuracy is not needed. However, in geometry of complex domains, accuracy at different points of the domain such as near the boundary wall is of importance. Hence, a fine mesh is normally applied at the region where accuracy is required and a coarse mesh in the remaining region. The result is unstructured grids. Figure 2 shows structured grids (left picture) and unstructured grids (right picture [45].
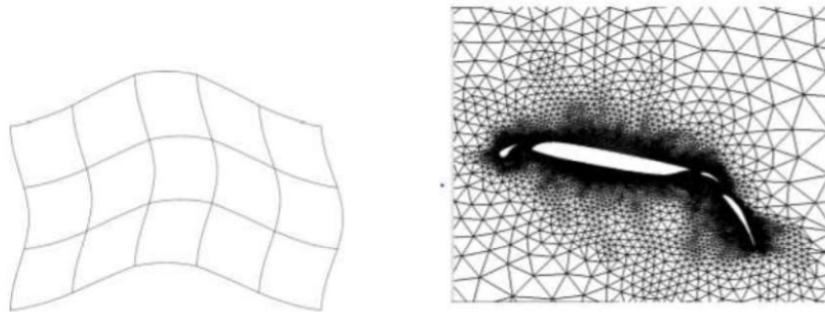
Figure 2. Structured grids and Unstructured grids [45]
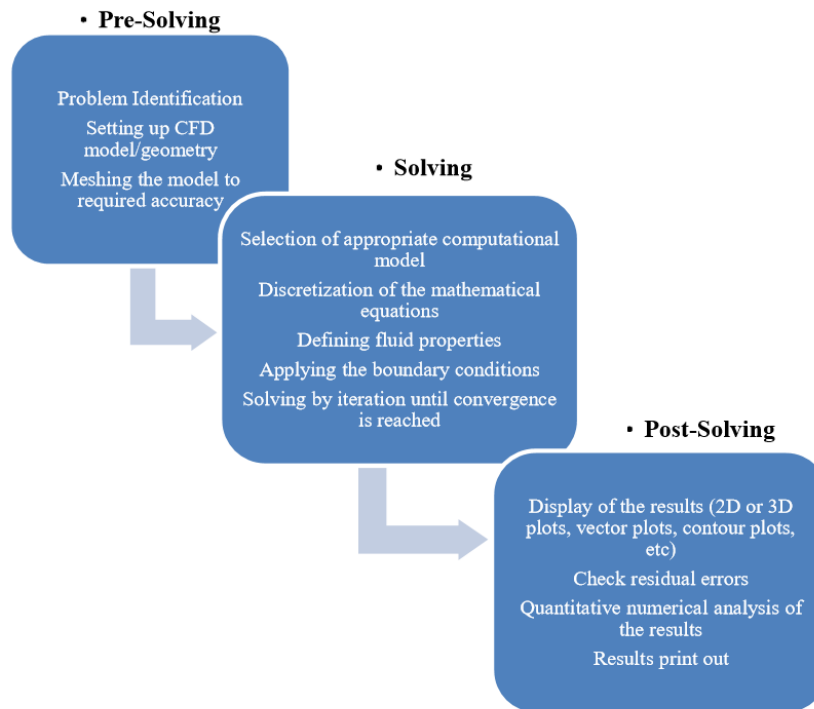
FDM can be applied directly when the governing equations are in the Cartesian coordinate system but not in curvilinear coordinates unless transformed. This method is not widely used for industrial applications because of its simplicity and various limitations on its usage.

The finite element method (FEM) was introduced in 1956 mainly for structural analysis. Researchers started gaining interest in FEM for numerical calculations of various equations and later in the 1990s it gained interest for application in solving Euler and Navier-Stokes equations [31]. According to Jamaleddine et al. [10], this method is "based on a piecewise representation of the solution in a root form of quantified functions". In the FEM, the

computational fluid domain is basically composed of finite elements such as triangular elements (in 2-Dimensions) or tetrahedral elements (in 3-Dimentions). The flow solution is generally computed over nodal points that are stated at the boundaries and/or inside the elements. These nodal points determine the number of degrees of freedom and affect the accuracy of the solution. FEM can be applied to flows that are inside or outside complex geometries and it is also suitable for modeling non-Newtonian fluids. FEM is considered numerically to be similar to FDM, but its accuracy is higher, and it can be used in combination with FVM depending on the flow physics.

3. CFD SOLVING APPROACH

Modelling and simulation of a CFD problem is normally achieved under three distinct procedures; (i) Pre-Solving, (ii) Solving, and (iii) Post-Solving. Under these procedures, several different steps are carried out to properly define and analyse the problem. Figure 3 depicts a summarised schematic view of procedures involved in analysing a CFD problem.

- **Pre-Solving**

Problem Identification

Setting up CFD model/geometry

Meshing the model to required accuracy

- **Solving**

Selection of appropriate computational model

Discretization of the mathematical equations

Defining fluid properties

Applying the boundary conditions

Solving by iteration until convergence is reached

- **Post-Solving**

Display of the results (2D or 3D plots, vector plots, contour plots, etc)

Check residual errors

Quantitative numerical analysis of the results

Results print out

Figure 3. Summarised procedures in CFD analysis

Depending on the CFD problem and the results that are required by the analyser, the simulation procedures might differ from one analyser to another. According to Alexandros et al. [39], modelling of a CFD problem that involves convection drying and diffusion of molecules involves two different modelling approaches: (i) conjugated modelling, and (ii) non-conjugated modelling. Conjugated modelling is carried out when the time-dependent heat and mass transfer equations in the food product and in the drying media are calculated simultaneously. This model requires applying different thermophysical properties to different regions that represent the food product and air stream domains. Non-conjugated modelling is

Johannes P. Angula and Freddie Inambao

carried out when heat and mass transfer equations in food products are solved separately to the flow characteristics. Flow characteristics such as flow velocity, temperature, and moisture level are considered unaffected during the simulation period [39]. Some of the advantages and disadvantages reported in the literature on the application of CFD in food drying processes are indicated in Table 2.

Table 2. Advantages and disadvantages of CFD methods in drying [3, 12, 37, 38]

Advantages	Disadvantages
Provides more detailed output that allows for a better understanding of heat, mass, and momentum transfer in the drying process including radiative effect	In some case there is a need for very small-time steps because of different time scales of fluid flow properties resulting in long computation times
It is easie and cheaper to make design changes in CFD than conducting multiple experiments	Incapability of controlling thermal processes
Ability to reduce scale-up problems of the drying models	Provides insufficient data on physicochemical properties of food products during drying
Graphical results are immediately available after every simulation step	Drying process causes most products to shrink which results in a very difficult mesh generation of the fluid domain
Provides data that can be used to improve final product quality	It requires a better understanding of modeling and fundamental principles of fluid dynamics to reduce the chances of computational errors and wrong results
Provides a meaningful and safe way to simulate unusual conditions such as hot temperature or adverse weather conditions	High computational cost because some CFD codes requires powerful computers and knowledgeable CFD experts
It provides enough information for any region of interest the analyst chooses to examine	
It offers very good reliability in the design and analysis processes in food industries	
When evaluating plant problems, CFD highlights the root cause and not only the effect	
Different conceptual models can be simulated in order to select the optimum design model	

4. PREVIOUS WORKS ON CFD IN SOLAR DRYING

A conference paper was presented by Demissie et al. [1] on the development of an indirect solar food dryer. In their study, ANSYS Fluent 18.1 was used in CFD analysis to predict the transient three-dimensional flow field and temperature profile inside the dryer. Findings from their study indicated a good agreement between the predicted CFD results and experimental results with a temperature difference of 4.3 °C. Simulation results also anticipated a non-uniform temperature and velocity profile within the drying chamber in which drying products on shelves closer to the dryer inlet experience higher temperature and velocity. Due to the non-uniform temperature profile within the drying chamber, they recommended that care should be taken when loading food products in the dryer by positioning the high moisture products at the center of the chamber. In another similar study on the simulation of an indirect solar dryer using ANSYS Fluent software, Romero et al. [35] performed a comparative analysis of the simulation against experimental testing of the temperature distribution. Their results indicated a good correlation between simulated and experimental temperatures at the solar collector outlet but not a good correlation for the temperature inside the dryer cabinet. They explained that the bad correlation is due to the approximation of a constant heat transfer coefficient and they recommended a time-dependent heat transfer coefficient for future related studies.

Noh et al. [40] conducted a recent study on the CFD simulation to analyse the temperature and air flow distribution within a solar dryer. In their simulation analysis, ANSYS Fluent software was used. The simulation study was conducted on two different configurations of the pallets (straight and zig zag arrangement) against three different operating conditions (passive, active, and intermittent active ventilation effects) of the dryer. Their results concluded that the zig zag arrangement with intermittent active operating conditions could optimize the drying system. Their results were part of an indication that CFD simulation could accurately predict flow phenomena of a system before conducting the actual experiment. A similar study on the use of ANSYS Fluent software to accurately predict solar drying parameters was conducted by Román-Roldán et al. [41]. They investigated the turbulence kinetic energy, temperature, and flow velocity inside a solar dryer with an air heating system. Their numerical results were validated against those from experimental testing and the results were in good agreement with each other, with little discrepancy. The results of their study indicated that it was necessary to reduce the volume of the greenhouse dryer which resulted in an improvement of the air velocity and temperature inside. They validated the use of CFD to carry out the virtual design and simulation of the greenhouse solar dryer before the experiment. They stated that the use of CFD software can also allow for further study on the velocity and temperature field inside a greenhouse solar dryer for further improvement in its performance.

In another recent study conducted by Sanghi et al. [2], the drying of maize corns in a natural convection solar cabinet dryer was studied. The ANSYS CFD tool was used in the simulation process to predict the temperature, humidity, and flow velocity in the dryer. The results of their CFD simulation overpredicted the temperature by 8.5% and humidity by 21.4%. One of their objectives was to simulate the performance of the dryer in different weather conditions. The simulation was conducted for fair and overcast weather which was predicted with a 32% moisture removal difference between the two weather cast conditions. It was also reported that stagnation and backflow was occurring at the inlet of the dryer cabinet whereby humidity was seen to be increasing from the ambient humidity (which in fact is not supposed to differ under steady state conditions.) The CFD simulation accurately predicted this phenomenon which was found to be occurring due to the recirculation of air inside the cabinet. The authors emphasized the importance of using CFD in eliminating stagnation and improving natural convection in solar dryers which allow dryer performance to be enhanced. Aukah et al. [43] investigated the drying uniformity within a hybrid solar biomass dryer using ANSYS CFX software. In their simulation model, air flow turbulence within the chamber was modelled with the standard $k - \varepsilon$ turbulence model. They indicated that the simulation was done without considering the presence of trays and the drying product (maize) inside the chamber. Their results showed that the velocity and temperature profile was uniform in most parts of the drying chamber but there were some areas with less flow recirculation.

A case study was conducted on the development of a solar dryer for fruit preservation by Chaignon et al. [46]. In their study, modeling and simulation was conducted using COMSOL Multiphysics software to dry juicy fruits or fruit juices in a special membrane using Solar Assisted Pervaporation (SAP) technology, a technology developed by the Food Technology Department at Lund University. The study was conducted on direct and indirect types of solar dryers whose modeling work were based on research work by Olsson et al. [47]. Olsson et al. [47] modelled the dryer using Maple 2015 software. One of the main objectives in Chaignon et al. [46] study was to investigate the effect of several air flow parameters (such as solar dryer geometry, ambient condition, and solar dryer materials) and optimize the dryer based on identified parameters. In their modeling simulation, several assumptions were made to simplify the problem such as assuming steady state conditions, neglecting radiative heat losses, etc. They concluded that the CFD model simulated in COMSOL Multiphysics

software provided a good approximation to parameters for performance enhancement although discrepancy in results were picked up (maximum resulted error of 30%). Due to many assumptions made and possibly discrepancies in results, Chaignon et al. [46] recommended future works on similar modeling to:

- Increase measurements on the actual dryer for different weather conditions,

- Model the drying process using the method of transport of diluted species with heat transfer to obtain more precise results,

- Model the solar dryer under transient conditions,

- Study fluid behavior inside the dryer to improve design and performance of the solar dryer,

- Possibly measure the convective heat transfer coefficient, and

- Consider the sun as an external source of energy in the simulation process instead of considering it as a boundary heat source.

Another important drying technique is drying products in a Fluidized Bed Dryer (FBD). This discussion is beyond the scope of this study except for presentation of a case study conducted by Rosli et al. [9] on the simulation of FBD. In their study they validated the use of ANSYS Fluent software as a CFD tool to simulate the drying phenomena of sago waste. They investigated the effects of air velocity and temperature at the inlet of dryer, and the effect of particle size on attaining a moisture ratio of 0.25 using the multiphase Eulerian model. The authors recommended a detailed CFD analysis to be conducted on sago waste incorporating evaporation, mass and moisture transfer of sago moisture in similar future studies. In another case study conducted by Sapto et al. [32], a CFD tool was used to simulate and optimize the tray dryer design. In their simulation, they analyzed the air flow distribution, flow turbulence, temperature distribution, and pressure which yielded optimum parameters for the tray dryer design.

SolidWorks Flow Simulation (SWFS) software was used by Odewole et al. [33] to conduct a CFD analysis of a solar dryer. They investigated the effect of air flow distribution, flow velocity, and pressure field on transient moisture within the dryer. Some of the simulation parameters such as air temperature were accurately predicted, resulting in small deviations of about 0.02%. Their simulation of drying process for the green bell pepper was conducted using the standard turbulence model under steady state conditions. They the use of CFD application to dryer design as it can be used effectively to solve uneven drying problems in products under various conditions. In another study conducted by Gomez et al. [34] used STAR-CCM+ v12.02 software to model and simulate a convective dryer. Their objective was to investigate the air flow patterns that lead to non-uniformity within the dryer. The results of the air distribution showed that recirculation is the main culprit resulting in uneven drying inside the chamber due to low air velocity at two points. They recommended the introduction of air distributors or dampers to combat the issue of air recirculation inside the convective drying chamber.

Ambesange et al. [7] investigated flow through a solar dryer duct using FLUENT software. Their main objective was to conduct a CFD analysis in order to enhance flow-conditioning devices to accurately guide the air flow through solar dryer ducts. The focus was on analyzing the fluid flow and heat transfer characteristics within the dryer. Three tests conducted on the duct were (1) flow through the duct without trays, (2) flow through the duct with trays, and (3) flow through the duct with tray holes. According to their CFD results, test number 3 yielded satisfactory results with a duct having artificial roughness to enhance the Nusselt number and thereby increase heat transfer through induced turbulence. However, they noticed that an increase in artificial roughness also increased the friction factor which resulted

in heat losses. In another similar case study by Yunus et al. [36], a combination of GAMBIT and FLUENT simulation software was used to analyze a solar dryer with a biomass burner as a backup heater under different operational modes. Results from their simulation were validated with on-site experimental results which indicated good agreement with each other although discrepancy in temperature was spotted due to poor design. Their objective was to improve the hybrid solar dryer using CFD simulation and resulted in the option of biomass backup heating as opposed to other operational modes.

Ahumuza et al. [42] conducted a study on the development of a pineapple solar drying system which was optimized using OpenFOAM CFD software. The final design of their optimized solar cooker-dryer system was derived from the performance assessment of four existing solar dryers. Their results indicated that an incorporation of a biomass cooker would improve the drying efficiency of the system and reduce spoilage under forced convection. They simulated the air flow within the entire drying system and analysed the predicted temperature field and air velocity. Simulation results predicted that with the addition of a cooker the temperature inside the dryer would be raised and was expected to be in the range of 60 °C to 65 °C. This study indicated that OpenFOAM permitted viable ways to accurately simulate drying of food products.

5. CONCLUSION

A study was carried out on the applications of CFD tools in modeling and simulating product drying using solar energy. The principles of CFD in solving fluid flow properties have been discussed in this paper. In modeling the drying characteristics of food products, CFD is able to accurately predict the heat transfer, moisture evaporation, radiative effect, and flow velocity within solar dryers prior to experiment. It was discussed that there are many commercially available software packages that employ CFD codes which researchers can select from and use in their analysis. Accuracy of CFD in predicting fluid flow properties is concluded to be dependent on the model setup and the model equations applied for simulation. Many researchers have conducted studies on the application of CFD in food processing and some have used it in their solar dryer performance assessment. With an increase in technology advancement and research, the use of CFD in solar drying systems is emphasized. Although some researchers were able to investigate fluid flow behavior inside the drying chambers, there are still possibilities for further improvement. Aa number of studies were found that reported on indirect and hybrid solar dryers but few were found on mixed-mode solar dryers. This indicates that there is a need for further research on the use of CFD related to mixed-mode solar dryers. In general, computational fluid dynamics is an exceptional tool in modeling fluid properties, finding wide-ranging application from aerospace to solar drying of agricultural food products. CFD provides tools to improve and optimize drying systems.

REFERENCES

[1]   Demissie, P., Hayelom, M., Kassaye, A., Hailesilassie, A., Gebrehiwot, M. and Vanierschot, M. Design, Development and CFD Modeling of Indirect Solar Food Dryer. Proceedings of the 10th International Conference on Applied Energy, Hong Kong. *Energy Procedia*, 158, 2019, pp. 1128-1134. DOI: 10.1016/j.egypro.2019.01.278.

[2]   Sanghi, A., Kingsly, R. P. A. and Maier, D. CFD Simulation of Corn Drying in a Natural Convection Solar Dryer. *Drying Technology,* 36(7), 2018, pp. 859-870. DOI: 10.1080/07373937.2017.1359622.

[3]   Malekjani, N. and Jafari, S.M. Simulation of food drying processes by Computational Fluid Dynamics (CFD); recent advances and approaches. *Trends in Food Science & Technology,* 78, 2018. DOI: 10.1016/j.tifs.2018.06.006.

[4]   Kumar, M., Sansaniwal, S. K. and Khatak, P. Progress in Solar Dryers for Drying Various Commodities. *Renewable and Sustainable Energy Reviews,* 55, 2016, pp. 346-360. DOI: 10.1016/j.rser.2015.10.158.

[5]   Hossai, M. A., Amer, B. M. A. and Gottschalk, K. Hybrid Solar Dryer for Quality Dried Tomato. *Drying Technology,* 26 (12), 2008, pp. 1591-1601. DOI: 10.1080/07373930802467466.

[6]   Janjai, S., Lamlert, N., Intawee, P., Mahayothee, B., Bala, B. K., Nagle, M. and Muller, J. Experimental and Simulated performance of a PV-Ventilated Solar Greenhouse Dryer for Drying of Peeled Longan and Banana. *Solar Energy,* 83(9), 2009, pp. 1550-1565. DOI: 10.1016/j.solener.2009.05.003.

[7]   Ambesange, A. I. and Kusekar, S. K. Analysis of Flow Through Solar Dryer DUCT using CFD. *International Journal of Engineering Development and Research,* 5(1), 2017.

[8]   Norton, T. and Sun, D. W. CFD: An Innovative and Effective Design Tool for the Food Industry. In: Aguilera J., Simpson R., Welti-Chanes J., Bermudez-Aguirre D., Barbosa-Canovas G. (eds) Food Engineering Interfaces. Food Engineering Series. New York, NY: Springer, 2010, pp. 55-68. doi.org/10.1007/978-1-4419-7475-4_3.

[9]   Rosli, I. M., Nasir, A. M. A., Takriff, S. M. and Chem, L. P. Simulation of a Fluidized Bed Dryer for the Drying of Sago Waste. *Energies*, 11(9), 2018, pp. 2383. DOI: 10.3390/en11092383.

[10]   Jamaleddine, T. and Ray, B. M. Application of Computational Fluid Dynamics for Simulation of Drying Processes: A Review. *Drying Technology,* 28, 2010, pp. 120-154. DOI: 10.1080/07373930903517458.

[11]   Sun, D. and Xia, B. Applications of Computational Fluid Dynamics (CFD) in the food industry: A Review. *Computers and Electronics in Agriculture.* 34(1-3), 2002, pp. 5-24. DOI: 10.1016/S0168-1699(01)00177-6.

[12]   Pragati, K. and Sharma, H.K. Concept of Computational Fluid Dynamics (CFD) and its Applications in Food Processing Equipment Design. *Journal of Food Processing and Technology.* 2011. DOI: 10.4172/2157-7110.1000138.

[13]   Moses, J. A., Norton, T. Alagusundaram, K. and Tiwari, B. K. Novel Drying Techniques for the Food Industry. *Food Engineering Reviews,* 6(3), 2014, pp. 43-55. https://doi.org/10.1007/s12393-014-9078-7.

[14]   Albaali, G. and Farid, M. M. Fundamentals of Computational Fluid Dynamics. In: Sterilization of Food in Retort Pouches. New Your, NY: Springer, 2006, pp. 33-44. DOI: 10.1007/0-387-31129-7_4.

[15]   Fox, W.R., Pritchard, J. P. and Macdonald, T. A. Introduction to Fluid Mechanics. 7th Edition. New Delhi, India: John Wiley & Sons, 2010, pp. 161-205.

[16]   COMSOL INC. Navier-Stokes Equations. In: Multiphysics CYCLOPEDIA., 2017. https://www.comsol.com/multiphysics/navier-stokes-equations.

[17]   Norton, J. T. and Sun, D. Computational Fluid Dynamics (CFD) – an Effective and Efficient Design and Analysis Tool for the Food Industry: A Review. *Trends in Food Science & Technology,* 17(11), 2006, pp. 600-620. DOI: 10.1016/j.tifs.2006.05.004.

[18]   Defraeye, T. Advanced Computational Modelling for Drying Processes – A Review. *Applied Energy,* 131, pp. 323-344. https://doi.org/10.1016/j.apenergy.2014.06.027.

47

[19]   Guerrero, J. Introduction to Computational Fluid Dynamics: Governing Equations, Turbulence Modelling Introduction and Finite Volume Discretization Basics. 2015. DOI: 10.13140/RG.2.1.1396.4644.

[20]   Launder, B. and Spalding, D. B. The Numerical Computation of Turbulent Flow Computer Methods. *Computer Methods in Applied Mechanics and Engineering,* 3(2), 1974, pp. 269-289. DOI: 10.1016/0045-7825(74)90029-2.

[21]   Sadrehaghighi, I. Turbulence Modeling – A Review. CFD Open Series, Patch 1.85.9, 2019. DOI: 10.13140/RG.2.2.35857.33129/2.

[22]   Wilcox, D. C. Formulation of the k-ω Turbulence Model Revisited. *AIAA Journal,* 46(11), 2008, pp. 2823-2838. doi: 10.2514/1.36541.

[23]   Bellakhal, G., Chahed, J. and Masbernat, L. K-Omega Turbulence Model for Buddy Flows. Proceedings of the 5th International Conference on Multiphase Flow, Yokohama, Japan. 2004.

[24]   Norton, T., Tiwari, B. and Sun, D. Computational Fluid Dynamics in the Design and Analysis of Thermal Processes: A Review of Recent Advances. *Critical Reviews in Food Science and Nutrition,* 53(3), 2012, pp. 251-275. https://doi.org/10.1080/10408398.2010.518256.

[25]   Pope, S. Turbulent Flows. Cambridge: Cambridge University Press. 2000.

[26]   Sagaut, P. Large Eddy Simulation for Incompressible Flow. 3rd Edition. New York: Springer, 2006, pp. 45-85.

[27]   Georgiadis, J.N., Rizzetta, P.D. and Fureby, C. Large-Eddy Simulation: Current Capabilities, Recommended Practices, and Future Research. *AIAA Journal*, 48(8), 2010, pp. 1772-1784. DOI: 10.2514/1.J050232.

[28]   Kuriakose, R. and Anandharamakrishnan, C. Computational Fluid Dynamics (CFD) Applications in Spray Drying of Food Products. *Trends in Food Science & Technology,* 21(8), 2010, pp. 383-398. DOI: 10.1016/j.tifs.2010.04.009.

[29]   Van Leer, B. and Powell, G.K. Introduction to Computational Fluid Dynamics. In: Encyclopedia of Aerospace Engineering. New York, NY: John Wiley & Sons, 2010. DOI: 10.1002/9780470686652.eae048.

[30]   Versteeg, H. K. and Malalasekera, W. An Introduction to Computational Fluid Dynamics: The Finite Volume Method. Addison-Wesley, New York, NY: Longman, 1995.

[31]   Blazek, J. Computational Fluid Dynamics: Principles and Applications. 1st Edition. Oxford: Elsevier Science, 2001.

[32]   Sapto, W. W., Wong, C. Y., Kamarul, A. M. and Nurul Hidayah, A. CFD Simulation for Tray Dryer Optimization. *Journal of Advanced Manufacturing Technology,* 5(2), 2011, pp. 1-10. http://eprints.utem.edu.my/id/eprint/4650.

[33]   Odewole, M. M., Sunmonu, O. M., Oyeniyi, K. S. and Adesoye, A. O. Computational Fluid Dynamics (CFD) Simulation of Hot Air Flow Pattern in Cabinet Drying of Osmo-Pretreated Green Bell Pepper. *Nigerian Journal of Technological Research,* 12(1), 2017, pp. 36-45. DOI: 10.4314/njtr.v12i1.7.

[34]   Gomez, M. A. D.., Velasco, C. A. G., Ratkovich, N. and Daza, G. C. J. Numerical Analysis of a Convective Drying Chamber from Drying Air Velocity and Temperature Perspective. Proceedings of the 3rd World Congress on Momentum, Heat and Mass Transfer. Budapest, Hungary. 2018. DOI: 10.11159/icmfht18.134.

[35]   Romero, V. M., Cerezo, E., Garcia, M. I. and Sanchez, M. H. Simulation and Validation of Vanilla Drying Process in an indirect Solar Dryer Prototype Using CFD Fluent Program. *Energy Procedia,* 57, 2014, pp. 1651-1658. DOI: 10.1016/j.egypro.2014.10.156.

[36] Yunus, M.Y. and Al-Kayiem, H.H. Simulation of Hybrid Solar. Proceedings of the 4th International Conference on Energy and Environment. 16(1), 2013. DOI: 10.1088/1755-1315/16/1/012143.

[37] Bin, X. and Sun, E.D. Applications of Computational Fluid Dynamics (CFD) in the Food Industry: A Review. *Computers and Electronics in Agriculture,* 34(1), 2002, pp. 5-24. DOI: 10.1016/S0168-1699(01)00177-6.

[38] Bakker, A., Haidari, A. and Oshinowo, M.L. Realize Greater Benefits from CFD. *Chemical Engineering Progress.* 97(3), 2001, pp. 45-53.

[39] Alexandros, V., Tzempelikos, D., Mitrokos, D. and Filios, A. CFD Modeling of Convective Drying of Cylindrical Fruit Slices. In: Sun, D., ed., Computational Fluid Dynamics in Food Processing, 2nd Ed. Boca Raton, FL: CRC Press, 2018, pp. 339-364.

[40] Noh, M. A., Sohif, M., Rusian, H. M. and Baru, A.P. CFD Simulation of Temperature and Air Flow Distribution Inside Industrial Scale Solar Dryer. *Journal of Advanced Research in Fluid Mechanics and Thermal Sciences,* 45(1), 2018, pp. 156-164.

[41] Román-Roldán, N., López-Ortiz, A., Ituna-Yudonago, J., García-Valladares, O. and Pilatowsky-Figueroa, I. Computational Fluid Dynamics Analysis of Heat Transfer in a Greenhouse Solar Dryer "Chapel-Type" Coupled to an Air Solar Heating System. *Energy Science & Engineering,* 2019, pp. 1-17. DOI: 10.1002/ese3.333.

[42] Ahumuza, A., Zziwa, A., Kambugu, R., Komakech, A.J. and Kiggundu, N. Design and Simulation of an Integrated Solar Cooker-Dryer System. *RUFORUM Working Document Series (ISSN 1607-9345).* 14(2), 2016, PP. 1075-1084. http://repository.ruforum.org.

[43] Aukah, J., Muvengei, M., Ndiritu, H. and Onyango, C. Simulation of Drying Uniformity inside Hybrid Solar Biomass Dryer using ANSYS CFX. Proceedings of the Sustainable Research and Innovation Conference. 2015, pp. 336-344. ISSN: 2079-6226. http://sri.jkuat.ac.ke/ojs/index.php/proceedings/article/view/315.

[44] Chauhan, S.P., Kumar, A. and Tekasakul, P. Applications of Software in Solar Drying Systems: A Review. *Renewable and Sustainable Energy Reviews,* 51, 2015, pp. 1326-1337. https://doi.org/10.1016/j.rser.2015.07.025.

[45] Zuo, W. Introduction of Computational Fluid Dynamics. FAU Erlangen-Nürnberg, JA, St. Petersburg: JASS, 2005.

[46] Chaignon, J. and Henrik, D. Modelling of a Solar Dryer for Fruit Preservation in Developing Countries. Master's thesis. Lund University, Lund, Sweden, 2017, pp. 1-11. DOI: 10.18086/swc.2017.30.01.

[47] Olsson, J. and Henrik, D. Modelling of a Solar Dryer for Food Preservation in Developing Countries. 2016, pp. 1-48. https://lup.lub.lu.se/student-papers/search/publication/8890943.

49

CHAPTER 4

4. METHODOLOGY

4.1 Introduction

The ongoing advancement in computational modeling has contributed significantly to technology improvement and the development of robust systems. This includes the use of CFD codes in designing and optimizing solar drying systems. As explained in previous chapters, the sets of governing equations describing the fluid flow and drying characteristics in the modeled solar dryer are based on Navier-Stokes equations and conservation of energy. These equations are solved numerically by iteration on discretized domains of the fluid region of interest.

This chapter presents the methodological approach applied to the conducted research works. As briefly identified in Chapter 1, the research study is composed of works conducted on CFD and those of the experiments. In this chapter, the methodology has two parts. Part 1 of the methodology describes the approach to CFD application regarding the solar dryer. This covers the modeling and simulation of the solar dryer to predict its drying capacity using maize ear as the grains in drying. Part 2 covers the experimental methods to validate the predicted results of Part 1 and optimize the dryer system accordingly. Both the CFD analysis and experiments were conducted during the month of October.

4.2 Research Site

The research was conducted at the University of KwaZulu-Natal, Howard college campus in Durban located at 29.9° South, 30.98° East, and at an elevation of 151.3 meters above sea level. The city has a hot humid subtropical climate with temperatures ranging from as low as 9.4 °C in winter to as high as 30.8 °C in summer. According to metrological data from the Virginia weather station in Durban, the relative humidity of this coastal town can be as high as 95 %. Further research also indicates that the daily average sunlight hours of Durban is around 6 hours and 24 minutes per year. While the annual average values of direct normal irradiance (DNI) and global horizontal irradiance (GHI) are 1574 kWh/m^2 and 1638 kWh/m^2, respectively [1].

4.3 Part 1: Modeling and Simulation

This part describes the use of CFD in solar drying. A model of the actual solar dryer was created and simulated to predict the drying of maize ears. The summarized flow chart for the methods applied in this part are shown in Figure 4-1. As indicated, the flow chart comprises three sections: Pre-Solving, Solving, and Post-Solving. It should be noted that only the first two sections (Pre-Solving and Solving) are part of the methodology, and discussed in this chapter.
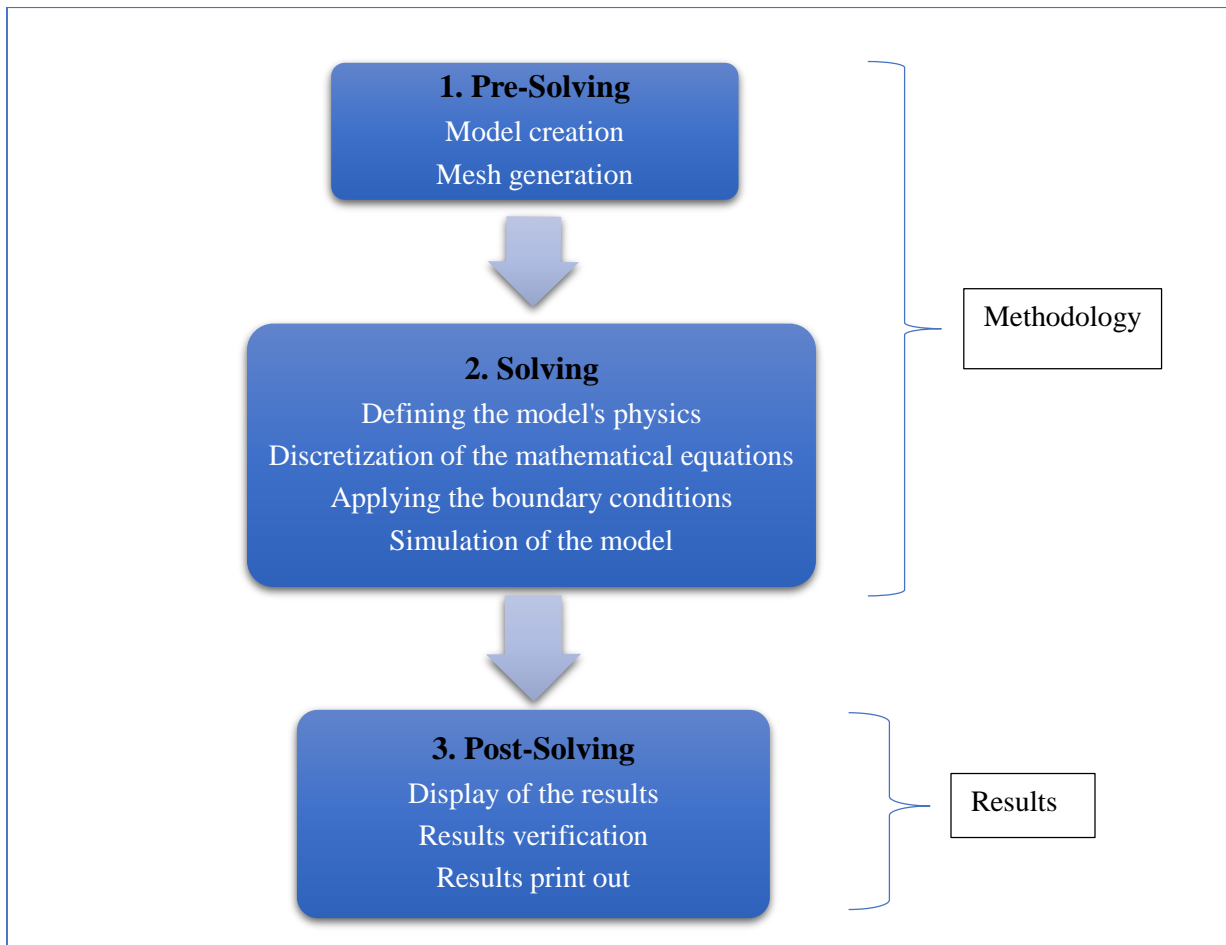
Figure 4-1 Summarized flow chart of modeling and simulation.

4.3.1   Model Creation

As previously explained regarding CFD analysis, the accuracy of the results is dependent on many factors including the software used in modeling and simulation. Despite the type of software, the user knowledge in using the software is also a contributing factor. The choice of which CAD software to use in creating the model geometry was between Autodesk Inventor and SolidWorks software. Autodesk Inventor and

SolidWorks are both 3D modeling software with exceptional reputations and widely used in many engineering applications including modeling and designs. One of the advantages of 3D CAD is the flexibility to allow the user to easily make changes on the model geometry before and after simulation.

Both of these software codes were freely available for usage in the Department of Mechanical Engineering, hence there was no need of purchasing a copy. The researcher was better acquainted with and confident in using SolidWorks software to design and create 3D models. Hence, in this study, SolidWorks 2018 software was used to create the model of the actual mixed-mode solar grain dryer to be used in the experiment. Figure 4-2 shows the overall model of the solar dryer that was created for the drying simulation purpose.
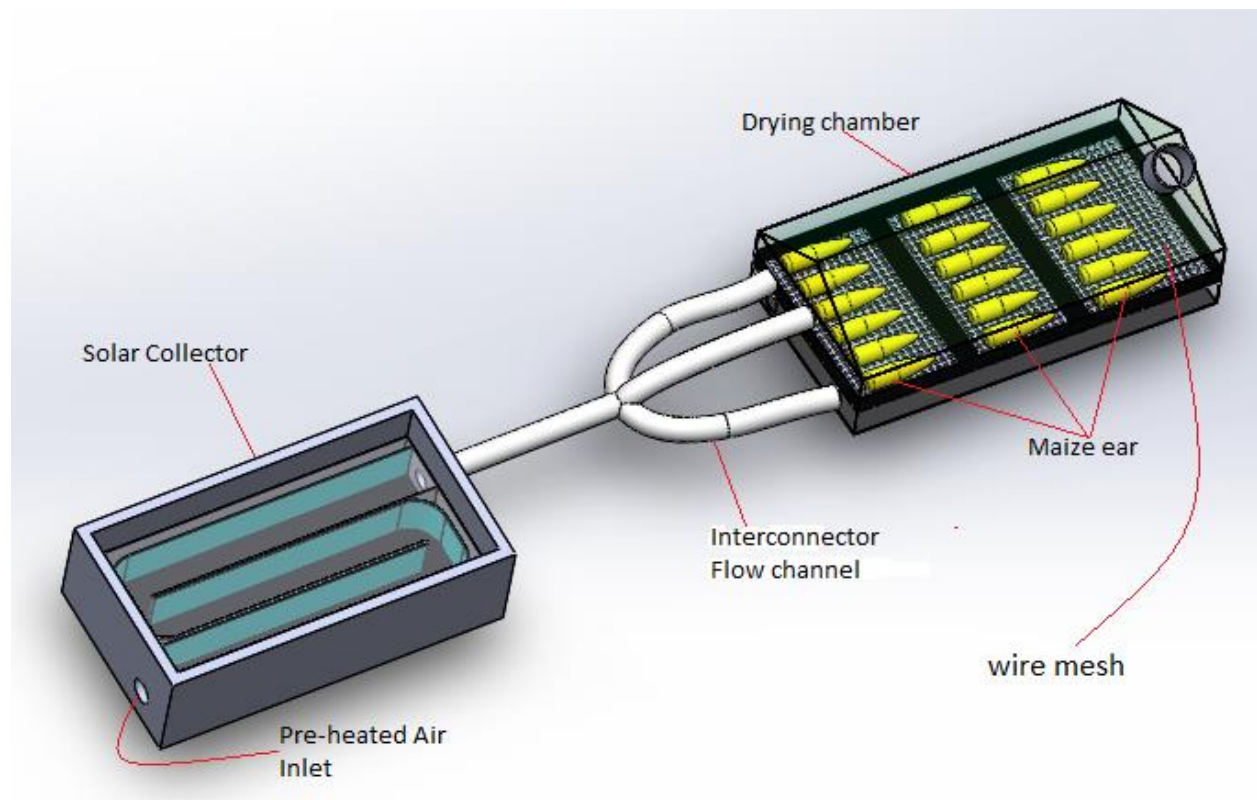
Figure 4-2 CFD Model of the mixed-mode solar dryer system.

The model was created using the measured dimensions of the existing solar dryer that was used for experimental validation. As seen in Figure 4-2, a model representation of maize ears was included in the drying chamber to mimic the actual phenomena during drying. Different arrangements of the maize ears inside the dryer will be discussed in later sections to study the fluid behavior inside the chamber. One of the important factors in conducting CFD analysis is to consider the available computational power yet retain acceptable and quality results. Hence, during model creation it was necessary to focus on the key

components of the dryer system that have vital roles during drying and create a simplified system. A simplified yet accurate system allowed mesh generation and discretization to be carried out within a short period of time without overloading the computer. During this study, all works pertaining to CFD analysis were carried out under the available computational power consisting of a:

- Processor: Intel® Core™ i7-2600 CPU,
- Processor speed: 3.40 GHz and 3.40 GHz,
- RAM: 8.00 GB, and
- Hard Drive rotational speed: 7200 RPM.

4.3.2 Simulation Software Selection

Selection of the right 3D simulation software to appropriately predict the actual drying phenomena of the solar dryer is crucial in this study. The simulation also needed to be carried out with a convenient and yet accurate software. Research findings indicated that there are many robust and reputable CFD software codes that are capable of modeling and simulating heat and mass transfer problems such as ANSYS Fluent, Comsol Multiphysics, Star CCM+, OpenFOAM, PHOENICS, CFD 2000, etc. [2, 3, 4]. Apart from these CFD codes, further research findings indicated that software such as SolidWorks and Autodesk have flow simulation packages within their programs that the user can use to accurately simulate flows.

In this study, it was necessary to keep the expenditure low yet deliver good quality research findings. It was therefore necessary to make use of the materials that were locally and freely available within the School of Engineering. The selection of the right simulation software was between four software codes that were freely available for students within the Department of Mechanical Engineering. The choice was between:

- ANSYS Fluent,
- Start CCM+,
- SolidWorks Flow Simulation, or
- Autodesk Flow Simulation.

Both ANSYS Fluent and Star CCM+ have proven to be very good CFD codes with high accuracy in simulating various flow regimes including those of complex geometries. However, the researcher was not familiar with using Star CCM+, hence, the choice was reduced to three simulation software codes (ANYSYS Fluent, SolidWorks and Autodesk Flow Simulation packages) that the researcher was familiar with. Both SolidWorks and Autodesk Flow Simulation packages have proven to be very good in accurately simulating heat transfer problems, but have limited capacity on flows involving mass transfer. This resulted

in selection of ANSYS Fluent to simulate the drying phenomena of the solar dryer in this study. The use of ANSYS Fluent in simulating solar dryers is also emphasized in various studies such as those conducted by Demissie et al. [5], Romero et al. [6], and Román-Roldán et al. [7], among others.

4.3.3 Mesh Generation

The process of mesh generation is the next step to follow after creating a model. This process is crucial in achieving good quality results, hence a well-defined mesh is necessary. Considering the available computational power, it was necessary to divide the CFD analysis of the solar dryer system into three individual sub-systems (1) Preheater-to-solar collector, (2) Interconnector flow channel, and (3) Drying chamber. In this way, each sub-system was analyzed independently using the outputs of the preceding sub-system as its inputs.

4.3.3.1 Preheater-to-Solar Collector System

The main reason a heater was introduced in this study was to pre-heat the ambient air to a set temperature which in turn raises its temperature and lowers its humidity before entering the solar collector. For the purpose of CFD analysis, the preheater is represented by a pre-defined input temperature required at the solar collector inlet. Hence, mesh generation was only carried out on the solar collector.

The general approach to CFD analysis involves concentrating on the regions of interest. Thus, in creating the mesh of the solar collector it was necessary to focus on the region of the solar collector flow channel which was composed of the air passage and the drying air volume. The air passage is responsible for capturing the solar energy and the air volume is responsible of conveying this energy to the drying chamber. Because the model was created in the SolidWorks platform, it had to be imported into ANSYS Fluent as a body. Figure 4-3 shows the flow channel before and after the mesh had been generated.
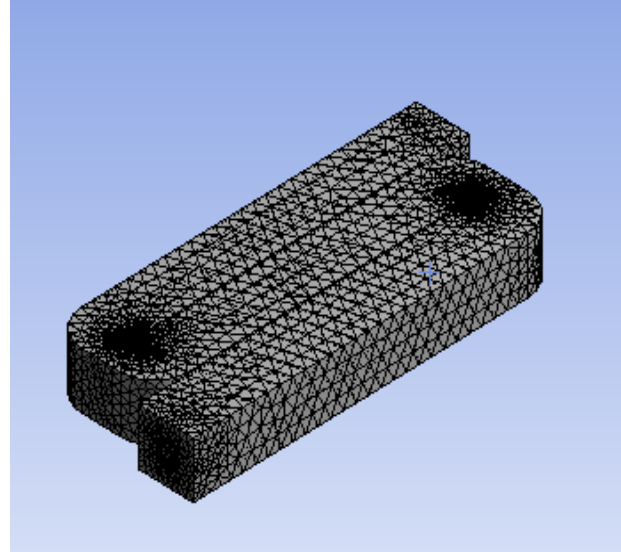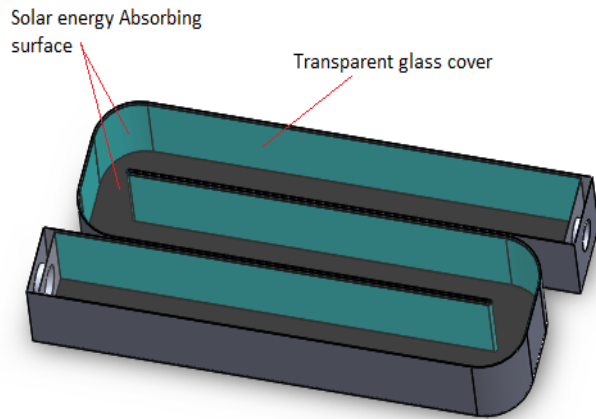
Figure 4-3 Unmeshed (left) and 3D Mesh of the solar collector flow channel (right) in ANSYS Fluent.

The main component of the solar collector was the channel where the drying air flows through and gains heat. As shown in Figure 4-3 (left), the channel was modeled with the actual dimensions of the existing solar dryer. For better visualization the inner surface walls in the model are shown with a green color but in reality, both the inner surface walls and base were painted with a black color to improve absorptivity. Because the flow channel body consisted of two geometries, a mesh was created for the air passage geometry and another mesh for the air volume geometry. The ANSYS software version 19.2 used in this study was for academic purposes and its meshing capability was limited to 512K cells/nodes [8]. Considering the software limitation and computational power, various meshing trials resulted in the final choice of applying the following mesh criteria:

- 8 mm mesh element size for the whole body except at contact regions where the element size was reduced to 3 mm to improve accuracy. Contact regions are where the air volume particles interact with the solid walls of the absorber during convection heat transfer.
- For the air volume geometry, a minimum element size of 0.3 mm was allowed to capture curvature flow. This was essential because the flow channel consisted of sharp corners.
- Tetrahedron mesh type for the whole body.
- Five inflation layers were applied on the walls and base of the air volume geometry. This was necessary in order to improve the quality of the results since these were the areas where convection heat transfer would take place between the solar energy absorbing surface and the drying air.

Figure 4-4 below shows a closer view of the inflation layers and the tetrahedron mesh generated for the drying air volume as extracted along the air passage of the solar collector.

55
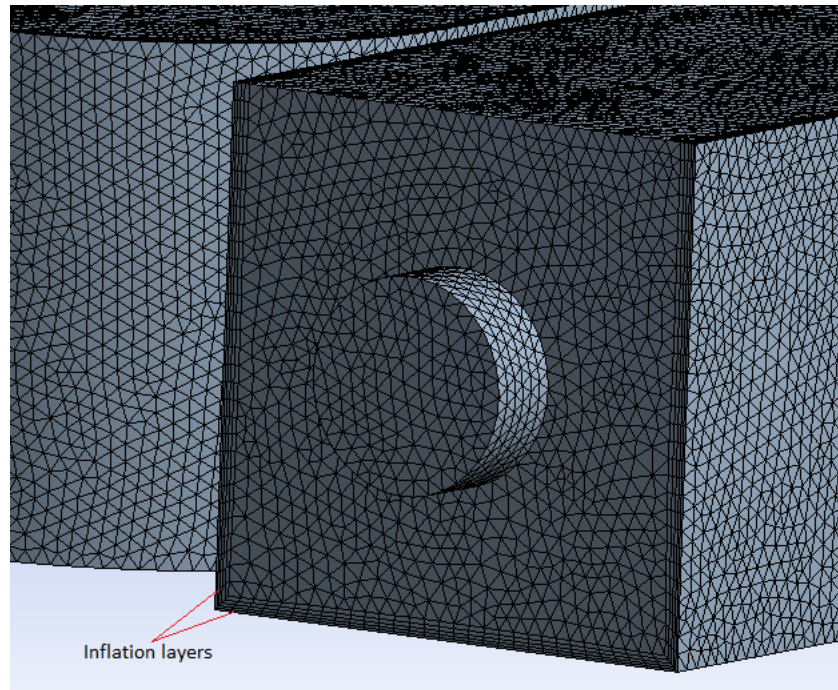
Figure 4-4 Closer view of the mesh and inflation layers for the air volume in ANSYS Fluent.

4.3.3.2 Interconnector Flow Channel

The actual interconnector flow channel on the existing solar dryer was made up of four insulated flexible ducts joined together with a 4-way pipe fitting. In this case, the body that was created for meshing was the air volume occupying the flow channel. It was created in SolidWorks and imported into ANSYS Fluent. Figure 4-5 shows the meshed interconnector flow channel as carried out for CFD analysis. To maintain consistency, the mesh criteria applied to this body were kept the same as those of the air volume from the solar collector.
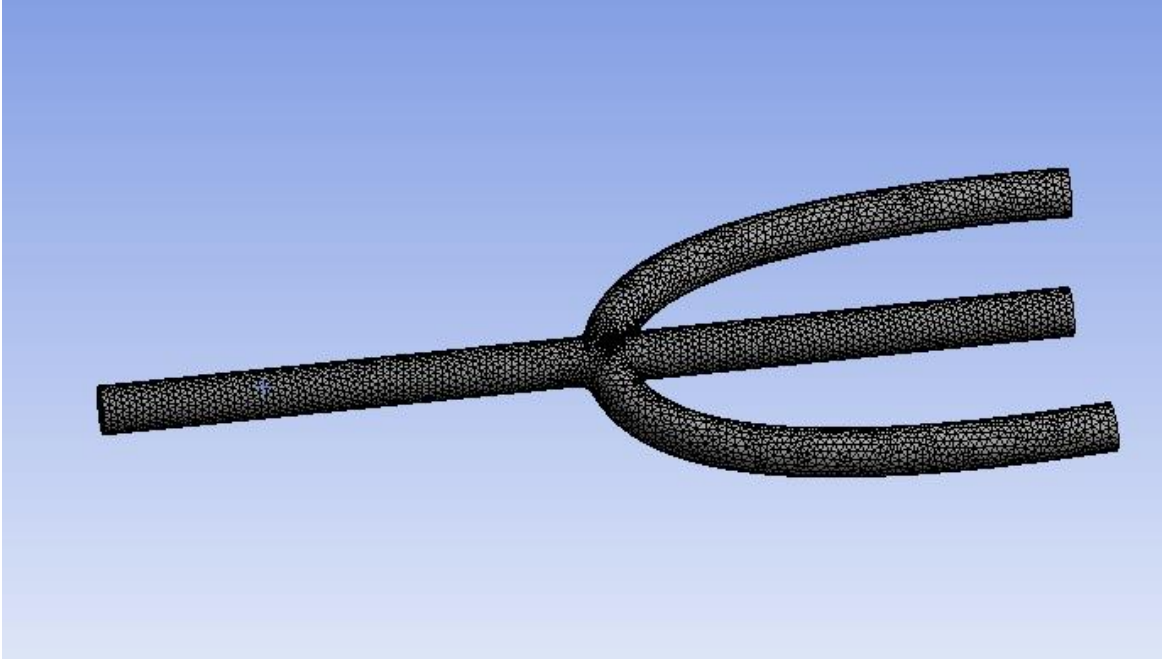
Figure 4-5 3D Mesh of the interconnector flow channel.

4.3.3.3 Drying Chamber

The drying chamber is the most critical part of the dryer system and careful consideration is needed during meshing to ensure the real drying scenario is predicted accurately. To perform CFD analysis on the drying chamber, a fluid volume occupying the internal space of the chamber needed to be created for meshing purposes. The fluid volume was created in SolidWorks by extracting it from the solid body of the drying chamber using a Boolean operation method. This volume is of central interest since it is responsible for moisture evaporation from the maize ear surfaces during the drying period. The drying chamber model including the maize ears indicated with a light green color while the fluid volume is indicated with a brown color for visualization purposes. Figure 4-6 shows the structural body model of the drying chamber with its cross-sectional view indicating the extracted volume.
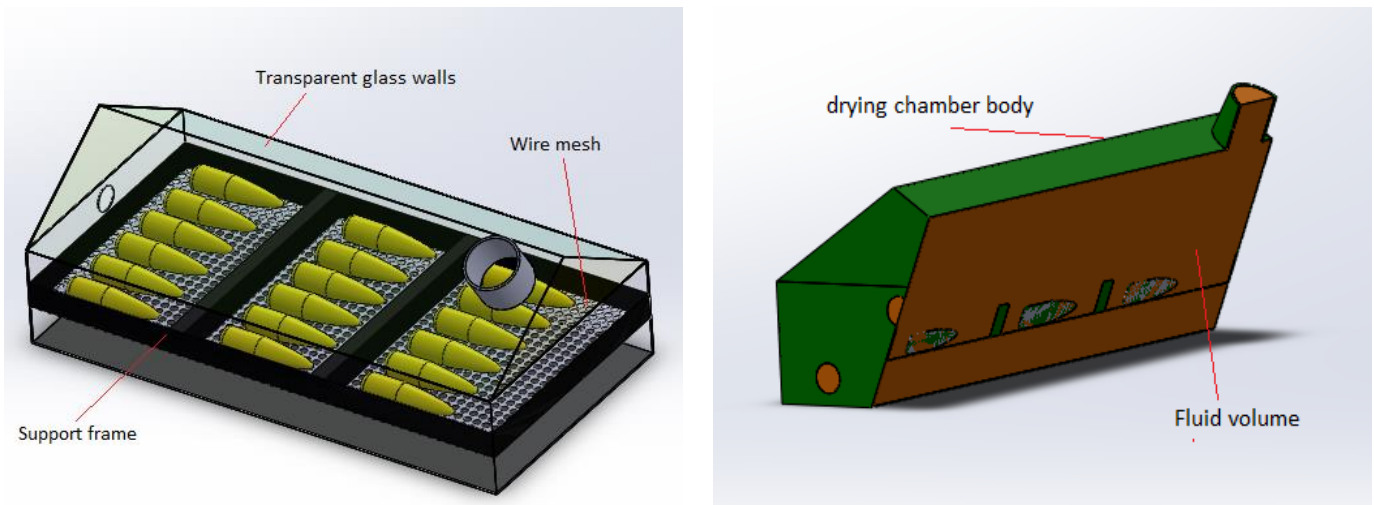
Figure 4-6 Drying chamber model (left) and cross-sectional view of the chamber (right) created in SolidWorks.

In optimizing the mesh quality for the drying chamber, one has to consider the complexity of the fluid domain and the computational power available for numerical analysis during solving. There is a combination of heat and mass transfer inside the drying chamber, particularly around maize ears where evaporation of moisture is anticipated to take place. This necessitated the need for refining the mesh in the regions close to the maize ears. Various mesh trials with different criteria were evaluated to identify the most suitable setup for the CFD analysis. In setting up the mesh, the criteria selected for further CFD analysis was as follows:

- 8 mm mesh element size for the whole drying chamber body except at contact regions where the element size was further reduced to 2 mm to improve accuracy and capture the heat and mass transfer during evaporation.

- A local minimum size of 0. 6 mm was allowed so as to capture curvature flow. It can be seen that in this case the element sizes around the curvatures were bigger than those of the meshes in the previous section. This is because in the drying chamber there were many curvatures which might have increased the computational cost if the local minimum sizes were lowered significantly.

- Again, in this scenario, tetrahedron meshes were still used, primarily to promote consistency during numerical calculations but also to lower computational cost. Research indicated that it is easier to achieve a good mesh quality and compatible with meshing complex geometry using a tetrahedron mesh [8].

- The element order was set to quadratic instead of linear order. This is because in quadratic element order the mesh is created with middle nodes to increase the degree of freedom and improve results accuracy.
- The quality of the mesh was kept at medium level with a more refined mesh closer to the wire mesh as shown in Figure 4-7 and Figure 4-8. The wire mesh holds the maize ears and contains tiny holes that allow drying air to circulate around the maize ears in order to promote evaporation of moisture.
- The number of inflation layers in regions of potential interest such as around the maize ears, flow inlets and outlet were increased to seven layers to improve accuracy.

The tetrahedron mesh generated from the fluid volume body which was imported in ANSYS Fluent is shown in Figure 4-7 and Figure 4-8.
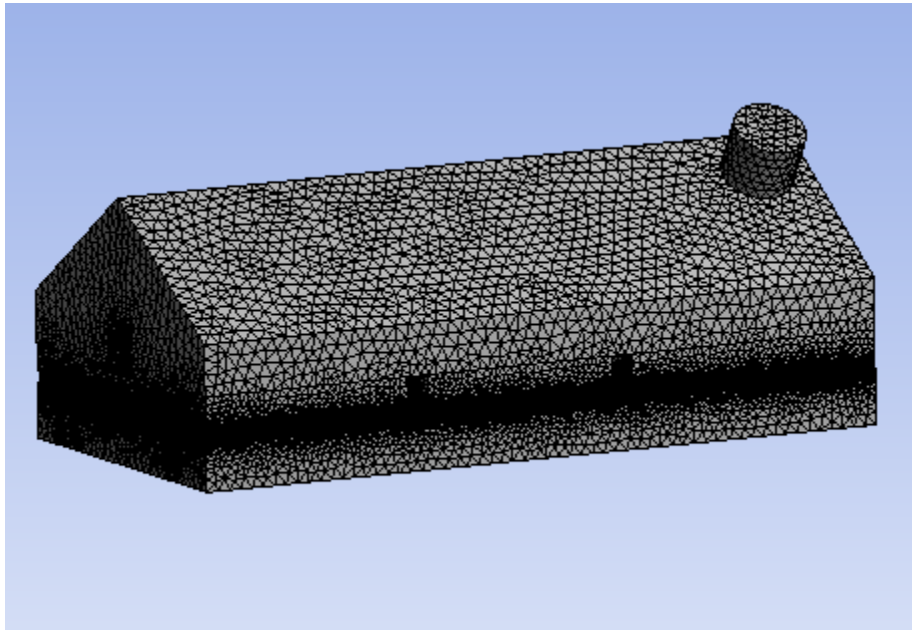
Figure 4-7 3D Mesh of the fluid volume inside the drying chamber.
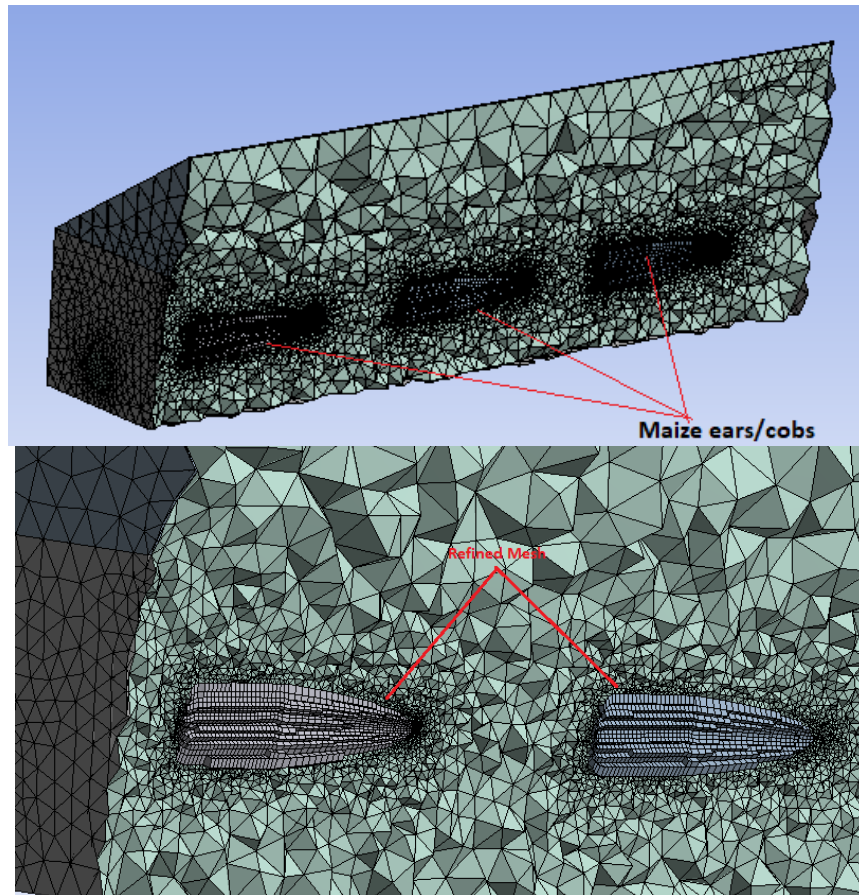
Figure 4-8 Cross-sectional view of the mesh (Top) and closer view of the refined mesh (bottom).

4.3.4 Simulation Assumptions

In this study it was necessary to employ several assumptions in the modeling and simulation of the solar dryer to accurately predict its performance. Valid assumptions are generally acceptable in engineering designs to assume characteristics of complex systems and processes which are otherwise difficult or impractical to achieve. In modeling the forced convection mixed-mode solar grain dryer with a preheater, the following assumptions were made:

- The analysis is considered under steady-state conditions for a constant solar irradiation. This is to simplify the CFD analysis but in reality the solar irradiation will vary with time throughout the day. Other factors such as weather conditions have effects on the amount of solar irradiation received by the solar dryer system.

- All maize ears inside the drying chamber are assumed to have the same initial moisture content. In reality the initial moisture content will vary from one maize ear to another due to various factors

such as time harvested, size of maize cob, susceptibility to moisture reabsorption, etc. All these factors affect the evaporation rate of different maize ears.

- The initial temperature of grains on the maize ears is the same as the drying air temperature inside the chamber. In practice different components inside the chamber will initially absorb heat as the drying chamber warms-up leading to an increase in internal temperature.

- The small amount of heat loss inside the solar collector and around the interconnector flow channel is neglected for the purpose of CFD analysis.

- It is assumed that all the incident sun rays received by the solar dryer system are Direct Normal Irradiance (DNI) rays and the surfaces that are not perpendicular to incident sun rays receive an effective 20% of the DNI. The average DNI for Durban was used for the CFD analysis although in reality the DNI will vary each day depending on the weather conditions.

- Internal walls of the interconnector flow channel are considered very smooth in order to neglect internal flow losses. In practice there will be losses due to surface roughness inside the duct, but theses will be minimal.

- The drying chamber of the actual solar dryer consists of a black-painted frame structure which is neglected in the CFD analysis. This is simply because the effective area of the structure inside the chamber is less significant for drying although in practice a small portion of the incident solar irradiation will be absorbed by the structure.

- The glazing material covering the entire drying chamber does not absorb any incident solar irradiation. Although most of the incident solar irradiation is transmitted through the glass, in reality a small portion of the incident rays will be absorbed.

4.3.5   Model Descriptions

In this section, the three sub-systems of the dryer system are fully described by defining and assigning relevant boundary conditions which allow the respective equations governing the fluid dynamics to be computed. However, before defining the model, the inputs to simulations need to be defined. It is clear that one of the factors affecting solar drying is atmospheric conditions. Because atmospheric air temperature

and relative humidity are parameters that change with time it was necessary to come up with average input parameters for the drying air entering the preheater to be used for the CFD analysis. Essentially this eliminated the need for having various temperatures and relative humidity of air at the preheater inlet for all the simulations, although these parameters were measured during the experiment. Therefore, to simulate drying for October weather conditions, the simulation was conducted based on the local weather data collected for the past three years (2017-2019) in order to incorporate adverse weather conditions of the month. The weather data used in this study were obtained from the Virginia weather station in Durban.

The data extracted from the weather station were daily values. Therefore, it was necessary to calculate the weekly average data in order to simplify the analysis as shown in Table 9-1 (Appendix A). With the use of this weather data, it was possible to determine and make use of the average minimum temperature and average maximum temperature as input parameters for the drying air entering the preheater. The flowing sub-sections give a thorough overview of the model descriptions for the solar dryer system.

4.3.5.1 Preheater-to-Solar Collector System

In this study the preheater was used to heat the ambient air and increase the air temperature at the inlet to the solar collector from 30 °C and 40 C°. Using Table 9-1 it was necessary to select the most suitable input parameters (temperature and relative humidity) for the preheater which would enable the input parameters to the solar collect to be identified for CFD analysis. Considering the worst-case scenario of a low temperature/high humidity month which would correspond to a slower drying rate, the ambient air was assumed to have a calculated temperature and relative humidity of 15.2 °C and 90 %, respectively (see Appendix A for calculations). It is fundamentally known that increasing the temperature of air affects its relative humidity, therefore it was necessary to calculate the resulting relative humidity of air at the output of the preheater. Table 4-1 shows the calculated relative humidity of air corresponding to the desired output temperature of the preheater (see Appendix A for calculations).

**Table 4-1 Predicted temperature and relative humidity of air at inlet and outlet of the preheater.**

	Input	Output 1	Output 2	Output 3
Temperature (°C)	15.2	30	36	40
Relative Humidity (%)	90	39	28	23

To simulate forced convection in the drying process, the CFD analysis was conducted by varying the air flow velocity (0.5 m/s to 2 m/s) within the solar dryer system. In ANSYS Fluent the 3D meshed model of

the solar collector (shown in Figure 4-3) was discretized using the pressure-based solver and assigned different boundary conditions as follows:

- Inlet flow conditions – The temperature and relative humidity at inlet was set equal to the values of Output 1 in Table 6 for all air flow velocity (0.5 m/s, 1 m/s, and 2 m/s). This process was repeated using the same air velocity range for all the different input conditions (Output 2, and Output 3). Turbulence intensity was varied between 5 % and 8 % to account for minor turbulence through the flow passage.

- Outlet flow conditions – At outlet, it is a pressure outlet boundary condition whose pressure is the same as the atmospheric pressure at sea level, 1 bar.

- Viscous model setup – For all simulations carried out, the viscous model that was applied was the Realizable $k - \varepsilon$ model with standard wall functions. This model was suitable for the flow regime and offered accuracy at low computational cost.

- Energy setup – The energy model was activated and a surface-to-surface radiation model was used to account for the radiation effect. A heat flux of 155.8 W/m^2 was applied in relation to the absorber surface of the solar collector.

- Materials – The solid material was copper while the fluid was air. Default properties of air available in ANSYS Fluent library were used while the properties of the copper material used were as follows:
  - Density = 8978 kg/m^3
  - Specific heat = 381 J/kg.K
  - Thermal conductivity = 387.6 W/m.K

- Solution methods – Pressure-to-velocity coupling using SIMPLEC scheme and a skewness correction factor of 1 with least square cell-based gradient interpolation method was used. Hybrid initialization was used instead of standard.

- Calculation setup – The maximum number of iterations was first set to 200, however it was realized that the solutions seemed to be converging after 100 iterations as shown in Figure 4-9. Residual

errors were set to a maximum level of 0.0001 to ensure the solution converged with an acceptable accuracy.
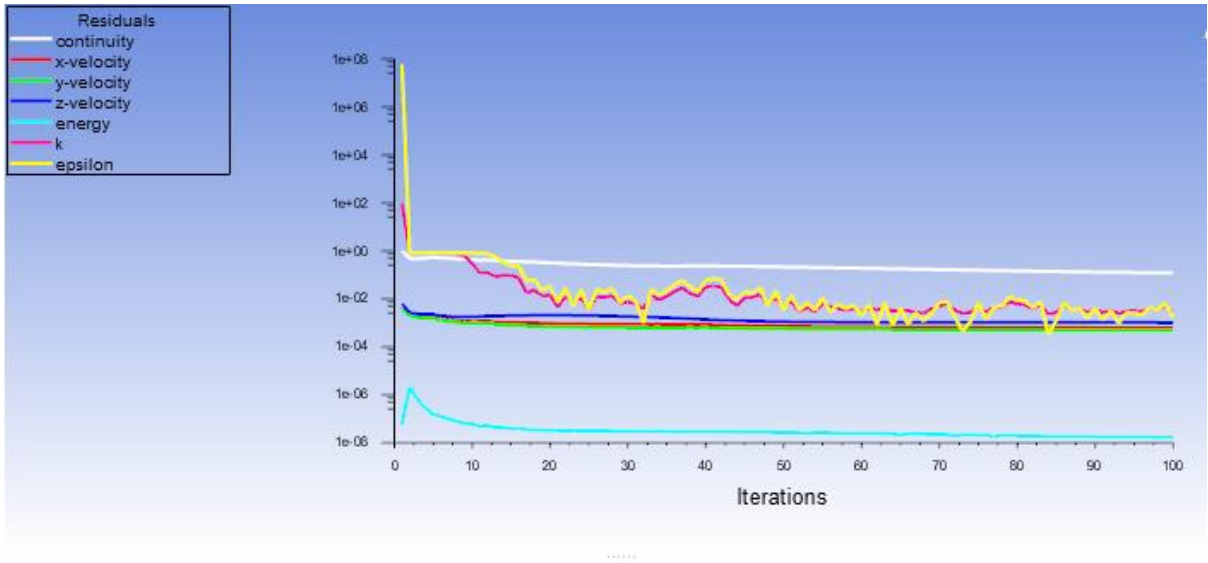
Figure 4-9 Residual errors at different iterations.

The schematic of the heat transfer within the solar collector is shown in Figure 4-10. As shown, the figure is a cross-sectional view of the flow passage (discussed in section 4.3.3.1), which is the component responsible for capturing solar irradiation.
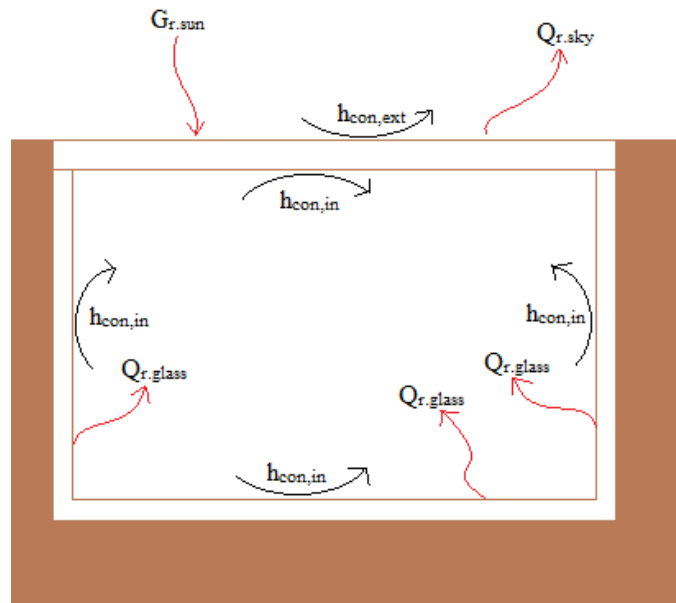
Figure 4-10 Schematic diagram of the heat transfers within the solar collector.

The brown color represents insulation around the air flow passage inside the solar collector. Therefore, it was considered that there would be no heat transfer from the absorber walls. All the heat absorbed by the absorber walls would be lost through convection and radiation heat transfer. Acronyms shown in Figure 4-10 are defined as follow:

- $h_{con,in}$ (W/m^2.K) is the internal convective heat transfer coefficient responsible for the total heat transfer from the absorber or perspex glass by forced convection.
- $h_{con,ext}$ (W/m^2.K) is the external convective heat transfer coefficient responsible for the total heat loss from the perspex glass by natural convection of ambient air.
- $G_{r.sun}$ (W/m^2) is the total effective solar irradiation received by the solar collector.
- $Q_{r.glass}$ (W/m^2) is the total radiative heat between the absorber surface and the perspex glass surface.
- $Q_{r.sky}$ (W/m^2) is the total radiative heat loss to the sky.

In order to model the solar drying phenomenon, the amount of solar irradiation for the proposed area where the experiment would be conducted needed to be considered. According to a case study conducted by Suri et al. (2015) on accuracy enhancement of South African solar resource maps, Durban has an average direct normal irradiance of 1574 kWh/m^2 per annum (4.31 kWh/m^2 per day). To calculate the effective solar irradiation $G_{r.sun}$ (W/m^2) received by the solar collector, the optical properties (shown in Table 4-2) of both the perspex glass and absorber material needed to be accounted for. The material used as the absorber was commercial black-painted copper.

Table 4-2 Optical properties of perspex glass and commercial black-painted copper [9, 10].

	Perspex	Black-painted copper
Transmissivity	92%	-
Reflectivity	8%	6.21%
Absorbance	0%	93.8%

In relation to Figure 4-10, the radiation from the sun will first hit the glass. Most of the radiation is transmitted to the absorber while a small portion is reflected. In this analysis absorbed radiation by the perspex glass was neglected. The amount of radiation transmitted was based on the transmissivity, τ_g and the amount reflected was based on the reflectivity, R_g. The transmitted radiations are absorbed by the absorber material based on the absorbance, α_{ab} and reflected between the absorber surface and the perspex glass surface based on the reflectivity R_{ab} and R_g. The overall relation was as given in Equation 4-1, giving an effective solar irradiation considered for heating up the absorber of the solar collector.

$$G_{r.sun} = \frac{G.\tau_g.\alpha_{ab}}{1-(R_{ab}.R_g)}$$
(4-1)

The effective solar irradiation $G_{r.sun}$ (W/m^2) was modeled in ANSYS Fluent as a heat flux applied on the absorber. Its value was computed from Equation 4-1 using the daily DNI value and the optical properties given in Table 4-2.

4.3.5.2 Interconnector Flow Channel

In this section of the solar dryer there would be no heat transfer taking place because the interconnector flow channel was an insulated flexible pipe. Its only primary function was to transfer air flow from the solar collector to the drying chamber without losing heat. The flow channel was modeled using the output results (temperature, flow velocity, relative humidity) of the solar collector as its inputs. Because of an adiabatic wall relationship, the temperature at the outlet of the flow channel was not of particular interest for the analysis. It was already anticipated that the temperature and humidity at the inlet would be the same as at the outlet because of the insulation on the wall. The parameter which would be affected by the geometry of the flow channel was the velocity. Hence, the flow velocity at all three outlets of the flow channel needed to be computed.

Procedures to discretize and apply boundary conditions were the same as those carried out for the solar collector except that in this case the material of concern was the fluid (air). Due to the simplicity of modeling the flow channel, it was possible to manually calculate the velocity at both outlets using the continuity equation. Since there is no change in temperature in this section, and the density of air was considered constant.

4.3.5.3 Drying Chamber

In this section, results of calculations at the outlets of the interconnector flow channel were carried over as inputs to the drying chamber model. Essentially, the results at the outlet of the solar collector were used except the flow velocity changed when the flow branched into three sections before entering the drying chamber.

The drying chamber was constructed from perspex glass with a black-painted aluminum frame structure, and its drying tray was made from black-painted aluminum with a wire mesh. For the purpose of the

simulation, the frame structure was ignored and only the glazing and the drying tray to hold the maize ear were considered in the CFD analysis.

To carry out the CFD simulation, it was crucial to understand the heat and mass transfer taking place within and/or across the drying chamber. Figure 4-11 indicates the schematic of the heat and mass transfer analog as perceived for the drying of maize ears. Because the dryer system operated in mixed mode, heat was gained from direct sun rays and as well from the heated air entering the drying chamber from the solar collector.
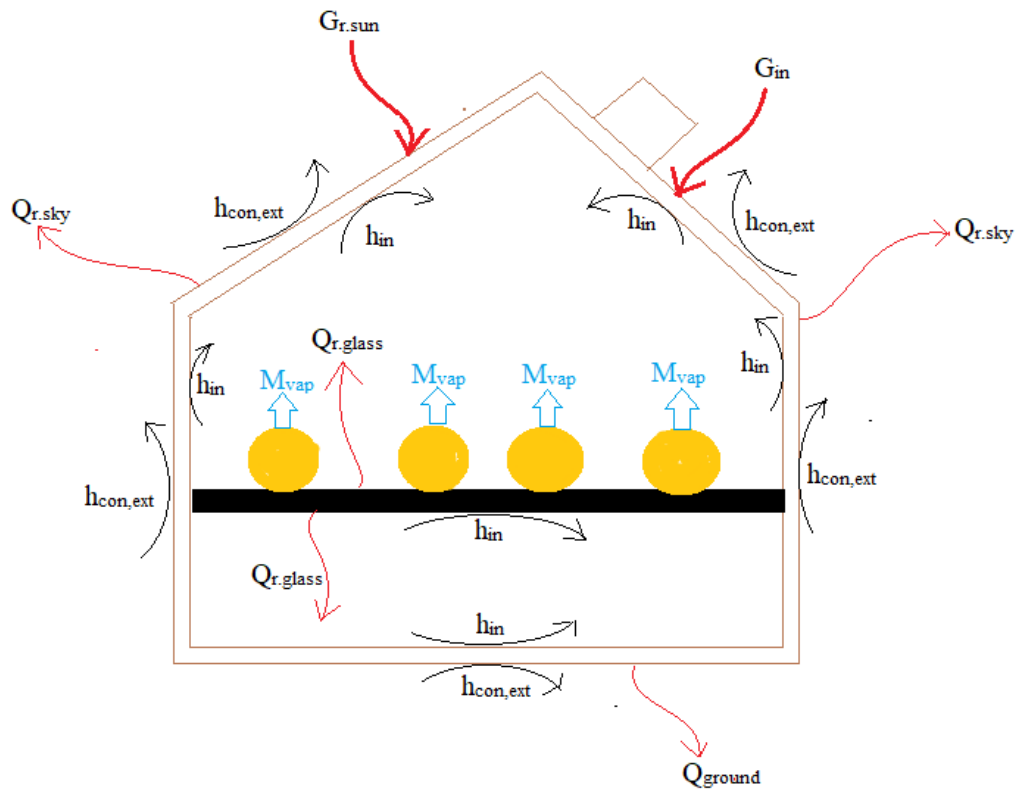
Figure 4-11 Schematic diagram of the heat and mass transfers within and/or across the drying chamber.

The different acronyms shown in Figure 4-11 are defined as follows:
- h_{in} (W/m².K) is the internal convective heat transfer coefficient leading to the total heat transfer inside the chamber and moisture evaporation from maize ears (indicated with orange color) through air circulation.
- $h_{con,ext}$ (W/m².K) is the external convective heat transfer coefficient responsible for the total heat loss from the perspex glass by natural convection of ambient air.
- $G_{r.sun}$ (W/m²) is the total effective solar irradiation received for the drying chamber.

- G_{in} (W) is the total heat gained from the hot air entering the drying chamber from the solar collector.
- $Q_{r.glass}$ (W/m²) is the total radiative heat between the surfaces of the drying tray (indicated with black color), maize ears and perspex glass.
- $Q_{r.sky}$ (W/m²) is the total radiative heat loss to the sky.
- Q_{round} (W/m²) is the total radiative heat loss to the ground.
- M_{vap} (kg/s) indicates the rate of moisture removal from the maize ears.

The solver setup for the drying chamber was similar to the one carried out in the solar collector section except that mass transfer was included in this case. This was necessary in order to model evaporation and condensation of moisture from the grains of the maize ears. The analysis aimed to predict drying of the grains by lowering its moisture content from 24 % to 13 % moisture content which is the level recommended for safe storage. Maize ears were included in the model as solid bodies (for thermal analysis) with a layer of water equivalent to their initial moisture content. The model setup was as follows:

- <u>Inlet flow conditions</u> – The temperature, relative humidity and air velocity from the results of the preceding sections (solar collector and interconnector flow channel) were used accordingly, as inlet flow parameters. Turbulence intensity was left as default at 5 %.

- <u>Outlet flow conditions</u> – Similar condition as for the solar collector.

- <u>Multiphase Model</u> – A eulerian model was selected with evaporation-condensation as the eulerian parameter under Lee model. The number of eulerian phases were set to 3 because there were three phases (water in the grains, air for drying, and moisture/vapor). Volume fraction parameter was set for implicit formulation. Evaporation frequency was tuned to 50 and the saturation temperature was initially set to default value.

- <u>Viscous Model Setup</u> – The realizable $k - \varepsilon$ model with enhanced wall treatment was applied to increase accuracy.

- <u>Energy setup</u> – Similar conditions as for the solar collector.

- <u>Materials</u> – The geometry of the meshed drying chamber consisted of four domain bodies including the fluid domain. Apart from air as the fluid material, three solid materials were defined. The solid materials defined were: (1) aluminum (drying tray), (2) perspex glass (glazing), and (3) maize ears.

Default properties of air available in ANSYS Fluent library were used while the properties of the three solid materials were defined as follows:

(1) Aluminum for the drying tray:
- Density = 2700 kg/m³
- Specific heat = 880 J/kg.K
- Thermal conductivity = 189 W/m.K

(2) Perspex glass (*Optical properties are as per Table 4-2*):
- Density = 1190 kg/m³
- Specific heat = 1270 J/kg.K
- Thermal conductivity = 0.189 W/m.K

(3) Maize ears. According to research conducted, thermal properties of maize ears are dependent on the temperature and moisture content. Based on the study conducted by [11] on maize ears, its thermal properties was computed as follows:
- Density = 760 kg/m³
- Specific heat, C_p (kJ/kg.K)
$$= 1.3066 + 1.2045M_d + 0.0198T \qquad (4.2)$$
- Thermal conductivity, T_c (W/m.K)
$$= 0.028 + 0.1321M_d + 3.4981 \times 10^{-3}T - 0.128M_d^2 - 2.24 \times 10^{-5}T^2 \qquad (4.3)$$

Whereby "T" and "M_d" are the temperature and moisture content of the maize ear, respectively. Thus, for every simulation trial, the properties of maize need to be computed based on the temperature and moisture content present.

- <u>Solution Methods</u> – Similar condition as for the solar collector.

- <u>Calculation setup</u> – Initially the maximum number of iterations were set to 250 but at 150 iterations the solutions seemed to be approaching convergence. The maximum level of residual error was set to 0.0001 as for the solar collector.

4.4 Part 2: Experimental Validation

In this part, a further study was conducted to validate some of the simulation works that were carried out in part 1. The experimental study was conducted using an existing solar dryer system which was adapted for the purpose of the study. The experiment was run on various tests and the data was collected.

4.4.1   Materials Used

- A solar dryer system
- 72 fresh maize ears (17 kg batch)
- A preheater/air heater
- PID temperature controller
- An RTD temperature sensor for the temperature controller
- Solid state relay for the temperature controller
- Supply of compressed air through an air dryer
- A needle flow control valve
- NI USB-6000 data logger
- Four temperature and humidity sensor probes
- Electrical wiring, piping and fittings
- Moisture meter
- Anemometer
- Laptop
- AC/DC voltage supply

4.4.2   Experiment Setup

4.4.2.1 Electronic Control and Data Acquisition

The experimental setup process began by first cleaning the solar dryer system and connecting all the necessary fittings to make them suitable for the experiment. The experiment was conducted in an open space with no obstruction to direct sunlight. Since the experiment included electronic control and data acquisition, necessary arrangements to connect the electronics were made. Four sensor probes (denoted S1, S3, S4, and S5 in Figure 4-12) were connected to the NI USB-6000 data logger to monitor the temperature and relative humidity at four positions across the solar dryer system as shown in the Figure 4-12. The heat

generated by the heating elements in the preheater was controlled by the PID temperature controller through a solid state relay (denoted as SSR in Figure 4-12) and a feedback temperature sensor, S2. Figure 4-12 shows the electrical control layout and connections between various components of the experiment.
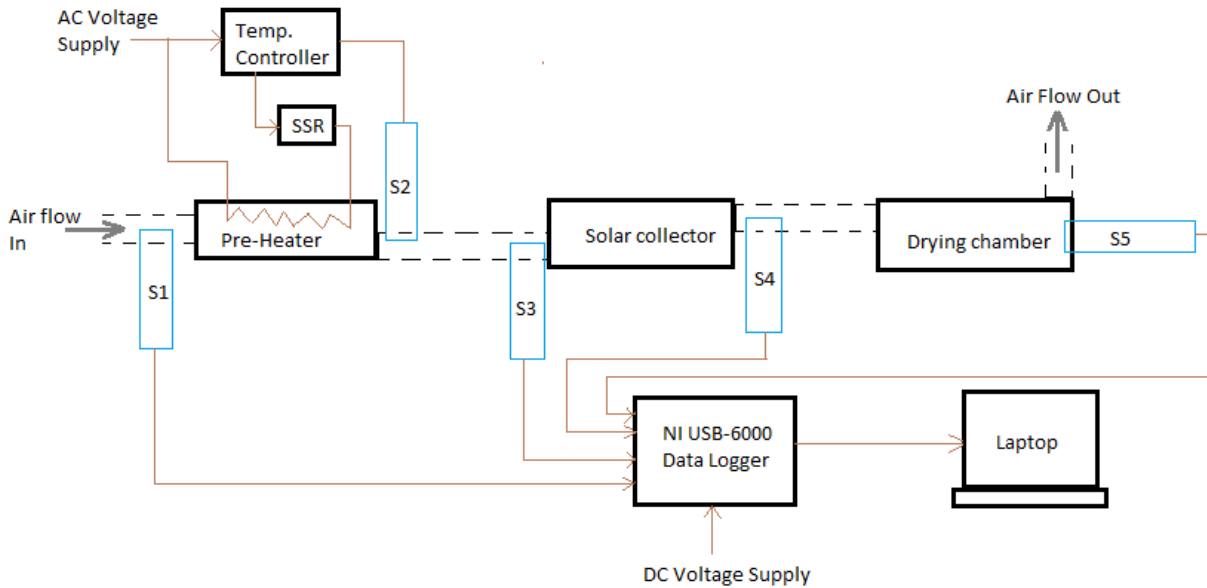

**Figure 4-12 Electrical control layout and connections of the solar dryer system.**

The four sensor probes (denoted S1, S3, S4, and S5 in Figure 4-12) used in the experiment were HTM2500LF probes. In each probe there were two separate sensors, one for measuring the temperature while the other measures humidity (see Appendix B for specifications). The temperature sensor S2 was a resistance temperature detector (RTD) type sensor. As shown in Figure 4-12, sensor probe S1 measured the temperature and humidity at the preheater inlet, sensor probe S3 and sensor probe S4 measured temperature and humidity at the solar collector inlet and outlet, respectively, and sensor S5 measured temperature and humidity at the drying chamber outlet.

As shown in Figure 4-12, the data were retrieved through DAQ Express software installed in a laptop which was linked to the NI USB-6000 data logger using a high-speed USB data cable. The data logger was powered by a separate DC voltage supply while the heating elements and temperature controller were powered by AC voltage supply. The dashed line indicates the flow of air through the solar dryer system. Due to financial constraints, some of the equipment used in the experiment (such as the preheater to heat the air) were sourced within the School of Engineering. During the process of setting up the experiment, it was noticed that the preheater/air heater that was available for usage was dismantled, and, anyway, it did not have a temperature control circuit for regulating the output air temperature from the heater. This

necessitated the need to incorporate a suitable temperature control circuit for the preheater. Through research, it was found that it would be most economical and efficient to use a PID controller to control the temperature of the preheater in conjunction with a thermocouple sensor and a relay to switch the heating element on/off. Figure 4-13 and Figure 4-14 show photos of the preheater before it had a temperature controller and after the temperature controller was incorporated in its circuit, respectively.
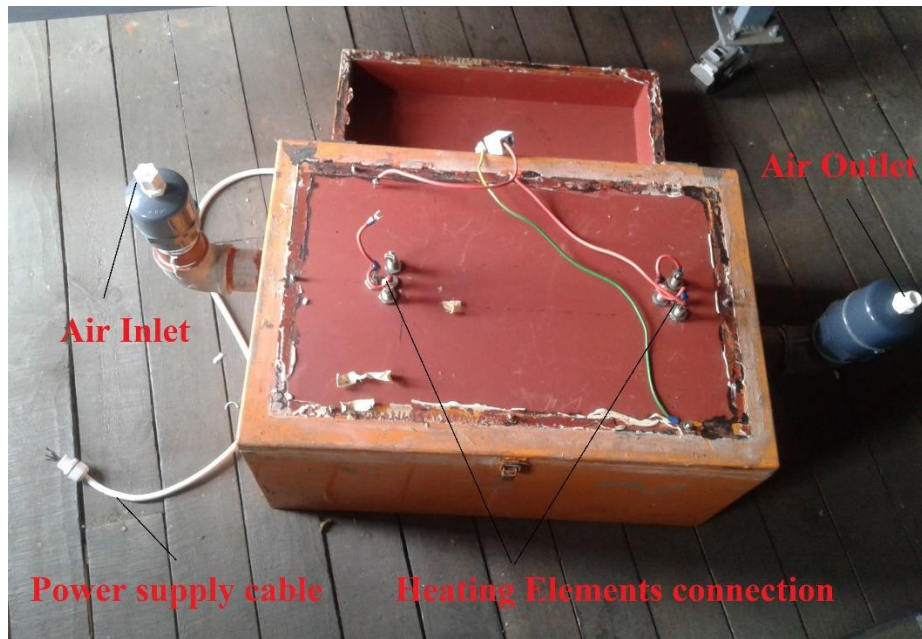
Figure 4-13 Preheater before modification.
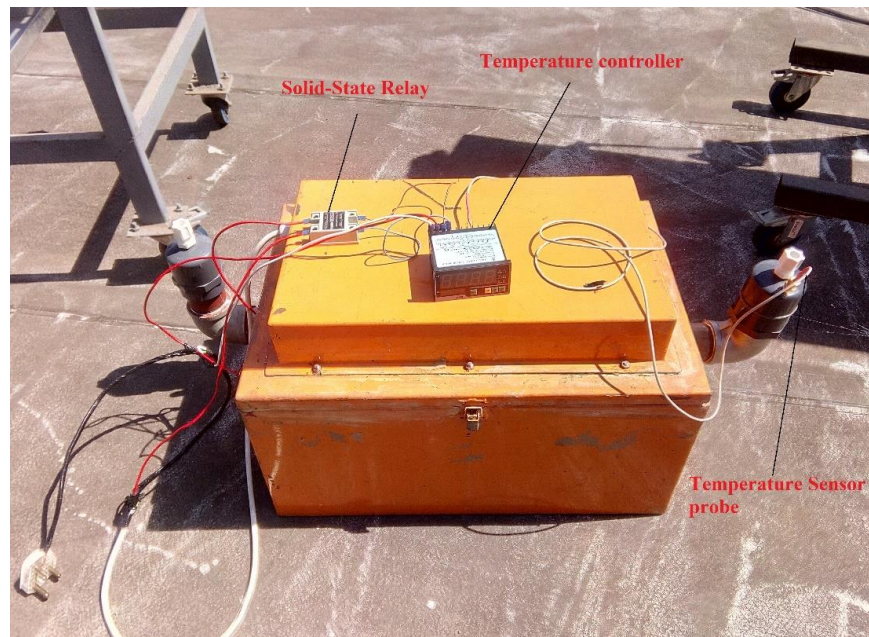
Figure 4-14 Preheater after modification.

The PID temperature controller was selected and purchased based on the power ratings of the heating elements. Another modification that was made on the preheater was to lower the power consumption of the heating elements. Initially the preheater was constructed with three heating elements that were connected in parallel and drawing a total current of 20 amperes (see Appendix B for the heating elements). To prevent high power consumption and possible overheating of circuit wiring, one heating element was disconnected, leaving the preheater with two heating elements connected in parallel which reduced the wattage from a maximum 4500 watts to 3000 watts.

4.4.2.2 Complete System Setup

The full setup of the experimental forced convection mixed-mode solar dryer with a preheater system is shown in Figure 4-15. More photos of the different components of the solar dryer system can be found in Appendix C. The system was set up on the roof top of a building where there were no obstructions and sufficient sunlight could be captured for optimum drying performance.
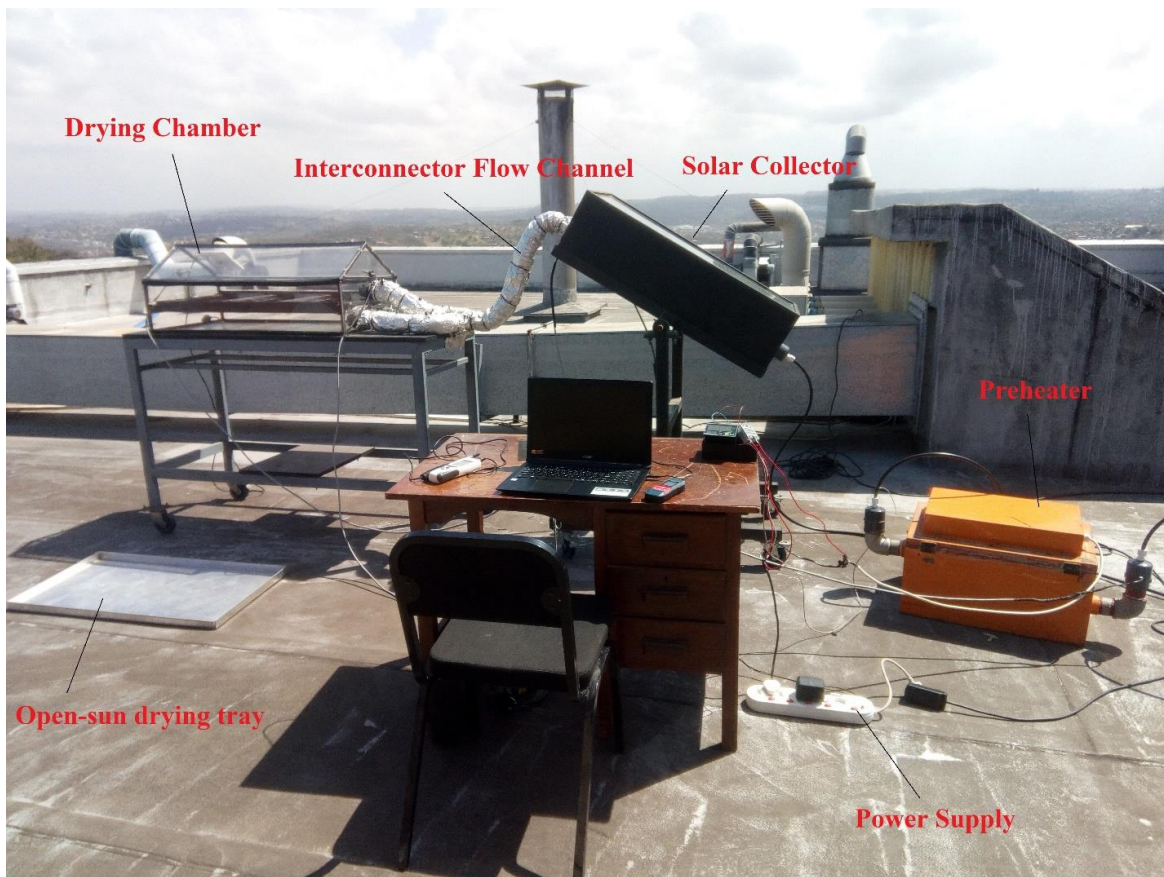
Figure 4-15 Complete experimental setup of the solar dryer system.

To induce a forced convection flow of air for the dryer system, a flow of compressed air through a filter-pressure regulator and a needle flow control valve was used for the experiment. A blower could have been used, but it was found that it would be cheaper to use the compressed air supply that was already installed on-site. Although thermal conductivity of polyethylene is very small, the polyethylene tubing between the preheater and solar collector was insulated to prevent a significant loss in air temperature. A bag containing 72 fresh maize cobs was purchased from a local farmer in the vicinity of Durban and a moisture analyzer was used for determining the moisture content.

4.4.3 Experimental Procedures

To obtain the correct readings of the measurements during the experiment, it is of vital importance that sensors are calibrated. Calibration of the sensors was the initial step in conducting the experiment and it was a necessity since some of the sensors were used sensors. A portable digital temperature-humidity probe (shown in Appendix B) was used in the calibration of the sensors. During the calibration process a dry-run test was carried out whereby the readings from the four sensors were compared with the one measured by the portable digital sensor probe. By comparing the readings, the sensors were found to be functioning accurately and their readings were in close tolerance with those of the portable digital sensor probe. Hence, they were deemed calibrated and functioning as required. Upon completion of sensor calibration, the experiment was conducted as follows:

a) Securely position the sensor probes at their respective ports of the dryer system. One sensor probe at the inlet of the preheater, one sensor probe at the outlet of the solar collector, one sensor probe at the inlet of the drying chamber and another one at its outlet.

b) Prepare 8 maize cobs by removing the corn husks and measure the moisture content of each maize cob using the moisture meter. Since the moisture content of each cob differed slightly from one another, an average moisture content was used as the initial moisture content of all 8 maize cobs. Record the initial moisture content.

c) Turn on the compressed air supply line to induce a high flow of air.

d) Set the air flow at the inlet of the solar collector to approximately 0.5 m/s. This is achieved by adjusting the handle of the installed needle flow control valve and using the anemometer to achieve the desired air flow.

e) Set the temperature of air at the outlet of the preheater to approximately 30 °C. This is achieved by setting the desired temperature on the digital display of the temperature controller.

f) Evenly place 6 maize cobs on the tray in the drying chamber and 2 maize cobs on the tray in the open sun. Ensure the tray is closed and sealed.

g) Connect the USB cable from the NI USB-6000 data logger to the laptop the laptop and open the DAQ Express software application.

h) Once the software application opens, choose analog inputs and add 8 input channels, because there are two input signals (temperature and humidity) from each sensor probe.

i) On the software application, change the sampling rate to 9 minutes (0.00185185 Hz) so that the measurements are taken every after 9 minutes. This will avoid the sensors taking measurements every second which is not a necessity for the experiment and will take up too much memory space on the computer.

j) Using the software application, start recording the readings from the four HTM2500LF sensors until the desired final moisture content of maize cobs is achieved.

k) While the laptop monitors and stores readings from the four sensors, use the moisture meter to keep measuring and recording the moisture content of the maize ears inside the drying chamber and in the open sun every after 20 minutes for the first hour then every 15 minutes thereafter.

l) Maintain the drying parameters until a moisture content safe for grain storage is achieved. The recommended moisture content for safe storage of grains is 13 % wb or less.

m) Once a moisture content of less than 13 % wb is achieved, repeat the above steps for the following drying parameters:

- Air flow at 0.5 m/s and preheater temperature of 35 °C.
- Air flow at 0.5 m/s and preheater temperature of 40 °C.
- Air flow at 1 m/s and preheater temperature of 30 °C.
- Air flow at 1 m/s and preheater temperature of 35 °C.
- Air flow at 1 m/s and preheater temperature of 40 °C.
- Air flow at 2 m/s and preheater temperature of 30 °C.
- Air flow at 2 m/s and preheater temperature of 35 °C.
- Air flow at 2 m/s and preheater temperature of 40 °C.

n) Safely disconnect all electronic device from the power supply and analyze the data.

4.5 References

1. Suri, M., Cebecauer, T., Meyer, A.J. and Van Niekerk, J.L. Accuracy-Enhanced Solar Resource Maps of South Africa. Proceedings of the 3rd Southern African Solar Energy Conference, Kruger National Park, South Africa. 2015, pp. 450-456. http://hdl.handle.net/2263/49525.

2. Sun, D. and Xia, B. Applications of Computational Fluid Dynamics (CFD) in the Food Industry: A Review. *Computers and Electronics in Agriculture*. 34(1-3), 2002, pp. 5-24. DOI: 10.1016/S0168-1699(01)00177-6.

3. Pragati, K. and Sharma, H.K. Concept of Computational Fluid Dynamics (CFD) and its Applications in Food Processing Equipment Design. *Journal of Food Processing and Technology*. 2011. DOI: 10.4172/2157-7110.1000138.

4. Defraeye, T. Advanced Computational Modelling for Drying Processes – A Review. *Applied Energy,* 131, pp. 323-344. https://doi.org/10.1016/j.apenergy.2014.06.027.

5. Demissie, P., Hayelom, M., Kassaye, A., Hailesilassie, A., Gebrehiwot, M. and Vanierschot, M. Design, Development and CFD Modeling of Indirect Solar Food Dryer. Proceedings of the 10th International Conference on Applied Energy, Hong Kong. *Energy Procedia*. 158, 2019, pp. 1128-1134. DOI: 10.1016/j.egypro.2019.01.278.

6. Romero, V.M., Cerezo, E., Garcia, M.I. and Sanchez, M.H. Simulation and Validation of Vanilla Drying Process in an Indirect Solar Dryer Prototype Using CFD Fluent Program. *Energy Procedia*. 57, 2014, pp. 1651-1658. DOI: 10.1016/j.egypro.2014.10.156.

7. Román-Roldán, N., López-Ortiz, A., Ituna-Yudonago, J., García-Valladares, O. and Pilatowsky-Figueroa, I. Computational Fluid Dynamics Analysis of Heat Transfer in a Greenhouse Solar Dryer "Chapel-Type" Coupled to an Air Solar Heating System. *Energy Science & Engineering*. 2019, pp. 1-17. DOI: 10.1002/ese3.333.

8. ANSYS Meshing User's Guide. Retrieved 2020.
    https://studentcommunity.ansys.com/thread/meshing-user-guide-for-ansys-19-2/.

9. Perspex CC Technical Data Sheet. Retrieved 2020. www.perspex.com.

10. Oliva, A.I., Maldonado, R.D., Diaz, E.A. and Montalvo, A.I. A High Absorbance Material for Solar Collectors' Applications. *IOP Conference Series Materials Science and Engineering*, 45(1), 2013. DOI: 10.1088/1757-899X/45/1/012019.

11. Verma, R.C. and Prasad, S. Mechanical and Thermal Properties of Maize. *Journal of Food Science and Technology*. 37(5), 2000, pp. 500-505.
    https://www.researchgate.net/publication/297790797_Mechanical_and_thermal_properties_of_maize.

CHAPTER 5

5. MODELLING AND CFD SIMULATION OF TEMPERATURE AND AIRFLOW DISTRIBUTION INSIDE A FORCED CONVECTION MIXED-MODE SOLAR GRAIN DRYER WITH A PREHEATER

This chapter presents work that was published under the title "Modelling and CFD Simulation of Temperature and Airflow Distribution Inside a Forced Convection Mixed-Mode Solar Grain Dryer with a Preheater" in the *International Journal of Innovative Technology and Exploring Engineering (IJITEE)*. A journal accredited by the Department of High Education and Training (DHET) of South Africa.

To cite this article:

Johannes P. Angula and Freddie Inambao, Modelling and CFD Simulation of Temperature and Airflow Distribution Inside a Forced Convection Mixed-Mode Solar Grain Dryer with a Preheater. *International Journal of Innovative Technology and Exploring Engineering* (IJITEE*)*, 10(4), 2021, pp. 33-40.

The link to this article:

DOI: 10.35940/ijitee.B8283.0210421

Modelling and CFD Simulation of Temperature and Airflow Distribution Inside a Forced Convection Mixed-Mode Solar Grain Dryer with a Preheater

Johannes P. Angula, Freddie Inambao

Abstract: In this study, a 3D Computational Fluid Dynamics (CFD) model was developed to simulate the drying process of maize ears/cobs in a mixed-mode solar grain dryer. The dryer system is aimed to operate under forced convection and is integrated with a preheater to heat air prior to entering the solar collector. The 3D model was developed with great accuracy using SolidWorks software and the CFD simulation was carried out using ANSYS Fluent software. The study was aimed at analyzing and predicting temperature and airflow distribution in the mixed-mode solar dryer system. The CFD simulation was conducted at different airflow velocities varying from 0.5 m/s to 2 m/s for different temperature values of the preheater. Results from the simulation of the solar collector were satisfactory, indicating a minimum and maximum temperature of 59.7 °C and 70.5 °C at minimum and maximum drying conditions, respectively. The variation of temperature inside the drying chamber was predicted with an average maximum of 64.1 °C at the inlets. Results of airflow distribution in the solar collector and drying chamber indicated high turbulence and flow recirculation. This is a desirable flow combination that promotes good moisture evaporation from the maize ears during the drying process. This study proves that the use of computer software can allow one to clearly gain an understanding of the development, heat and mass transfer process, and performance of dryers used in the food drying industry. This approach can promote improvements in existing drying processes and increase food productivity.

Keywords: Modelling & CFD simulation, Maize ears, Solar drying, Temperature distribution, Air flow distribution

I. INTRODUCTION

Advances in drying technologies over time have significantly improved food productivity and quality. Amongst the various drying technologies used, solar drying is one of the most efficient and cost-effective for drying food and agricultural products [1]. This technology uses solar radiation from the sun to generate thermal energy which is used in the drying process. The use of solar energy has gained popularity in food drying applications due to the ongoing reduction in natural resources, high natural fuel costs, and environmental damage [2], [3]. To develop an efficient solar dryer one needs to take into consideration the weather conditions and drying parameters which significantly affect the solar dryer's performance. Recent studies on food drying applications rely on the use of Computer-Aided Design (CAD) and Computational Fluid Dynamics (CFD) codes to model and simulate the drying phenomena. The use of CFD codes has gained popularity in the design industry as it is regarded as a promising tool for modeling and simulating designs, making costly experimental trials unnecessary [4]–[6]. CFD is a powerful and innovative computational method that uses numerical calculations and algorithms to solve and analyze problems associated with fluid flow in specified regions of interest [7], [8]. With sufficient simulation results, one gains an understanding of the performance of a dryer at various drying conditions. This allows the actual solar dryer to developed, tested and optimized. This study involves the use of CAD and CFD codes to model and simulate the drying of maize ears/cobs using a forced convection mixed-mode solar grain dryer integrated with a preheater. The CFD code used in this study to simulate the solar dryer system is ANSYS Fluent, while the CAD code used in the design or model creation is SolidWorks. The aim was to develop a three-dimensional model of a mixed-mode solar dryer system and simulate it against various drying parameters to predict the temperature and airflow distribution within the dryer system

II. THEORY

The approach to CFD analysis of the solar dryer involves the computation of the governing equations for the model. Using the CFD code, the kinetics of the fluid are analyzed and solved primarily using the compressible Navier-Stokes partial differential equations given by equation 1 [9] and equation 2 [10]. Equation (1) is referred to as a continuity equation while (2) is referred to as momentum law conservation. In solar drying, heat transfer occurs; hence, an additional equation to incorporate the energy transfer is included in the computation. The heat transfer process is governed by the first thermodynamic law, as expressed by (3) [11].

$$\nabla \cdot \rho \vec{V} + \frac{\partial \rho}{\partial t} = 0 \qquad (1)$$

Johannes P. Angula*, Department of Mechanical Engineering, University of KwaZulu-Natal, Durban, South Africa. Email: 210546069@stu.ukzn.ac.za

Freddie Inambao, Department of Mechanical Engineering, University of KwaZulu-Natal, Durban, South Africa. Email: Inambaof@ukzn.ac.za https://orcid.org/0000-0001-9922-5434

33

$$\underbrace{\rho \left(\frac{\partial \vec{v}}{\partial t} + \vec{v}.\nabla \vec{v} \right)}_{1} - \underbrace{\nabla p}_{2} +$$
$$\underbrace{\nabla . \left[\mu (\nabla \vec{v} + (\nabla .\vec{v})^T) - \frac{2}{3}\mu(\nabla .\vec{v})I \right]}_{3} + \underbrace{F}_{4} \qquad (2)$$

$$\frac{\partial}{\partial t}(\rho C_a T) + \frac{\partial}{\partial x_j}(\rho u_j C_a T) - \frac{\partial}{\partial x_j}\left(\gamma \frac{\partial T}{\partial x_j} \right) = S_T \qquad (3)$$

The preceding equations are essentially a simplification of the sets of equations in rectangular coordinates. In equation 2, term 1 is a representation of the inertial forces acting on the fluid; term 2 represents the effect of thermodynamic forces on the fluid particles, term 3 indicates the impact of the dynamic viscosity of the fluid, while term 4 represents all other external forces acting on the fluid. The drying of maize ears (cobbs) was modelled using the evaporation-condensation model found in the ANSYS Fluent program. It is available with the mixture and Eulerian multiphase models. The transfer of mass during moisture evaporation phases is described by (4) and (5). If the temperature T is greater than the saturation temperature T_{sat}, evaporation will occur in the drying chamber. Hence the transfer of mass during evaporation:

$$\dot{m}_{e \to v} = coeff * \alpha_l \rho_l \frac{(T-T_{sat})}{T_{sat}} \qquad (4)$$

If the temperature T is less than the saturation temperature T_{sat}, condensation will occur in the drying chamber. Hence the transfer of mass during condensation:

$$\dot{m}_{e \to v} = coeff * \alpha_v \rho_v \frac{(T-T_{sat})}{T_{sat}} \qquad (5)$$

The process of drying is generally associated with turbulent flows which makes it almost impossible to computationally solve turbulent flows using direct Navier-Stokes partial differential equations. Hence, Navier-Stokes partial differential equations coupled with other transport equations are considered to accurately model turbulence in the fluid domain. Other turbulence models that can be used are the Reynolds Averaged Navier-Stokes (RANS) model and the Large Eddy Simulation (LES) model. More information about the RANS and LES models can be found in literature such as [11]–[14].

III. METHODOLOGICAL APPROACH

The approach to this research work included the use of CAD and CFD codes to develop and simulate the model as required for different drying parameters. The CAD software used to create the model of the solar dryer system was SolidWorks 2018, and the CFD code used for simulating the developed model was ANSYS Fluent 19.2. The simulation results can be validated against the experimental results which helps necessary improvements to be made.

A. Model Creation and Meshing

In this study of analyzing a solar dryer in forced convection and mixed-mode operation integrated with a preheater, a decision was made to divide the entire solar dryer system into three models. This was necessitated due to the model's complexity and, most importantly, to reduce computational time and cost. Fig. 1 shows the models of the solar dryer system which were created using SolidWorks software.

As can be seen in Fig.1, the three models are the solar collector model, the interconnector flow channel model, and the drying chamber model. Each model was imported into ANSYS Fluent and analyzed separately. The output results from the first model were used as input results on the proceeding model. To accurately simulate a CFD problem, the model needed to be correctly meshed. The three meshed models of the solar dryer system are shown in Fig. 2. Essentially, what was meshed is the fluid volume created from the solid body in SolidWorks using the Boolean operation method and imported into ANSYS Fluent. A closer view of the mesh within close proximity of the maize ears contact surfaces is shown in Fig. 3. In this region, the mesh is refined to smaller mesh elements to improve the modeling process's accuracy. The mesh criteria applied to the three models are specified in Table 1. Necessary adjustments were also made to the mesh in refining certain areas of the model, such as using inflation layers, refined mesh size, elements order, etc.
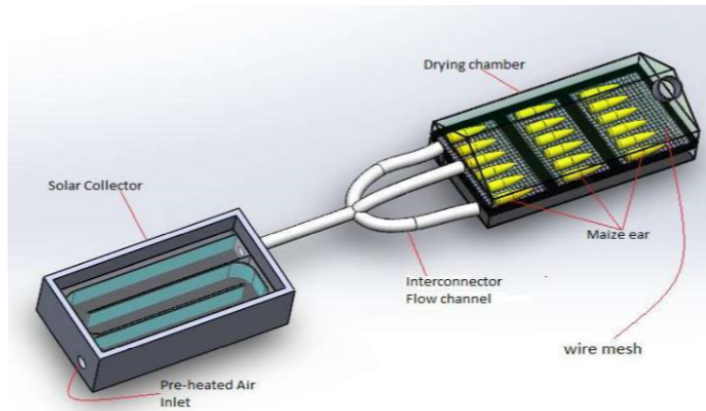
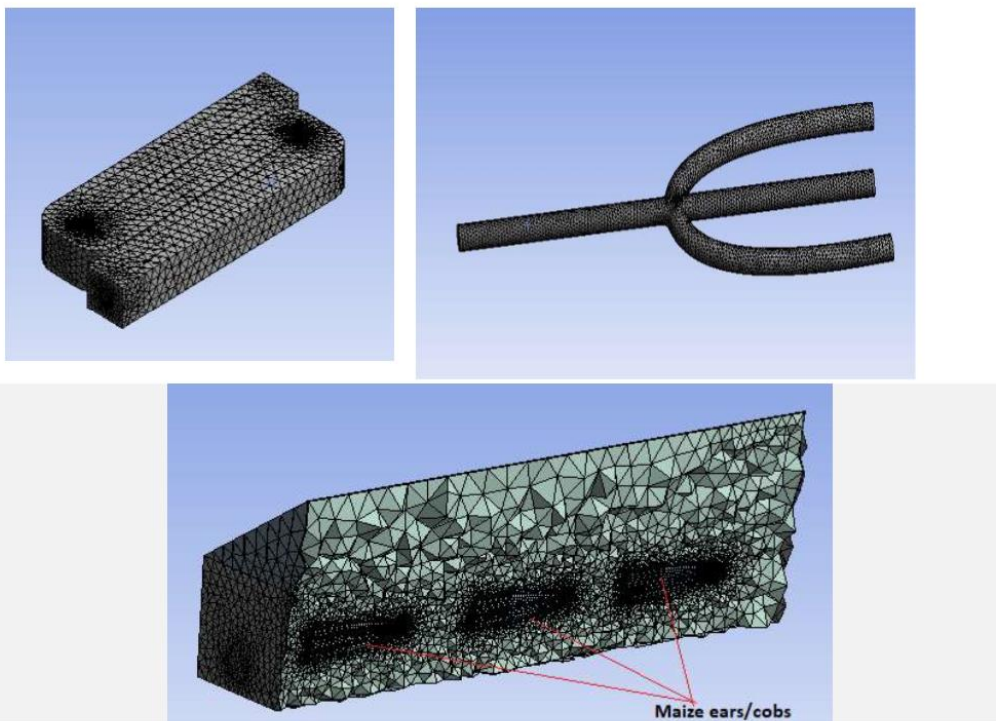Fig. 1. CFD model of the mixed-mode solar dryer system

Fig 2. 3D Mesh of the solar collector fluid volume (top left), interconnector flow channel fluid volume (top right), and a cross-sectional view of the drying chamber (bottom center)
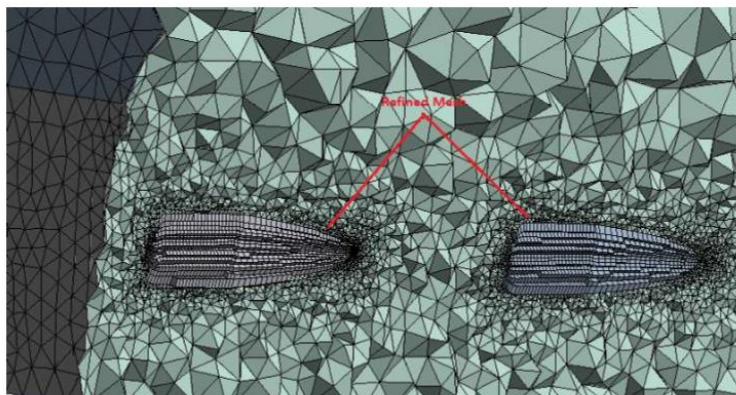

Fig. 3. Closer view of the refined mesh in the drying chamber

Table 1. Mesh criteria applied to the CFD model of the solar dryer system

Applied mesh criteria	CFD Model
Body mesh element size: 8 mm	Solar collector, Interconnector flow channel, Drying chamber
Element size at contact regions: 3 mm	Solar collector, Interconnector flow channel
Element size at contact regions: 2 mm	Drying chamber
Element size at curvature: 0.3 mm	Solar collector, Interconnector flow channel
Element size at curvature: 0.6 mm	Drying chamber

Mesh type: Tetrahedron	Solar collector, Interconnector flow channel, Drying chamber
Number of inflation layers: 5 layers	Solar collector, Interconnector flow channel
Number of inflation layers: 7 layers	Drying chamber
Elements order: Quadratic	Drying chamber
Mesh quality: Medium	Drying chamber

B. Definition of the Model

The simulation of the model conducted in this study was carried out based on several assumptions that were put in place to simplify the model. This was necessary as some of the flow characteristics are complex and impractical to achieve with the available computational resources and power. The main assumptions that were considered were:

- Steady state conditions are assumed for constant solar irradiation.
- The initial moisture content of grains inside the drying chamber is the same.
- The initial temperature of grains is the same as the drying air temperature inside the drying chamber.
- All incident solar irradiation falling on the solar dryer system are Direct Normal Irradiation (DNI) rays, equivalent to the measured average DNI rays of the site location.
- Negligible heat loss around the solar dryer system.
- Incident solar irradiation absorbed by the glazing material of the solar dryer system is neglected.

The above assumptions facilitated the definition of the three meshed models of the solar dryer system, enabling various boundary conditions to be assigned as required for simulation purposes. The simulation was conducted before the experiment. Hence, the weather parameters were assumed based on the calculated average data collected over the past 3 years from the Virginia Weather Station in Durban. Due to Durban's weather conditions that rarely exceed 30 °C, the presence of the preheater allows the ambient air temperature to be varied before entering the solar collector. It was considered that the drying air be preheated between 30 °C and 40 C°. For the purpose of the simulation, the preheater's effect was modelled as direct input values of temperature and calculated values of relative humidity. This was because the preheater used during the experiment has a temperature controller. The simulation was conducted using the pre-set output temperature and relative humidity values from the preheater, which served as the solar collector's input air flow values. The output temperature and relative humidity at the preheater outlet were 30 °C & 39%, 36 °C & 28%, and 40°C & 23%, respectively. Table 2 shows the boundary conditions that were applied to each model component of the solar dryer system.

Table 2. Applied boundary conditions of the solar dryer system at different drying airflow velocities and preheater temperatures

Boundary conditions	Model component 1: Solar collector	Model component 2: Interconnector flow channel	Model component 3: Drying chamber
Inlet flow conditions	Temperature: 30 °C Relative humidity: 39 % Flow velocity: 0.5 m/s Turbulence intensity: 8 %	Temperature: using output values from solar collector. Relative humidity: using output values from solar collector. Flow velocity: using output values from solar collector.	Temperature: using output values from interconnector flow channel. Relative humidity: using output values from interconnector flow channel. Flow velocity: using output values from interconnector flow channel. Turbulence intensity: 5 %
Outlet flow conditions	Pressure outlet Pressure value: 1 atm	Same conditions as solar collector	Same conditions as solar collector
Multiphase Model	-	-	Eulerian model with evaporation-condensation as the Eulerian parameter under Lee model. Eulerian phases number: 3 Volume fraction parameter: Implicit formulation Evaporation frequency: tuned to 50 Saturation temperature: default set
Viscous Model setup	Viscous model: Realizable $k - \varepsilon$ model with standard wall functions	Same conditions as Solar collector	Viscous model: Realizable $k - \varepsilon$ model with enhanced wall treatment
Energy setup	Energy model: active surface-to-surface radiation mode used. Heat flux on absorber surface: 155.8 W/m^2	No heat transfer, it has an adiabatic wall	Same conditions as solar collector

Materials	Solid material: Copper Solid material density: 8 978 kg/m^3 Specific Heat: 381 J/kg.K Thermal conductivity: 387.6 W/m.k Fluid: Air Fluid properties: ANSYS Fluent default values	Fluid is sir using default properties	*Aluminium for the drying tray* Density: 2 700 kg/m^3 Specific Heat: 880 J/kg.K Thermal conductivity: 189 W/m.K *Perspex glass* Density: 1190 kg/m^3 Specific Heat: 1270 J/kg.K Thermal conductivity: 0.189 W/m.K *Maize ear* Density: 760 kg/m^3 Specific Heat [6]: $= 1.3066 + 1.2045 M_d + 0.01987$ Thermal conductivity [6]: $= 0.028 + 0.1321 M_d + 3.4981 \times 10^{-3} T - 0.128 M_d^2 - 2.24 \times 10^{-5} T^2$
Solver	Pressure based	Pressure based	Pressure based
Solution methods	Coupling: Pressure to velocity using SIMPLEC Skewness correction factor of 1 with least square cell-based method. Hybrid initialization	Same conditions as solar collector	Same conditions as solar collector
Calculation setup	Maximum iterations: 100 to 200 Residual errors: 0.0001	Same conditions as solar collector	Same conditions as solar collector

In Table 2 "T" and "M_d" are the maize ear's temperature and moisture content, respectively. The simulation was repeated for all the previously mentioned preheater output conditions at an airflow velocity of 1 m/s and 2 m/s

IV. RESULTS AND DISCUSSION

The results obtained from CFD simulations are shown in Fig. 7, Fig. 8, Fig. 9, and Fig. 10. Due to the complexity of the model and simulation parameters, the maize cobs' final moisture content could not be determined through simulation. However, the temperature and velocity profile across different solar dryer system components during the predicted drying process are presented. In addition, the corresponding airflow distribution across the solar collector and drying chamber are also presented. To have a glimpse of the dryer performance as simulated at different drying parameters, the results shown in the figures are only for minimum and maximum drying parameters. Fig. 7 and Fig. 8 show the results of temperature distribution and velocity profile across the solar collector at minimum and maximum drying conditions. In this study, conditions at minimum drying were considered to be when the solar dryer system was operating as a natural convection solar dryer without a preheater. This is presented with an airflow velocity of 0.5 m/s and preheater temperature of 30 °C in the simulation process. While conditions at maximum drying are presented with the maximum airflow velocity of 2 m/s and 40 °C preheater temperature that were considered for simulation purposes.
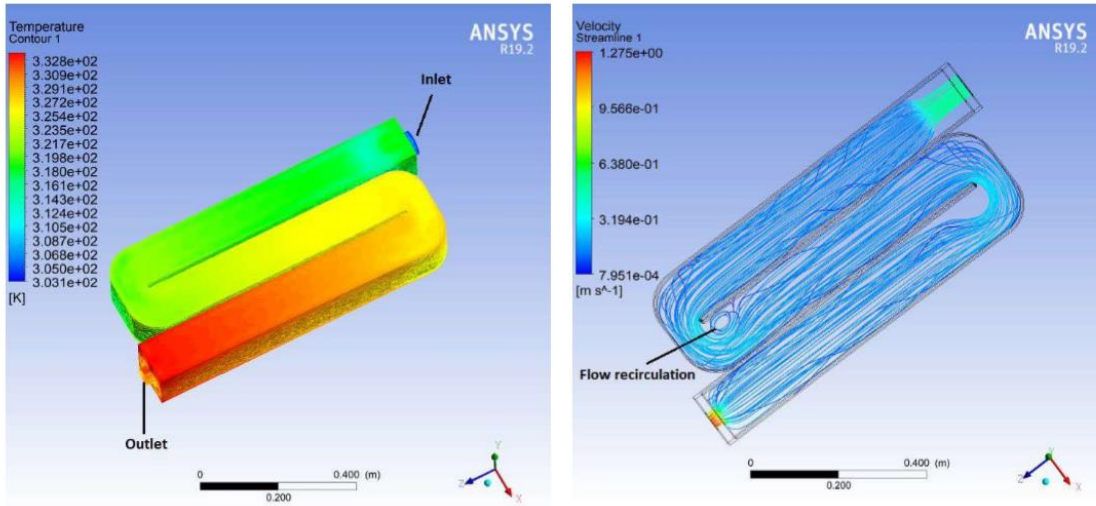
Fig. Temperature distribution (left) at 30 °C preheated air and velocity profile (right) at 0.5 m/s airflow across the solar collector
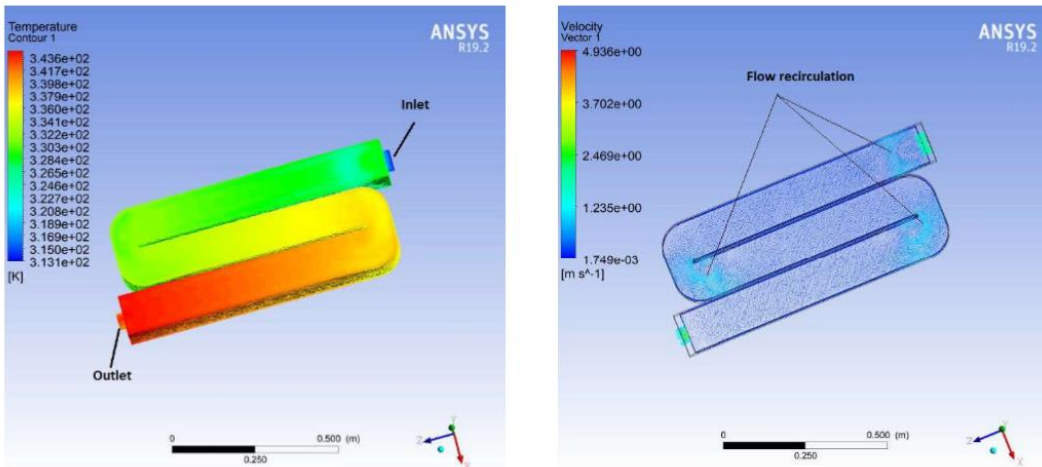
Fig. 8. Temperature distribution (left) at 40 °C preheated air and velocity profile (right) at 2 m/s airflow across the solar collector

The temperature distributions shown in Fig. 7 and Fig. 8 are very similar, however the temperature readings across the solar collector differ at various points along the air flow channel. It is evident that air starts heating up from the inlet as it navigates through the flow channel and gains its highest temperature toward the solar collector outlet. As shown in Fig. 7, at 30 °C preheated air, a maximum temperature of 332.8 K (59.7 °C) is predicted at the outlet when the airflow is set to 0.5 m/s, while at 40 °C preheated air, a maximum temperature of 343.6 K (70.5 °C) is predicted at the outlet when the airflow is set to 2 m/s. The presence of flow recirculation and turbulence inside the solar collector is also predicted, as shown by the velocity profile.

The flow exiting the solar collector is transferred to the drying chamber through an insulated interconnector flow channel. There were no results of the temperature profile across the interconnector flow channel since it is assumed that it is completely insulated, and there is no heat transfer across it. Thus, the airflow entering the interconnector will exit at the same temperature as it enters. However, its flow velocity will differ at the exit because of the change in areas. Using the solar collector and interconnector flow channel results, the temperature distribution and flow velocity profile across the drying chamber were obtained as shown in Fig. 9 and Fig. 10, respectively.
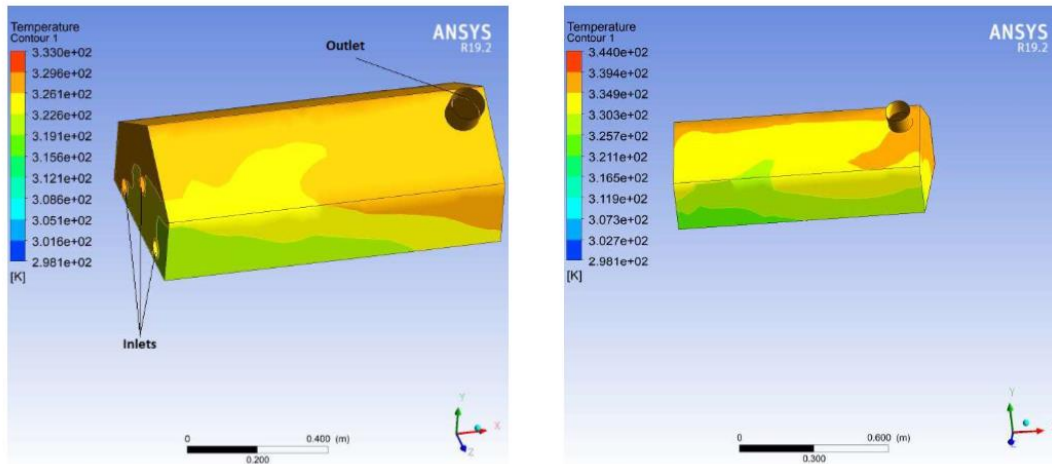
Fig. 9. Temperature distribution at 30 °C preheated air (left) and temperature distribution at 40 °C preheated (right) across the drying chamber during drying process
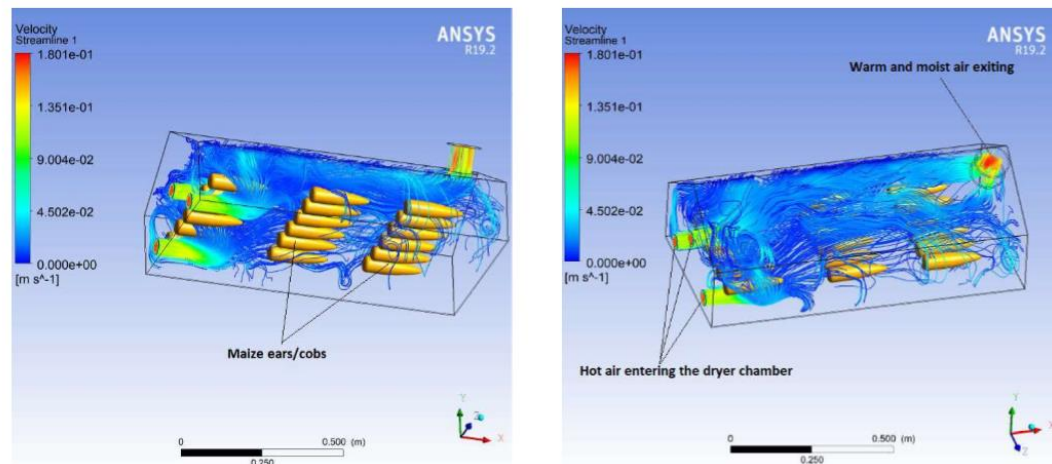

Fig. 10. Airflow distribution inside the drying chamber during drying process

The simulation results indicate the temperature profile across the drying chamber predicts temperature varying across the drying chamber. During the drying process, different chamber regions will have experienced different temperatures due to the heat and mass transfer processes. The results were also affected by the position of the sun at the time of drying. The highest temperatures as shown in Fig. 9 occur near the inlets when hot air enters the drying chamber. The average minimum temperature in the drying chamber was predicted to be around 327.9 K (54.8 °C), while the average maximum temperature was about 337.2 K (64.1 °C).

The flow behavior inside the drying chamber as shown in Fig. 10 during the drying process, predicts severe flow turbulence and recirculation. This is necessary during the drying process to accelerate the evaporation of moisture from the grains. The profile also indicates that more air flow is expected in the upper portion of the drying chamber than the bottom. Due to moisture evaporation, warm and moist air will exit the drying chamber at a relatively low velocity and at a temperature which is higher than ambient temperature.

V. CONCLUSION

In this study, a forced convection mixed-mode solar grain dryer with a preheater was modelled using SolidWorks and CFD simulation was carried out using ANSYS Fluent. Due to the complexity of the model and available computational resources, several assumptions were taken into consideration during the simulation process to simplify the problem. The solar dryer system was modelled and simulated with great accuracy. The simulation was run at a flow velocity varying from 0.5 m/s to 2 m/s for different temperature values of the preheater.

The results of temperature distribution indicated a maximum temperature of 70.5 °C predicted at the solar collector outlet for maximum drying conditions, and a maximum temperature of 59.7 °C at the solar collector outlet for minimum drying conditions. Due to the effect of mixed-mode solar drying, the average maximum temperature in the drying chamber was predicted to be around 64.1 °C. A small percentage of condensation is also expected to occur within some areas of the drying chamber. The simulation predicted a satisfactory airflow distribution within the drying chamber, indicating heavy flow turbulence and recirculation around the maize ears/cobs. The provision of multiple flow inlets at the drying chamber enable a perfect flow distribution and enhances moisture evaporation from the maize ears. Based on the results obtained, it is evident that increasing both the drying air velocity and temperature at the inlet of the solar collector improves the drying process of solar grain dryers.

REFERENCES

1. O. V. Ekechukwu, and B. Norton, "Design and measured performance of a solar chimney for natural-circulation solar-energy dryers," *Renewable Energy*, vol. 10 no. 1, 1997, pp. 81-90. https://doi.org/10.1016/0960-1481(96)00005-5.
2. P. Demissie, M. Hayelom, A. Kassaye, A. Hailesilassie, M. Gebrehiwot and M. Vanierschot, "Design, development and CFD modeling of indirect solar food dryer," Proceedings of the 10th International Conference on Applied Energy, Hong Kong. Energy Procedia, vol. 158, 2019, pp. 1128-1134. https://doi.org/10.1016/j.egypro.2019.01.278.
3. A. Lingayat, V. P. Chandramohan and V. R. K. Raju, "Design, development and performance of indirect type solar dryer for banana drying," *Energy Procedia*, vol. 109, 2017, pp. 409-416. https://doi.org/10.1016/j.egypro.2017.03.041.
4. P. D. Tegenaw, M. G. Gebrehiwot and M. Vanierschot, "Design and CFD modeling of a solar food drier," Proceedings of the 6th European Drying Conference, Belgium. Euro Drying, June 2017, pp. 183–184.
5. Y. Amanlou and A. Zomorodian, "Applying CFD for designing a new fruit cabinet dryer," *Journal of Food Engineering*, vol. 101, no. 1, 2010, pp. 8-15, https://doi.org/10.1016/j.jfoodeng.2010.06.001.
6. T Norton, B. Tiwari and D. W. Sun, "Computational fluid dynamics in the design and analysis of thermal processes: a review of recent advances," *Critical Review in Food Science and Nutrition*, vol. 53, no. 3, pp. 2013, 251-275. https://doi.org/10.1080/10408398.2010.518256.
7. A. A. Ambesange and S. K. Kusekar, "Analysis of flow through solar dryer DUCT using CFD," *International Journal of Engineering Development and Research*, vol. 5, no. 1, 2017.
8. T. Norton and D. W. Sun, "CFD: An innovative and effective design tool for the food industry." In *Food Engineering Interfaces*, J. Aguilera, R. Simpson, J. Welti-Chanes, D. Bermudez-Aguirre, ands G. Barbosa-Canovas, (Eds). Food Engineering Series. New York, NY: Springer, 2010, pp. 55-68. https://doi.org/10.1007/978-1-4419-7475-4_3.
9. W. R. Fox, J. P. Pritchard and T. A. Macdonald. Introduction to Fluid Mechanics. 7th ed. New Delhi, India: John Wiley & Sons, 2010, pp. 161-205.
10. COMSOL INC. Navier-Stokes Equations. In *Multiphysics Cyclopedia*, 2017. Available at https://www.comsol.com/multiphysics/navier-stokes-equations.
11. J. T. Norton and D. W. Sun, "Computational fluid dynamics (CFD) – an effective and efficient design and analysis tool for the food industry: a review," *Trends in Food Science & Technology*, vol. 17, no. 11, 2006, pp. 600-620. https://doi.org/10.1016/j.tifs.2006.05.004.
12. J. Guerrero. *Introduction to Computational Fluid Dynamics: Governing Equations, Turbulence Modelling Introduction and Finite Volume Discretization Basics*. 2015. https://doi.org/10.13140/RG.2.1.1396.4644.
13. I. Sadrehaghighi. *Turbulence Modeling – A Review. CFD Open Series, Patch 1.85.9*, 2019. https://doi.org/10.13140/RG.2.2.35857.33129/2.
14. S. Pope. *Turbulent Flows*. Cambridge: Cambridge University Press, 2000.

AUTHOR PROFILES

Johannes P. Angula holds a BSc Mechanical Engineering from the University of KwaZulu-Natal, South Africa. He has worked as a locomotive maintenance engineer and, research and development engineer for 5 years. His area of research focuses on renewable and green energy technologies with emphasis on solar drying systems. Mr. Angula is a member of the Engineering Council of Namibia and has published three articles on solar drying, computational fluid dynamics (CFD) in solar drying, and on the optimization of solar dryers through thermal energy storage systems.

Professor Freddie Inambao holds an MSc and Ph.D. (Technical Sciences) from Volgograd Polytechnic Institute, Russia. He has lectured in several Universities: University of Zambia, University of Botswana, University of Durban-Westville and University of KwaZulu-Natal (UKZN). Professor Inambao is a Principal Advisor of the Green Energy Solutions Research Group (UKZN). Professor Inambao's research and educational efforts focus on: energy efficiency, alternative energy systems, renewable energy, energy management, energy audit, energy and fuels, HVAC, low temperature power generation; water purification and desalination. Professor Inambao has directly supervised and graduated more than 30 MSc, Ph.D students and postdoctoral associates and is currently supervising over 20 postgraduates: He is author of more than 130 articles in peer-reviewed international journals and 130 conference proceedings, a co-author of 12 books and two chapters in books. Professor Inambao is a recipient of several prestigious awards: Top 30 Publishing Researcher Award for 2016 to 2019 UKZN; College of Agriculture, Engineering and Science Research Awards 2019; JW Nelson Research Productivity Award for 2013 to 2019.

NOMENCLATURE

∇	Vector operator
$\vec{V}$	Fluid velocity (m/s)
t	Time (m)
ρ	flow density (kg/m^3)
μ	fluid dynamic viscosity (kg/m.s)
p	local thermodynamic pressure (N/m^2)
C_a	specific heat capacity of the fluid (W/kg.K)
T	temperature of the fluid (K)
x_i	rectangular coordinate (m) of the fluid element
u_i	fluid velocity component in the respective coordinate
γ	thermal conductivity (W/m.K)
S_T	Energy added or work done on the fluid element (J)
coeff	Coefficient that must be fine-tuned and can be interpreted as a relaxation time
α_l	Liquid volume fraction
ρ_l	Liquid density (kg/m^3)
α_v	Vapor volume fraction
ρ_v	Vapor density (kg/m^3)
$\dot{m}_{i \to v}$	Transfer of mass during evaporation or condensation

CHAPTER 6

6. PERFORMANCE EVALUATION OF A FORCED CONVECTION MIXED-MODE SOLAR GRAIN DRYER WITH A PREHEATER

This chapter presents work that were published under the title "Performance Evaluation of a Forced Convection Mixed-mode Solar Grain Dryer with a Preheater" in the *International Journal of Innovative Technology and Exploring Engineering* (IJITEE). A journal accredited by the Department of High Education and Training (DHET) of South Africa.

To cite this article:

Johannes P. Angula and Freddie Inambao, Performance Evaluation of a Forced Convection Mixed-mode Solar Grain Dryer with a Preheater, *International Journal of Innovative Technology and Exploring Engineering* (IJITEE), 10(4), 2021, pp. 41-51.

The link to this article:

DOI: 10.35940/ijitee.D8443.0210421

Performance Evaluation of a Forced Convection Mixed-Mode Solar Grain Dryer with a Preheater

Johannes P. Angula, Freddie Inambao

Abstract: In this study the performance of a forced convection mixed-mode solar grain dryer integrated with a preheater was evaluated. The type of grains used in the experiment were 72 freshly harvested maize cobs with a total mass of 17 kg. The experiment was conducted at various airflow speeds and preheater temperatures ranging from 0.5 m/s to 2 m/s and 30 °C to 40 °C, respectively. The aim of the study was to improve the performance of an existing indirect solar dryer which was converted to a mixed-mode solar dryer. The initial thermal efficiency of the indirect solar dryer before modification was 36 %. The results from the experiment indicated a maximum thermal efficiency of 58.8 % with a corresponding drying rate of 0.0438 kg/hr. The minimum thermal efficiency for the mixed-mode solar grain dryer system was 47.7 %, with a corresponding drying rate of 0.0356 kg/hr. The fastest drying time of maize cobs was achieved in 4 hours and 34 minutes from an initial moisture content of 24.7 % wb to 12.5 % wb. The findings show a significant improvement in the dryer system's performance. This is a clear indication that operating a solar dryer system in mixed-mode operation with forced convection and the assistance of a preheater or backup heater can significantly improve drying processes and increase food preservation.

Keywords: Mixed-mode operation, Solar drying, Maize cobs, Thermal efficiency, Preheater, Forced convection.

I. INTRODUCTION

The use of solar energy in agricultural applications such as solar grain dryers is widely accepted in many parts of the world as a green energy solution [1]. Solar drying of grains involves using solar thermal energy to remove moisture from grains in order to obtain a moisture level that is desirable for safe storage of the grains. According to Kenneth et al. [2], the storage temperature of grains and the amount of moisture in the grains can determine the maximum storage time without compromising on its quality. Research shows that maize grains can be safely stored and preserved for a long period if the level of moisture content is not more than 13 % wb [2], [3]. Maize is a family of grains, and grains are one of the healthiest foods and a primary source of carbohydrate consumed worldwide. Maize is a staple food in many parts of the world, particularly in underdeveloped and developing countries such as South Africa. In South Africa, maize is consumed by about 60 % of the country's population [4]. It forms part of a healthy diet of human beings and it is also served as a delicacy to animals. Research indicates that most maize farmers in South Africa, including subsistence farmers,

rely on the open-air sun drying method for maize; a conventional drying method that leads to unfavorable outcomes [1]. In general, there are three types of solar drying techniques that can be used to dry crops; (i) direct solar drying, (ii) indirect solar drying, and (iii) mixed-mode solar drying. More details on the different types of solar drying techniques can be found in many available literature such as [5]–[8]. With the use of appropriate drying techniques such as using a forced convection mixed-mode solar dryer with a preheater or backup heater, the drying process can be significantly improved, particularly in high humidity areas such as coastal towns. This study was based on the operation principles of mixed-mode solar drying in which maize cobs were the subject of the drying process. This method uses a forced convection mixed-mode solar dryer which is integrated with a preheater for maximum performance. The solar dryer used for the experiment was a modification of an existing solar dryer developed by the Department of Mechanical Engineering at the University of KwaZulu-Natal, Durban, South Africa [9]. Initially, the solar dryer was designed as an indirect solar dryer system for drying faecal sludge. It was reported that this prototype solar dryer had a thermal efficiency of 36 % and was able to dry synthetic faecal sludge in 12 hours from an initial moisture content of 70 % wb to 20 % wb. Despite the longer drying time, it was also found that the solar collector could not heat air to a sufficiently high temperature due to the inconsistency of incident solar irradiation and the high humidity of the atmosphere. In order to improve the thermal performance and drying process for the existing indirect solar dryer system it was necessary to change its operation to mixed-mode. The main modification made was to incorporate a preheater and forced convection airflow in order to increase the drying rate. The aim of this study was to improve the performance of the solar dryer by increasing its thermal efficiency and drying rate.

II. RESEARCH SITE

The research was conducted at the University of KwaZulu-Natal, Howard College campus in Durban located at 29.9° South, 30.98° East, and at an elevation of 151.3 m above sea level. The city has a hot humid subtropical climate with temperatures ranging from as low as 9.4 °C in winter to as high as 30.8 °C in summer. According to meteorological data from the Virginia weather station in Durban, the relative humidity of this coastal city can be as high as 95 %. Research indicates that the daily average sunlight hours in Durban is around 6 hours and 24 minutes per year.

Johannes P. Angula*, Department of Mechanical Engineering, University of KwaZulu-Natal, Durban, South Africa. Email: 210546069@stu.ukzn.ac.za

Freddie Inambao, Department of Mechanical Engineering, University of KwaZulu-Natal, Durban, South Africa. Email: Inambaof@ukzn.ac.za https://orcid.org/0000-0001-9922-5434

41

Performance Evaluation of a Forced Convection Mixed-Mode Solar Grain Dryer with a Preheater

The annual average values of Direct Normal Irradiance (DNI) and Global Horizontal Irradiance (GHI) are 1574 kWh/m2 and 1638 kWh/m2, respectively [10].

III. METHODOLOGY

A. Materials and Experiment Setup

To set up the experiment, the following materials were used for the experiment:

- A solar dryer system
- 72 fresh maize mealies (17 kg batch)
- A preheater/air heater
- PID temperature controller
- An RTD temperature sensor for the temperature controller
- Solid-state relay for the temperature controller
- Supply of compressed air through an air dryer
- A needle flow valve
- NI USB-6000 data logger
- Four temperature and humidity sensor probes
- Electrical wiring, piping and fittings

- Moisture meter
- Anemometer
- Laptop
- AC/DC voltage supply

Experimental data were measured using four positioned HTM2500LF sensor probes (denoted S1, S3, S4, and S5 in Fig. 1) and logged by a data logger for analytical purposes through the use of a laptop. The experiment was conducted for the same number of trials under the same temperature and airflow velocity conditions of the preheater as performed during the simulation. A few electrical modifications were made to the equipment, such as to employ a temperature controller on the preheater and rewiring of the heating elements to lower their amperage. This was done because, initially, the preheater did not have a temperature control circuit. The preheater temperature control circuit included a PID temperature controller, a solid-state relay (SSR), and an RTD temperature sensor probe (denoted S2 in Fig. 2). Fig. 2 shows the control layout schematic for the experimental setup, while Fig. 2 shows the complete experimental setup.
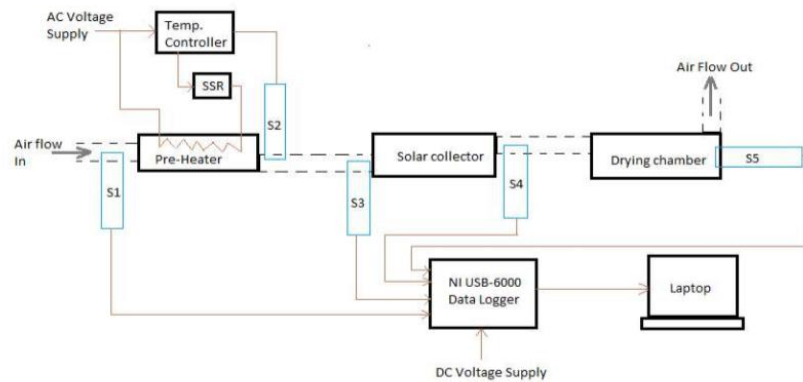

Fig. 1. Electrical control layout and connections of the solar dryer system

Fig. 2. Complete experimental setup of the solar dryer system

42

B. Experimental Procedures

Calibration of the sensors preceded the experimental procedures to ensure correct measurements were taken by each sensor positioned across the dryer system. The experimental procedures undertaken in this study were as follows:

a) Securely position one sensor probe at the preheater's inlet, one sensor probe at the solar collector outlet, another one at the inlet of the drying chamber, and the last one at the drying chamber outlet.

b) Prepare 8 maize cobs by removing the corn husks and measuring each maize cob's moisture content using the moisture meter. Average moisture content is used as the initial moisture content.

c) Through an air dryer, turn on the compressed air supply line.

d) With the use of a needle flow control valve and an anemometer, adjust the airflow to 0.5 m/s at the solar collector's inlet.

e) With the use of the temperature controller, set the temperature of the preheater to 30 °C.

f) Securely position 6 maize cobs in the drying chamber and the remaining 2 dehusked maize cobs on the open-sun drying tray.

g) Connect the USB cable from the NI USB-6000 data logger to the laptop and open the DAQ Express software application.

h) Once the software application opens, choose analogue inputs and add 8 input channels because there are two input signals (temperature and humidity) from each sensor probe.

i) On the software application window, change the sampling rate to 9 minutes (0.00185185 Hz) so that measurements are taken every 9 minutes.

j) Start recording the four sensor probes' readings until a final moisture content of less than 13 % wb is achieved.

k) While the laptop monitors and stores readings from the four sensors, use the moisture meter to keep measuring and recording the moisture content of maize cobs inside the drying chamber and in the open sun every 20 minutes (for the first 1-hour) then every after 15 minutes (after 1-hour drying).

l) Maintain the drying parameters until a moisture content safe for grain storage is achieved. The recommended moisture content for safe storage of grains is 13 % wb or less.

m) Once a moisture content of less than 13 % wb is achieved, repeat the above steps for the following drying parameters:

- Airflow at 0.5 m/s and preheater temperature of 35 °C.
- Airflow at 0.5 m/s and preheater temperature of 40 °C.
- Airflow at 1 m/s and preheater temperature of 30 °C.
- Airflow at 1 m/s and preheater temperature of 35 °C.
- Airflow at 1 m/s and preheater temperature of 40 °C.
- Airflow at 2 m/s and preheater temperature of 30 °C.
- Airflow at 2 m/s and preheater temperature of 35 °C.
- Airflow at 2 m/s and preheater temperature of 40 °C

n) Safely disconnect all electronic devices from the power supply and analyse the data.

The type of maize cobs and the moisture meter used in the experiment are shown in Fig. 3. For each experiment conducted, 8 maize cobs were used and tested for the right level of moisture content.

.

Fig. 3. Sample maize cobs (left) and moisture meter (right) measuring the moisture content of one of the dehusked maize cobs

Performance Evaluation of a Forced Convection Mixed-Mode Solar Grain Dryer with a Preheater

IV. RESULTS AND DISCUSSION

The entire experimental process was carried out in 11 days in the month of September and October (spring) that were chosen with good sunlight between 09h00 and 16h00. The first two days were used for the experimental setup and dry-run tests to ensure all equipment was functioning as needed, with the experiment being conducted on the remaining nine days. Based on the weather information, the data for Durban solar energy during the period of experiment indicated that the average daily incident solar irradiance was between 4.8 kWh/m^2 and 5.5 kWh/m^2 for September between 5.6 kWh/m^2 and 6.5 kWh/m^2 for October [11]. During the experiment, it was necessary to record the ambient weather temperature and relative humidity. Table 1 shows the minimum and maximum temperature and relative humidity values as recorded between 09h00 and 16h00.

The inconsistency of the weather patterns resulted in the fluctuation of atmospheric air temperature and relative humidity. As shown in Table 1, on some days the ambient temperature was as low as 16.4 ℃ and as high as 32.3 ℃. Due to Durban's highly humid weather, the ambient relative humidity fluctuated between 46 % and 81 % during the experiment. The variation of temperature and relative humidity for drying air across the dryer system was measured by four HTML2500LF sensor probes. The results are presented and discussed in the following sub-sections. Each graph shows the minimum and maximum value recorded during that period.

Table 1. Ambient weather conditions during the period of the experiments

	Ambient Temperature		Ambient Relative humidity	
	Minimum Temperature (℃)	*Maximum Temperature (℃)*	*Minimum Relative Humidity (%)*	*Maximum Relative Humidity (%)*
Day 1	18,9	27,8	52	81
Day 2	20,1	31,6	42	76
Day 3	19,8	28,2	50	79
Day 4	21,6	32,3	46	65
Day 5	17,8	26,8	58	71
Day 6	18,1	29,3	57	80
Day 7	16,4	28,4	51	68
Day 8	19,4	32,1	46	70
Day 9	20,4	29,5	48	74

The inconsistency of the weather patterns resulted in the fluctuation of atmospheric air temperature and relative humidity. As shown in Table 1, on some days the ambient temperature was as low as 16.4 ℃ and as high as 32.3 ℃. Due to Durban's highly humid weather, the ambient relative humidity fluctuated between 46 % and 81 % during the experiment. The variation of temperature and relative humidity for drying air across the dryer system was measured by four HTML2500LF sensor probes. The results are presented and discussed in the following sub-sections. Each graph shows the minimum and maximum value recorded during that period.

B. Variation of Temperature and Relative Humidity Across the Dryer System

The analog output logged by the data logger from the sensors was in voltages and needed to be converted from voltage to temperature and relative humidity values. The following polynomial equations (1) and (2), available in the data sheet for the HTM2500LF sensor probes, were used for the conversion.

Relative Humidity:

$$RH\ (\%) = (-1.92 \times 10^{-9} \times V^3) + (1.44 \times 10^{-5} \times V^2) + (3.4 \times 10^{-3} \times V) - 12.4 \tag{1}$$

Temperature:

$$T(℃) = (-2.428 \times 10^{-9} \times V^3) + (2 \times 10^{-5} \times V^2) - (7.419 \times 10^{-2} \times V) + 123.324 \tag{2}$$

Where V is the sensor output voltage in mV
results of these variations are shown in Fig. 4 and Fig 5

1) *Average Temperature and Relative Humidity at 30 ℃ Preheated Air*

The temperature of the weather in Durban is mostly below 30 ℃, although in some cases, the temperature surpassed 30 ℃. During the low-temperature periods, the air entering the solar collector was preheated to 30 ℃. The variations in temperature and relative humidity as the air navigated through the solar dryer system from the preheater were measured and recorded. As measured by the sensors, the results of these variations are shown in Fig. 4 and Fig 5.

The figures in Fig. 4 and Fig. 5 indicate the results for the first 3 hours and 9 minutes when maximum temperature gain across the solar collector was recorded. As shown in Fig. 4, there was a substantial gain in air temperature at the solar collector outlet, which corresponded to a relative reduction in humidity. A significant decrease in air temperature across the drying chamber was recorded. As shown in Fig. 5, there was a slight increase in the relative humidity within the drying chamber due to the moisture evaporation during the drying process
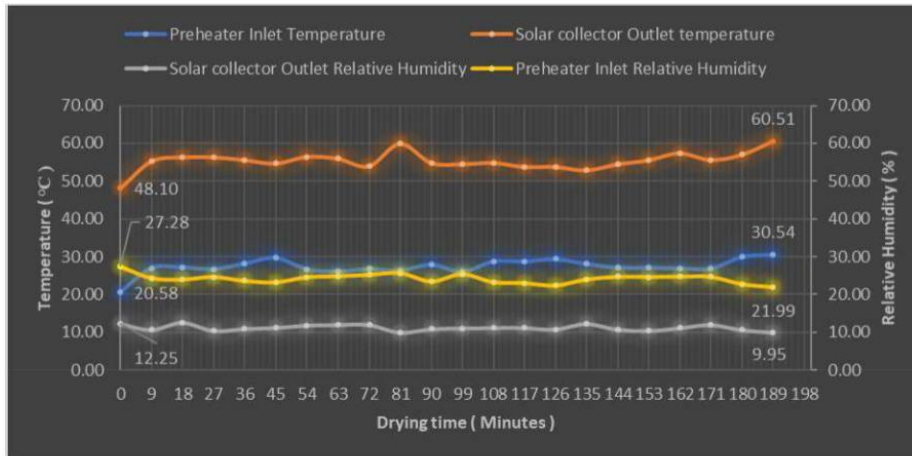
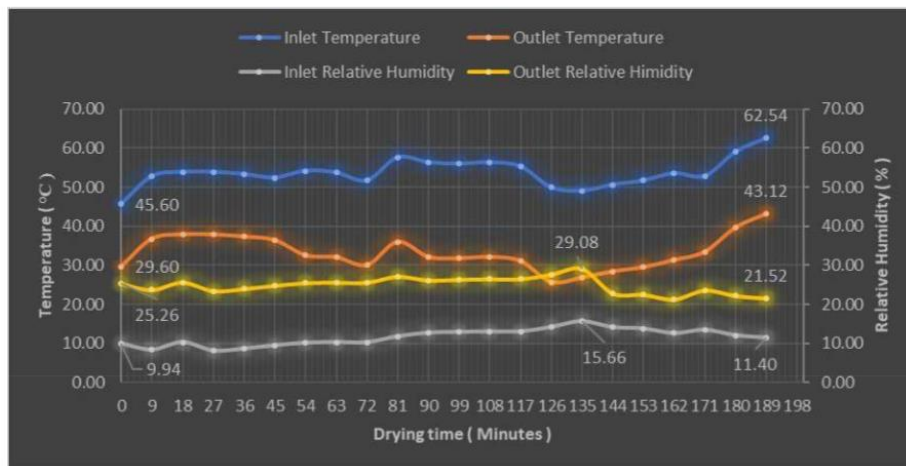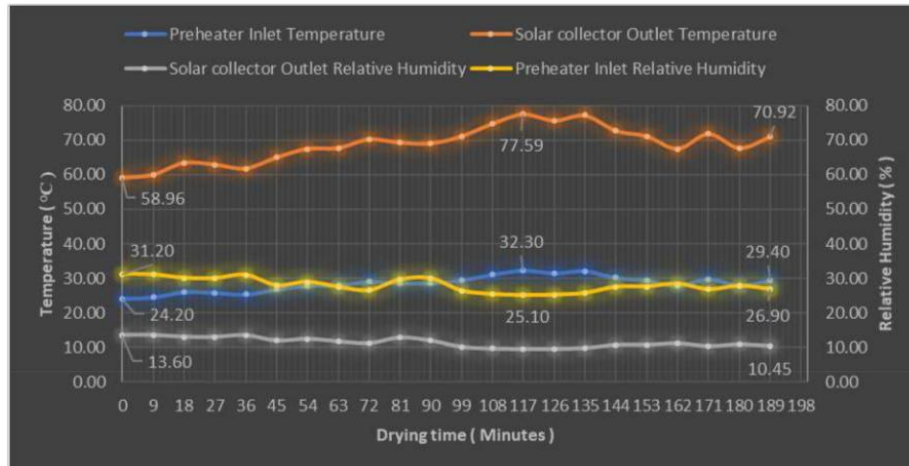**Fig. 4. Temperature and relative humidity variation across the preheater-to-solar collector unit**

Fig 5. Temperature and relative humidity variation across the drying chamber unit.

36 ℃.

2) Average Temperature and Relative Humidity at 36 ℃ Preheated Air

The graphs shown in Fig. 6 and Fig. 7 indicate the results during the first 3 hours and 9 minutes as measured by the sensors when air entering the solar collector was preheated to

It is also evident from the graphs that there was a gain in temperature during air heating (across the solar collector) and a reduction in air temperature during drying processes (across the drying chamber). However, the gain in air temperature was not consistent throughout the drying process.

45

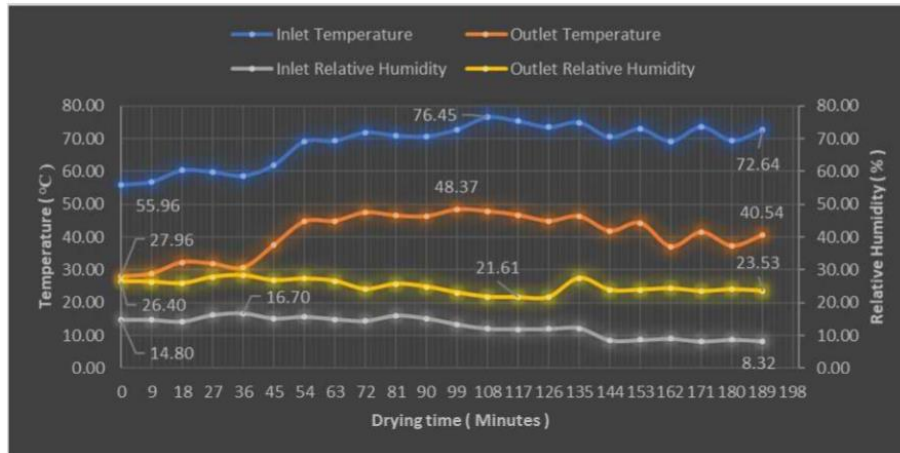**Fig. 6. Temperature and relative humidity variation across the preheater-to-solar collector unit**

Fig. 7. Temperature and relative humidity variation across the drying chamber unit

3) Average Temperature and Relative Humidity at 40 ℃ Preheated Air

The experiment included preheating the air to 40 ℃ before entering the solar collector unit. The temperature and relative humidity across the solar dryer system obtained during the first 3 hours and 9 minutes are shown in Fig. 8 and Fig. 9. The results indicate these were the highest drying air temperature recorded during the experiment.

High temperatures associated with very low relative humidity at the solar collector's outlet yielded maximum drying parameters at the drying chamber. A comparison of results from Fig. 4 and Fig. 8 indicates that preheating air from 30 ℃ to 40℃ results in a maximum temperature gain of about 18 ℃. The ambient weather conditions vary with time, consequently, these inconsistencies result in the fluctuations of the drying parameters, as shown by the graphs in all the above figures. Although the preheating of air significantly improves the drying process, it is crucial to consider the optimum temperature for drying specific food items. Depending on the application, different food items such as grains have various temperatures recommended for safe drying.
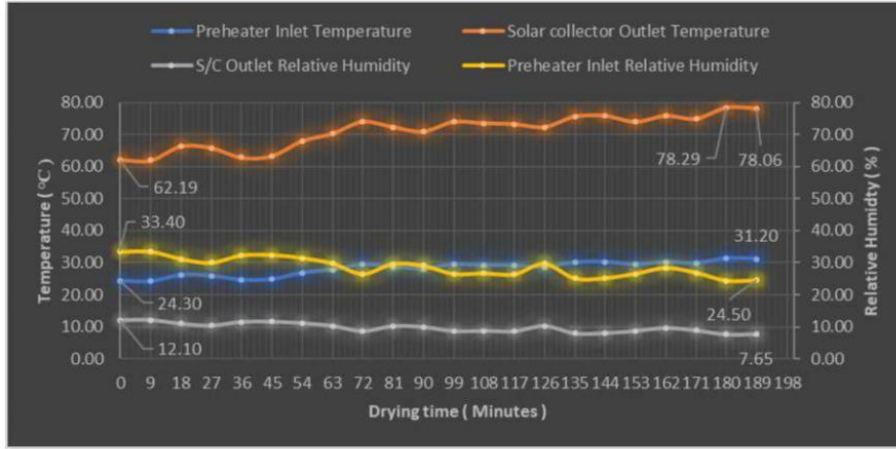
46

Fig. 8. Temperature and relative humidity variation across the preheater-to-solar collector unit
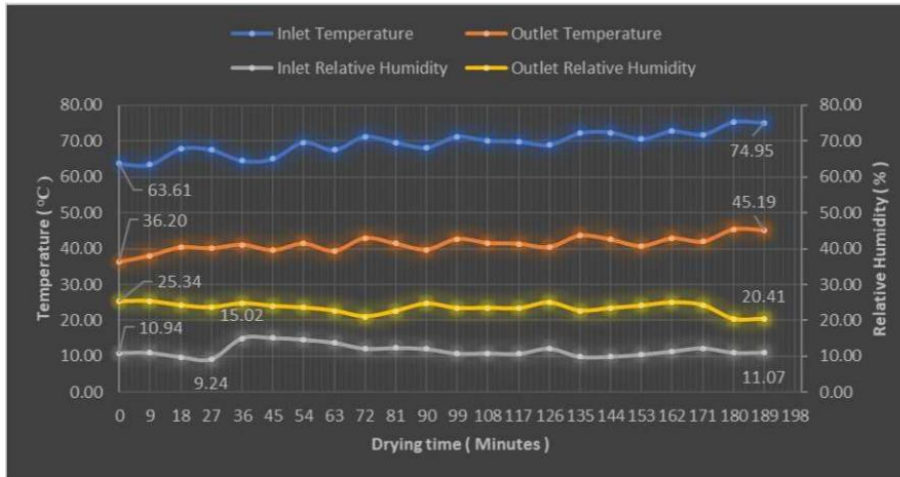

Fig. 9. Temperature and relative humidity variation across the drying chamber unit

C. Variation of Moisture Content During Drying Processes

The moisture content results measured using a moisture meter during the experimental period are shown in the figures below. Fig. 10 shows the results of day 1 to day 3, Fig. 11 shows the results of day 4 to day 6, and Fig. 12 shows the results of the last three days (day 7-9). Fig. 13 shows the results of moisture content during open sun drying that were recorded between day 1 and day 3. The final moisture content and the corresponding drying time are displayed at the end of each line graph. For example, in Fig. 10 air that was preheated to 30 ℃ with a flow speed of 0.5 m/s yielded a final moisture content of 12.8 % (wb) in 394 minutes (6 hours and 34 minutes)

47

Performance Evaluation of a Forced Convection Mixed-Mode Solar Grain Dryer with a Preheater
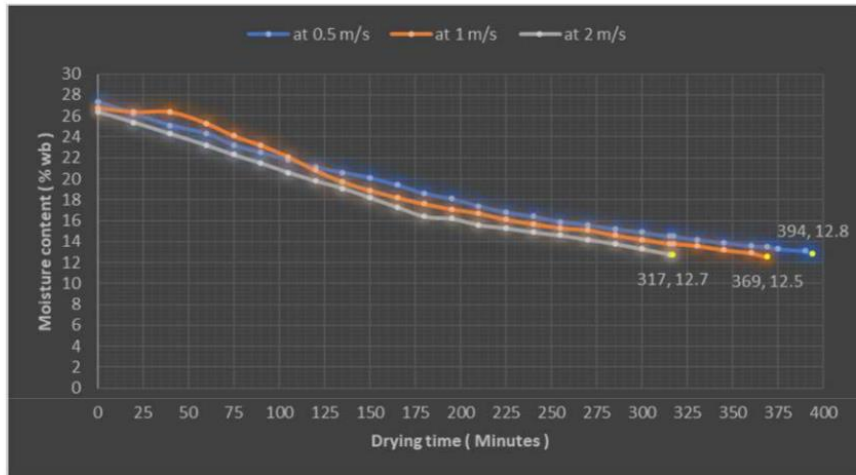

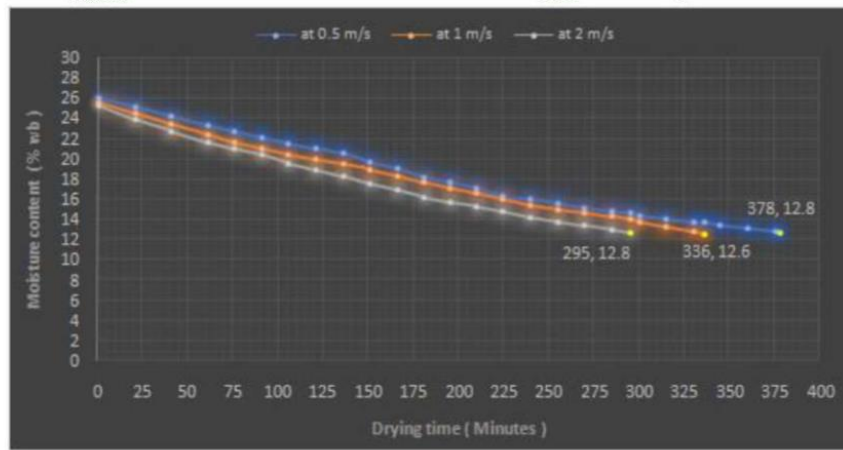**Fig. 10. Moisture content of maize corn at various air flow with 30 °C preheated air**

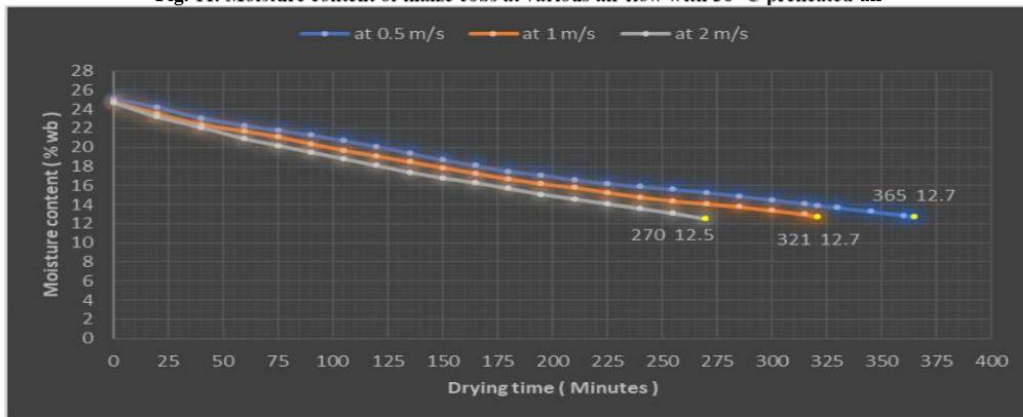**Fig. 11. Moisture content of maize cobs at various air flow with 36 °C preheated air**

Fig. 12. Moisture content of maize cobs at various air flow with 40 °C preheated air
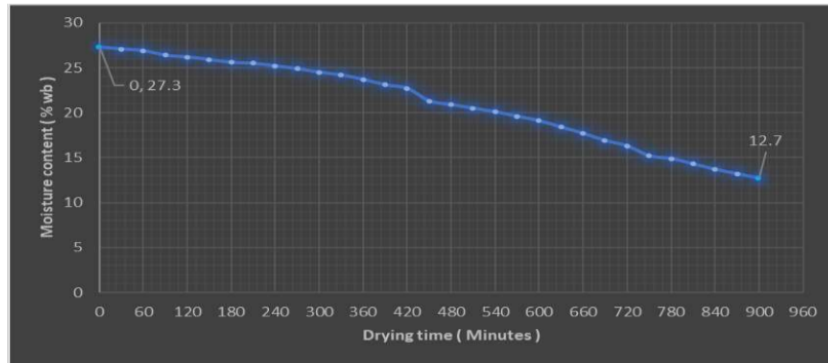
Fig. 13. Moisture content of maize cobs during open sun drying

Overall, the results shown in the above figures indicate that maximum drying was achieved at an airflow of 2 m/s using 40 °C preheated air. The average initial moisture content of the maize cobs was 24.7 % (wb), and this was reduced to a final moisture content of 12.5 % (wb) in 270 minutes (4 hours and 30 minutes) as shown in Fig. 12. The minimum drying of maize cobs using the solar dryer system occurred in 394 minutes (6 hours and 34 minutes) at an airflow of 0.5 m/s as shown in Fig. 10. Drying of maize cobs in the open sun was conducted in order to develop a reference of improvement. Open sun drying is associated with many disadvantages such as longer drying time. This can be seen in the results in Fig. 13 whereby drying of maize cobs was achieved in 900 minutes (15 hours). A drying period of 15 hours was achieved after two consecutive days of open sun drying experiment.

D. Performance Evaluation

This section analyzes the performance of the dryer system using the experimental results. The results enable the minimum and maximum thermal efficiencies of the dryer system to be calculated. In addition, minimum and maximum drying rates are also calculated to determine the hourly moisture removal from maize cobs.

1) Dryer Efficiency

The process of drying food products involves the removal of water that is contained within the food structure. In order for this process to happen, a minimum amount of heat is required to evaporate water from the food products. The minimum amount of heat required to evaporate water is referred to as the latent heat of vaporization. In practice, sensible heat needs to be incorporated in calculating the efficiency of the dryer. Sensible heat accounts for the heat required to raise the temperature of the food product being dried. In this study, the sensible heat was calculated based on the specific heat capacity of grains as defined by equation 4 provided in the study of Verma and Prasad [12].

In this study, the dryer system's efficiency was defined as the ratio of the latent heat of vaporization plus sensible heat to the useful heat gained by drying air as it navigates from the preheater through the solar collector to the drying chamber. Equation (3) indicates the formula used in calculating both maximum and minimum efficiency.

$$\eta_{sys} = \frac{(M_w \times L_v) + (M_g \times C_{pg} \times \Delta T)}{M_a \, C_{pa}(T_{dc} - T_{amb})} \quad (3)$$

Whereby:

M_w = Mass of evaporated water (kg)
L_v = Latent heat of vaporization (kJ/kg)
M_g = Mass of the dried product (kg)
ΔT = Change in temperature of maize grains (°C)
M_a = Total quantity air needed to evaporate water (kg)
T_{dc} = Temperature of drying air entering the drying chamber (°C)
T_{amb} = Temperature of ambient air (°C)
C_{pa} = Specific heat capacity of air (kJ/kg.K)
C_{pg} = Specific heat capacity of maize grains (kJ/kg.K)

$$= 1.3066 + 1.2045 M_d + 0.0198T \quad (4)$$

Whereby "T" and "M_d" are the dried grains' temperature and moisture content, respectively.

The mass of evaporated water is calculated based on the percentage of moisture content and the food products' total mass before drying. This relationship is given by (5).

$$M_w = M_p \left(\frac{M_i - M_f}{100 - M_f} \right) \quad (5)$$

Whereby:

M_p = Total mass of the maize grains = 1.41 kg (6 maize cobs were used per solar drying experiment with an average mass of 235 g each)
M_i = Initial moisture content of maize grains (% wb)
M_f = Final moisture content of maize grains (% wb)

Maximum dryer system efficiency

The maximum efficiency calculations were based on the experimental results for maximum drying, which was achieved when air was preheated to 40 °C at an air flow of 2 m/s. At maximum efficiency, drying of maize cobs was achieved in 4 hours and 30 minutes, and the volume of air needed for drying was 14.076 m³. Using information from Fig. 9 and Fig. 12, maximum efficiency can be calculated by substituting the following information.

M_i =24.7 %
M_f = 12.5 %
M_w = 0.197 kg
$M_g = M_p - M_w$ = 1.213 kg
M_a = *density × volume* = 16.666 kg (using air density of 1.184 kg at room temperature)

C_{pa} = 1.952 kj/kg.k (using final moisture content and assuming maize are at room temperature of 25 °C after drying)

ΔT = 20.19 °C

T_{amb} = 25 °C (assumed to be at room temperature)

T_{dc} = 74.95 °C

L_v = 2257 kj/kg

C_{pa} = 1.006 kj/kg.k

The above information yielded a maximum efficiency, η_{sys} = **58.8 %**

Minimum dryer system efficiency

The minimum efficiency calculations were based on the experimental results for minimum drying, which was achieved when air was preheated to 30 °C at an airflow of 0.5 m/s. At minimum efficiency, drying of maize cobs was completed in 6 hours and 34 minutes, and the volume of air needed for drying was 26.721 m³. Using information from Fig. 5 and Fig. 10, minimum efficiency can be calculated by substituting the following information:

M_i = 27.3 %

M_f = 12.8 %

M_w = 0.234 kg

$M_g = M_p - M_w$ = 1.176 kg

$M_a = density \times volume$ = 31.638 kg (using air density of 1.184 kg at room temperature)

C_{pa} = 1.956 kj/kg.k (using final moisture content and assuming maize are at room temperature of 25 °C after drying)

ΔT = 18.12 °C

T_{amb} = 25 °C (assumed to be at room temperature)

T_{dc} = 62.54 °C

L_v = 2257 kj/kg

C_{pa} = 1.006 kj/kg.k

The above information yielded a minimum efficiency, η_{sys} = **47.7 %**

2) *Drying Rate*

The drying rate of a solar dryer is defined as the ratio of the mass of evaporated water 'M$_w$' from the food product to the time 't$_d$' required to dry the food product. This relationship can be expressed by (5) as follows:

$$Drying\ rate\ (kg/hr) = \frac{M_w}{t_d} \qquad (5)$$

Using the information provided in the previous section, the following can be derived:

Maximum drying rate = **0.0438** kg/hr

Minimum drying rate = **0.0356** kg/hr

The solar dryer system's efficiency at minimum drying condition (47.7 %) is even higher than the initial efficiency (36 %) of the solar dryer system before modification. This is a clear indication that operating a solar dryer in mixed-mode operation with a preheater/backup-up heater and forced convection improves the dryer's performance. An efficient solar dryer will yield high drying capacity, resulting in enhanced grains harvest and storage capacity.

V. CONCLUSION

The performance of a forced convection mixed-mode solar grain dryer integrated with a preheater was evaluated in this study. The dryer system's performance results indicated a maximum thermal efficiency of 58.8 % with a corresponding drying rate of 0.0438 kg/hr. The minimum thermal efficiency for the dryer system was 47.7 %, with a corresponding drying rate of 0.0356 kg/hr. The fastest drying time of maize cobs was achieved in 4 hours and 34 minutes (within one day of drying) using the dryer system from an initial moisture content of 24.7 % wb to 12.5 % wb. Open sun drying yielded the slowest drying time of 15 hours (within 3 days of drying) from an initial moisture content of 27.3 % wb to 12.7 % wb. The results show a significant improvement of the mixed mode dryer system compared to the initial thermal efficiency of the indirect solar dryer before modification which was 36 %. This is a clear indication that operating a dryer system in mixed mode operation using forced convection drying air with the assistance of a preheater or backup heater can significantly improve drying processes. An efficient dryer system can lead to improved harvests and increased grain storage capacity.

REFERENCES

1. A. O. Akinola, and O. P. Fapetu, "Exergetic analysis of a mixed-mode solar dryer," *Journal of Engineering and Applied Sciences,* vol 1, 2006, pp. 205-10.
2. J. Kenneth, and P. E. Hellevang, Recommended Storage Moisture Contents and Estimated Allowable Storage Times, 2013. https://www.ag.ndsu.edu/publications/crops/grain-
3. Drying the Grain. n.d. https://www.shareweb.ch/site/Agriculture-and-Food-Security/focusareas/Documents/phm_postcosecha_drying_grain_e.pdf.
4. J. Du Plessis, Maize Production, Agricultural Research Council, 2003. https://www.arc.agric.za/arc-gci/Pages/Fact-Sheets.aspx.
5. A. Sharma, C. R. Chen, and N. Vu Lan, "Solar-drying systems: a review," *Renewable and Sustainable Energy Reviews*, vol. 13, , no. 6-7, 2009pp. 1185-1210. https://doi.org/10.1016/j.rser.2008.08.015
6. O. V Ekechukwu, and B. Norton, "Review of solar-energy drying systems II: an overview of solar drying technology," *Energy Conversion Management*, vol. 40 no. 6, 1999, pp. 615-655. https://doi.org/10.1016/S0196-8904(98)00093-4
7. W. Weiss, and J. Buchinger, Solar drying, Trainings course on the production and sale of solar thermal plants in Zimbabwe. Arbeitsgemeinschaft Erneuerbare Energie (AEE) of the Institute for Sustainable Technologies, Austria, 2001.
8. V. Belessiotis, and E. Delyannis, "Solar drying," *Solar Energy*, vol. 85, no. 8, pp. 1665-1691, 2010. https://doi.org/10.1016/j.solener.2009.10.001.
9. F. L. Inambo, and S. S. Stringel. Development of a Solar Dryer. Green Energy Solution Research Group. Department of Mechanical Engineering. University of KwaZulu-Natal, Durban, South Africa.
10. M. Suri, T. Cebecauer, A. J. Meyer, and J. L. Van Niekerk, Accuracy-Enhanced Solar Resource Maps of South Africa. Proceedings of the 3rd Southern African Solar Energy Conference, Kruger National Park, South Africa, pp. 450-456, 2015. http://hdl.handle.net/2263/49525.
11. Durban Solar Energy. n.d. https://weatherspark.com/m/96783/10/Average-Weather-in-October-in-Durban-South-Africa#Sections-SolarEnergy
12. R. C. Verma, and S. Prasad, "Mechanical and thermal properties of maize," *Journal of Food Science and Technology*, vol. 37, no. 5, 2000, pp. 500-505. https://www.researchgate.net/publication/297790797_Mechanical_and_thermal_properties_of_maize.

AUTHOR PROFILES

Johannes P. Angula holds a BSc Mechanical Engineering from the University of KwaZulu-Natal, South Africa. He has worked as a locomotive maintenance engineer and, research and development engineer for 5 years. His area of research focuses on renewable and green energy technologies with emphasis on solar drying systems. Mr. Angula is a member of the Engineering Council of Namibia and has published three articles on solar drying, computational fluid dynamics (CFD) in solar drying, and on the optimization of solar dryers through thermal energy storage systems.

Professor Freddie Inambao . holds an MSc and Ph.D. (Technical Sciences) from Volgograd Polytechnic Institute, Russia. He has lectured in several Universities: University of Zambia, University of Botswana, University of Durban-Westville and University of KwaZulu-Natal (UKZN). Professor Inambao is a Principal Advisor of the Green Energy Solutions Research Group (UKZN). Professor Inambao's research and educational efforts focus on: energy efficiency, alternative energy systems, renewable energy, energy management, energy audit, energy and fuels, HVAC, low temperature power generation; water purification and desalination. Professor Inambao has directly supervised and graduated more than 30 MSc, Ph.D students and postdoctoral associates and is currently supervising over 20 postgraduates: He is author of more than 130 articles in peer-reviewed international journals and 130 conference proceedings, a co-author of 12 books and two chapters in books. Professor Inambao is a recipient of several prestigious awards: Top 30 Publishing Researcher Award for 2016 to 2019 UKZN; College of Agriculture, Engineering and Science Research Awards 2019; JW Nelson Research Productivity Award for 2013 to 2019.

CHAPTER 7

7. OPTIMIZATION OF SOLAR DRYERS THROUGH THERMAL ENERGY STOREAGE: TWO CONCEPTS

This chapter presents work that were published under the title "Optimization of Solar Dryers through Thermal Energy Storage: Two Concepts" in the *International Journal of Engineering Research and Technology* (IJERT). A journal accredited by the Department of High Education and Training (DHET) of South Africa.

To cite this article: Johannes P. Angula and Freddie L. Inambao, Optimization of Solar Dryers through Thermal Energy Storage: Two Concepts, *International Journal of Engineering Research and Technology* (IJERT), 13(10), 2020, pp. 2803-2813.

The link to this article:

https://dx.doi.org/10.37624/IJERT/13.10.2020.2803-2813

Optimization of Solar Dryers through Thermal Energy Storage: Two Concepts

Johannes. P Angula

Department of Mechanical Engineering
University of KwaZulu-Natal, Durban, South Africa.

Freddie L. Inambao*

Department of Mechanical Engineering
University of KwaZulu-Natal, Durban, South Africa.

ORCID: 0000-0001-9922-5434

Abstract

The technology of storing thermal energy is primarily based on using materials that are deemed fit for storing thermal energy which can be discharged for later usage based on the application. Different applications might require thermal energy for heating or cooling purposes; hence, a suitable energy storage material must be selected to efficiently meet the application's demand. This paper focuses on innovative ways of storing solar thermal energy that can be used in to improve the drying processes of conventional solar dryer systems used for food drying. It aims at identifying the most suitable and economical materials that can be used for the design of an optimal thermal energy storage system/unit to store energy from the sun during sunshine hours and release it during non-sunshine hours. The energy stored is aimed at prolonging the drying process and improving thermal efficiency of the solar dryer systems. The research conducted has identified two conceptual designs that are economically viable for the design and construction of a thermal energy storage system. As discussed in this paper, concept 1 utilizes a rock-bed system and concept 2 utilizes a hot water tank to store solar thermal energy. A review of different experiments on thermal energy storage materials by various researcher is also presented in this paper.

Keywords: Thermal energy storage; solar energy; materials; design; performance; cost

I. INTRODUCTION

Solar drying of food and agricultural products provides an effective and economical means of preserving foods in most developing countries. The drying rate can be significantly improved through the use of efficient and optimized solar drying techniques. Solar energy is unreliable due to weather conditions and other factors; however, with the use of appropriate technologies, energy from the sun can be harvested and stored for later usage. One of the effective ways to optimize solar dryer systems is by integration of a thermal energy storage (TES) system. The TES system works on the basis of a thermal energy sensitive material (liquid, solid, or phase change material) that can store solar energy captured during peak hours and release it during off-peak hours so as to prolong the drying process [1].

Recent studies indicate that solar dryers with an integrated

thermal energy storage system are effective for continuous drying at a steady state in temperatures ranging from 40 °C to 60 °C [2]. TES systems are not only used in the solar drying process but are also widely used in buildings and industrial processes such as power generation [5]. Many benefits have been reported in the literature pertaining to the use of TES in energy systems such as [5, 9]:

- Improved thermal efficiency

- Reduction in the utilization of fossil fuel

- Better system reliability

- Environmentally friendly

- Improved energy security

- Improved running costs and general economic value

The ever-increasing global population results in increased food consumption leading to a situation of increased food insecurity which can be addressed through measures such as solar drying. Solar energy is considered as the most economical and feasible way of dealing with the preservation of food and agricultural products. Although solar energy is plentiful and widely accessible for usage, its availability is irregular and periodic. Solar energy is mostly dependent on weather conditions and geographical location, and it is only available during daytime. In applications where solar energy is required for drying, TES system can be employed to take advantage of the availability of solar energy in order to store it and use it when needed. This is particularly the case in regions with less average sunshine hours per day such as humid subtropical regions. Whether energy storage can be justified depends critically on the nature of the demand and supply, and the conditions of operation since some energy storage systems can be charged and discharged several times a day while others are inter-seasonal [7]. In many industrial drying processes, controlled drying uses fossil fuel. However, the use of fossil fuel for energy generation has many negative impacts such as high running cost, environmental effects, and gradual depletion of its reserve [3]. This necessitates further research on harnessing solar energy to improve the drying process and so lead to a reduction in the use of fossil fuel.

South Africa has good sunshine hours throughout the year. Most areas of the country have annual average of at least 2500 hours of sunshine while the daily solar irradiance ranges from a

minimum of 4.5 kWh/m^2 to a maximum of 6.5 kWh/m^2 [4]. South Africa has a high production of agricultural products such as maize (corn). Hence, the potential of solar drying with an integrated TES system can be considered a viable option for both industrial and domestic sector of the country. TES systems are of crucial importance to any system that utilizes mainly solar energy because they compensate for the temporally mismatches during off-peak periods [6]. This paper focuses on the concept of optimizing solar dryers by incorporating a thermal energy storage unit to enhance thermal efficiency and drying of food products. In this paper a brief overview of the principles pertaining to TES systems is presented. Conceptual designs of the proposed TES unit for improvement of drying efficiency of a solar dryer are discussed.

II. LITERATURE REVIEW

The necessity of storing solar energy for thermal applications cannot be overemphasized; it is an important aspect of renewable energy that addresses issues of thermal energy, cost, environmental impacts, etc. Energy storage is an opportunity to optimize solar energy dependent systems by mitigating the issues of intermittence of solar energy. The storing of thermal energy in materials is divided into three temperature categories. Depending on the type of application, thermal energy can be either stored for low temperature heating (up to 90 °C), medium temperature heating (90 °C to 300 °C) or for high temperature heating (300 °C to 1250 °C) [7]. The application of solar thermal energy storage is mostly associated with low temperature heat, hence in this study, the discussion is mainly on low temperature heat applications. As shown in fig.1, solar thermal energy can be stored in three forms of thermal energy storage, namely, sensible heat energy storage, latent heat energy storage and thermochemical energy storage.
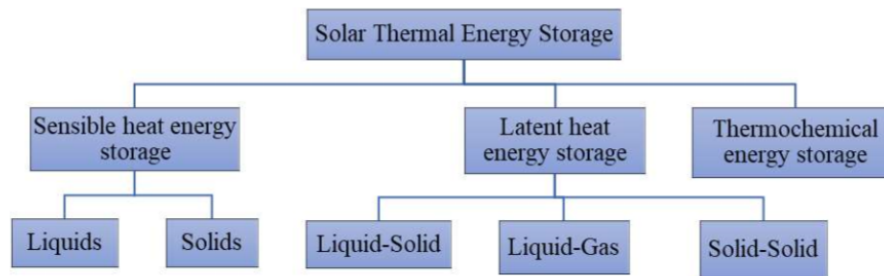

Fig. 1. Classification of TES systems of solar energy

The basic principles of these thermal energy storage systems are essentially the same. They mainly differ in their scale and energy storing method. The capacity of the storage system depends on the amount of time that the energy requires to be stored for [9]. All three energy storage systems are discussed in this paper but an emphasis is placed on sensible heat and latent heat energy storage systems because they are viable for low temperature applications.

A. Properties and Characteristics of TES materials

TES systems not only address the issues of intermittence of solar energy, but also enhance the efficiency and reliability of the entire system that requires thermal energy such as solar dryer systems [5]. Hence, careful considerations must be considered when designing a TES system for any application to ensure reliability and efficiency is enhanced. Alva et al. (2017) conducted a study on materials that are suitable for storing thermal energy. They identified various factors that need to be taken into consideration when selecting thermal energy storage materials suitable for the application. Some of the important factors to take into consideration are as follows [3,5,10]:

- Density of material – Materials with high density tend to store more energy, consequently improving the thermal efficiency of the system. TES systems

designed with high density materials result in high energy storage capacity but this depends on the storage process and material/medium type. The volume of the TES system is also reduced if a high-density material is used.

- Melting point of material – In applications where a phase change material is used for storing thermal energy, its melting point is crucial and careful consideration needs to be taken when designing the energy storage system.
- Enthalpy of fusion – A high enthalpy of fusion for a phase change material indicates a high energy storage material. Hence, these materials need to have high latent heat of fusion to ensure more heat is dissipated during phase change.
- Specific heat capacity of a material – In applications where sensible heat energy storage materials are used, the selection must consider those with a high specific heat capacity to improve energy storage.
- Thermal conductivity – TES systems designed with energy storage materials whose thermal conductivity is high have better rates of thermal charging and discharging, a requirement for an efficient TES system.

- Cost implications – Relates to affordability, maintenance/running cost and lifetime of the TES system. Materials need to be affordable and easily accessible.
- Flammability – As part of safety, careful consideration must be taken when selecting materials to avoid flammable materials.
- Thermal and Chemical stability – The lifespan of the TES system must not be significantly affected by thermal cycles as a result of heating and cooling of the material, and chemical reactions.
- Volume change – In applications where phase change materials are used, the selection must consider materials with a low thermal expansion coefficient to avoid a high change in volume during the process of phase change.
- Toxicity – As part of the health and safety issues, toxic and explosive materials need to be avoided or handled by an expert if the application requires such materials.
- Vapor pressure – Materials with low vapor pressure at operating temperatures are generally considered for the design of the TES system in order to minimize problems associated with containment and reduce costly insulation of the TES system.
- Storage duration – Relates to how long the energy can be stored in the system.
- Charging/discharging duration – Relates to the time required for charging/discharging the system.
- Congruent melting is required for phase change materials in order to have a constant storage capacity for every thermal cycle.
- Complete reversable process – For phase change material, the freezing/melting cycle must be completely reversable.
- Super cooling – For TES systems that utilizes phase change materials, the materials need to have a high nucleation rate to prevent the liquid from super cooling during the discharging

B. Common TES material for low temperature applications

Traditionally heat has been stored in sensible form by increasing the temperature of a liquid or solid. Usually a liquid or solid is used because the specific heat of gas is too low to be practically considered for thermal storage. This method is commonly practiced in many parts of the world for low temperature applications because it is inexpensive and easy to implement [11]. However, the other two TES techniques (storage of latent heat and thermochemical heat) offer better benefits because they store more energy per unit volume [7]. The following subsections give an overview of these various storage options in relation to the everyday use of energy storage applications.

1) Sensible heat energy storage. Sensible heat energy storage relies on the specific heat capacity and the temperature change of a TES material during the process of charging or discharging in which the temperature of the TES material increases when energy is absorbed and decreases when energy is withdrawn [11]. Further research indicates that the thermodynamic process during charging and discharging is completely reversable for the entire lifespan of the storage system, and it always take place under a constant pressure (mostly atmospheric pressure). Eq. 1 describes the sensible heat Q_s which is gained (during charging) or lost (during discharging) by the TES material when its temperature changes from T_1 to T_2.

$$Q_s = M \int_{T_1}^{T_2} C_\rho \, dT = V \int_{T_1}^{T_2} \rho \, C_\rho \, dT \quad (1)$$

Whereby:

- M, represent the mass (kg) of the TES material
- C_ρ, represent the isobaric specific heat capacity (J/kg. °C) of the TES material
- dT, is the differential temperature (°C)
- V, represent the volume (m³) of the TES material
- ρ, represent the density (kg/m³) of the TES material

Although there are other several parameters that effect the performance of the energy storage system as described in the previous section such as thermal conductivity, vapor pressure, temperature equalization in the material etc. Eq. 1 shows that the sensible heat energy is largely dependent on the material's density and specific heat capacity.

a) Liquid media storage. Liquid media storage can be used either for heating or cooling purposes with water and thermal oil being the most popular liquid sensible heat storage material. Water is used in many applications including hot-water storage tanks for domestic and industrial heating. Other liquid media storage includes oil-based fluid and molten salts. Table 1 shows the thermal properties of some of the commonly used liquid media in sensible heat storage systems.

TABLE I. Thermal properties of widely used liquid materials for sensible heat storage [11,12,13].

Materials	Density(kg/m³)	Specific Heat Capacity(J/kg. K)	Temperature Range(°C)
Water	1000	4190	0 to 100
Ethanol	780	2460	-117 to 79
Glycerin	1260	2420	17 to 290
Engine Oil	880	1880	-10 to 160
Butanol	809	2400	Up to 118
Caloria HT 43	867	2200	12 to 260
Propanol	800	2500	Up to 97
Liquid Paraffin	900	2130	Up to 200
Molten salt	1950	1570	Up to 400

For low temperature applications, water is seen as the best storage media of the available liquids due to several benefits listed below [8,13]:

- Cheap and easily available.
- Easily handled and controlled, harmless and non-flammable.
- Has a reasonable high density, high specific heat capacity, and high thermal diffusivity.
- Can be used without a heat exchanger.
- The process of charging and discharging can easily occur at the same time.
- It can be stored in all kinds of containers and can easily mix with additives.

Although water is seen to have many desirable benefits, there are also disadvantages associated with using water as a storage media, such as [8,13]:

- It is not desirable for medium and high temperature applications because it can only operate between 0 °C and 100 °C.

- At high temperature it is associated with high vapor pressure (above 5 bar).

- It can cause corrosion.

- Stratification is difficult to achieve.

Other liquid media such as ethanol and propanol can as well be used for low temperature applications, however they are highly flammable and not cost effective to implement. They require delicate handling which could increase the operational cost of the solar drying system if they are to be integrated in the energy storage system.

b) Solid media storage. In contrast to some of the disadvantages of water such as high vapor pressure and the limitations of other liquids, thermal energy can be stored as sensible heat in solids. For solid materials, soil and rock piles are the most commonly used storage materials due to their low cost and availability [8]. In general, solid storage materials are chemically inert, can store more energy than liquids, and have low vapor pressure. Thus, they can operate under no pressure containing vessel [13]. Because of their nature, when used in a thermal energy storage system, a fluid (usually air) is required to circulate and transfer the heat during charging and discharging process. This affects the thermal efficiency of the system since constant direct contact between the heat transfer fluid (air) and the solid material needs to be maintained [10]. Table 2 shows the thermal properties of some of the solid materials commonly used for thermal storage.

TABLE II. Thermal properties of solid materials used for sensible heat storage [11,13]

Material	Density (kg/m³)	Specific Heat Capacity (J/kg. K)	Thermal Conductivity (W/m.K)
Aluminum	2700	890	204
Iron	7850	465	59.3
Copper	8950	380	385
Wet Earth	1700	2100	2.5
Dry Earth	1260	795	0.25
Limestone	2500	910	1.3
Granite	3000	790	3.5
Concrete	2240	1130	0.9 - 1.3
Wood (oak)	480	2000	0.16
Sandstone	2200	710	1.8
Bricks	1700	840	0.69

The energy stored in TES systems utilizing these materials depend on many factors as discussed in previous sections such as thermophysical properties of the material, material size, and other heat transfer phenomena. Further details on solid materials for sensible heat storage can be found in the literature [1,10,13,14,15].

2) Latent heat energy storage. Latent heat is described as the energy absorbed or released at a constant temperature when the material changes from one phase to another e.g from solid to gas, liquid to gas, or solid to liquid [7,8]. Although the transformation of a material to a gas phase is possible, it is not common in thermal energy storage because gas occupies large volumes which can lead to high costs and other limitations [18]. The materials that undergo phase changes are commonly known as phase change materials (PCMs) and normally the PCMs used in thermal energy storage undergo solid to liquid transformation and vice versa. Research indicates that the storage of latent heat is based on the latent heat of melting rather than the latent heat of vaporization and such systems

provide a high energy storage density in comparison to sensible heat storage systems [16]. Table 3 shows some of the PCMs commonly used for thermal energy storage.

TABLE III.   Phase Change Materials used in thermal energy storage [11,16,17]

Materials	Melting Point °C	Density kg/m³	Latent Heat 10⁶ J/m³
Paraffin wax	58 - 60	900	180 – 200
Animal fat	20 - 50	900	120 - 210
Salt hydrates:			
$CaCl_2.6H_2O$	29	1802	190.8
$MgCl_2.6H_2O$	117	1569	168.6
$Mg(NO_3)_2.6H_2O$	89	1636	162.8
$Ba(OH)_2.8H_2O$	78	2070	265.7
$Na_2S_2O_3.5H_2O$	48	1750	200

Despite the PCMs outlined in Table 3, The thermal storage materials listed in Table 3 and others such as such as esters, glycols, tatty acids, alcohols, nitrate salts, carbonate salts, chloride salts, metal and alloys, etc. are discussed in detail the literature. Thermal analysis during phase transition is generally described by Eq. 2.

$$\Delta Q = H_2 - H_1 \qquad (2)$$

Eq. 2, can be expanded into Eq. 3 as expressed below:

$$\Delta Q = \int_{T_i}^{T_m} mC_{ps} dT + mf \Delta q + \int_{T_m}^{T_f} mC_{pl} dT \quad (3)$$

In Eq. 2, ΔQ (J) is the energy absorbed or released and H is the enthalpy before and after transition. The enthalpy is related to latent heat and volume of the materials. In Eq. 3, T_i, T_f and T_m are the temperatures (° C) at initial point, final point and melting point, respectively; m is the mass (kg) of PCM; C_{ps} is the specific heat capacity (kJ/kg.K) of the PCM during the solid phase (between T_i and T_m); C_{pl} is the specific heat capacity (kJ/kg.K) of the PCM during the liquid phase (between T_m and T_f); f is fraction melt; Δq is the change in latent heat (J/kg). Research indicates that in addition to the properties and characteristics discussed in section IIA, a thermal storage system utilizing a PCM needs to meet the following specific requirements [7,13]:

- Must melt in the desired temperature range.

- Must have a high heat of melting or large enthalpy for phase change.

- Must be chemically stable for all the reversable thermal processes without significant loss in performance.

- Subcooling during freezing and supersaturation during melting of the PCM must be minimal with no segregation.

- The PCM must be thermally stable with a low vapor pressure for the operating temperature range.

- A suitable heat exchanger is required for the heat transfer process between the PCM and the system requiring heat.

Due to advancement in technology and research, composite phase change materials have been introduced in thermal energy storages. Their primary function is to enhance the thermal conductivity of regular PCMs which are generally associated with poor thermal conductivity [10]. The discussion of composite phase change material is beyond the scope of this paper but literature is available for further research. Overall, PCMs are usually preferred over sensible heat materials for thermal storages, mainly because:

- A thermal storage system using PCMs operates at more or less a constant temperature, thus, the thermal gradient during charging and discharging remains small.

- PCMs store more heat per unit volume, thus, less volume is required for storage.

- PCMs have high thermal storage capacity for small temperature difference.

- The use of a heat exchanger allows both charging and discharging phases to occur simultaneously.

3) Thermochemical storage. Technology advancement and ongoing researches have come up with ways to overcome the burdens and uncertainties present in sensible and latent heat energy storages. Part of the technology advancement is the use of thermochemical energy storage systems. Thermochemical energy storage systems depend on the energy that is absorbed and released as the result of a change in enthalpy of a completely reversable chemical reaction. In thermochemical storage system, the charging process is referred to as an endothermic mode in which energy is absorbed and stored within the chemical bonds. The discharging process is referred to as an exothermic mode in which energy is released [8]. These systems are mainly developed for storing energy in

larger quantities than other type of TES systems and high temperatures are easily attainable due to faster reaction rates [13]. Research also indicates that energy losses in thermochemical storage systems are minimal and since the energy stored is mostly of great magnitude, they are commonly used in power plants for electricity generation. Hence, thermochemical energy storage is not of great advantage for low temperature application such as solar dryer systems. Detailed discussion on this type of TES system is not presented in this paper due to its complexity but there is extensive literature on the topic that can be consulted.

C. Solar dryer systems with integrated TES system

Sandali et al. (2018) investigated the thermal performance of a direct solar dryer with an integrated heat supply. Their study aimed to improve drying of the products by increasing the drying air temperature and promoting a continuous drying process during off peak hours using a geothermal water heat exchanger. The study found that the system was effective and significantly improved thermal performance of the solar dryer, particular during the night. The continuous use of geothermal water at constant temperature ensured there was a constant supply of heat for drying. However, one can economically utilize this system only in regions with geothermal water supply. Reyes et al. (2014) conducted a study on the performance evaluation of a heat exchanger that incorporated a solar energy accumulator. The heat exchanger used paraffin wax to store solar thermal energy and the wax was mixed with 5% w/w aluminum wool from recycled materials to improve thermal conductivity. Based on their results, 9.5 kg of paraffin wax was capable of storing 3000 kJ of energy which raised the temperature of 3.5 m3/h air flow by 20 °C in 2 hours. They concluded that this TES could extend the drying process and could even be used for heating purposes in household applications. Rabha et al. (2017) conducted a study to evaluate the performance of a forced convection solar dryer with an integrated paraffin wax thermal energy storage system as shown by the photograph in Fig 2.
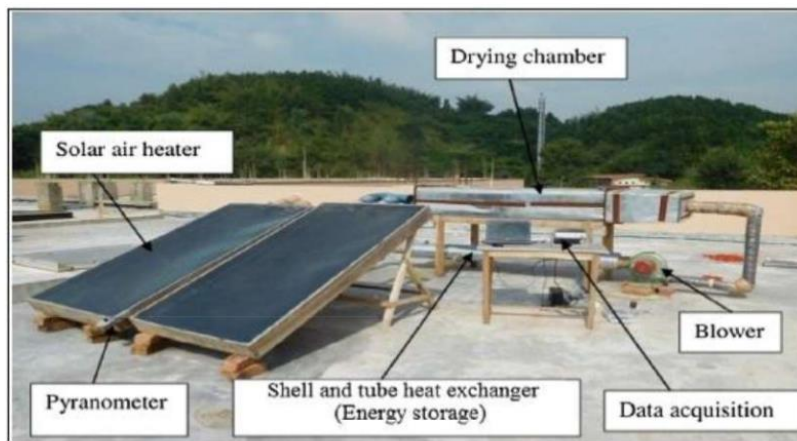

Fig. 2. Solar dryer system with integrated TES system [22].

As indicated in Fig 2, Rabha et al.'s dryer system consists of two double-pass solar air heaters to provide sufficient temperature to melt the paraffin wax. The wax is housed in a heat exchanger of shell and tube type. The test was conducted by drying a 20kg batch of red chilli in which the moisture content of red chilli was reduced from 73.5% (wet basis) to 9.7% (wet basis) in 4 days. Their study concluded that the system is effective in improving the thermal efficiency and providing a constant drying temperature during the cloudy period. However, with the addition of a second solar collector, costs were increased and drying period seemed to be longer. This can motivate the need for further improvements on the drying rate and lowering of the costs by eliminating the need for a two-double pass solar air heater.

Mohanraj et al. (2009) carried out a study on drying chilli. They analyzed the performance of a solar dryer system which incorporated a TES system that used gravel as a heat energy storage material. As shown in Fig 4, the solar dryer system is composed of a solar air heater with a heat storage unit, a drying chamber and a blower. The solar air heater is composed of a glass cover and commercially black painted copper absorber plate. In between the absorber plate and the insulation there is a gap which is filled with sand particles mixed with aluminum scraps for thermal storage during peak hours and to obtain hot air during off peak hours of the day. The drying chamber was designed with a capacity of holding 50 kg of chilli per batch. The solar air heater was inclined at an angle of 25° with respect to horizontal. They conducted the experiment at an air flow rate of 0.25 kg/s and managed to lower the moisture content of chilli from an initial moisture content of 72.8 % (wet basis) to a final moisture content of about 9.2 % and 9.7 % (wet basis) in just 24 hours. The incorporation of a heat storage unit to the dryer system was found to be effective in improving the performance of the system and prolonged the drying process by 4 hours per day. Thermal efficiency was found to be about 21%.
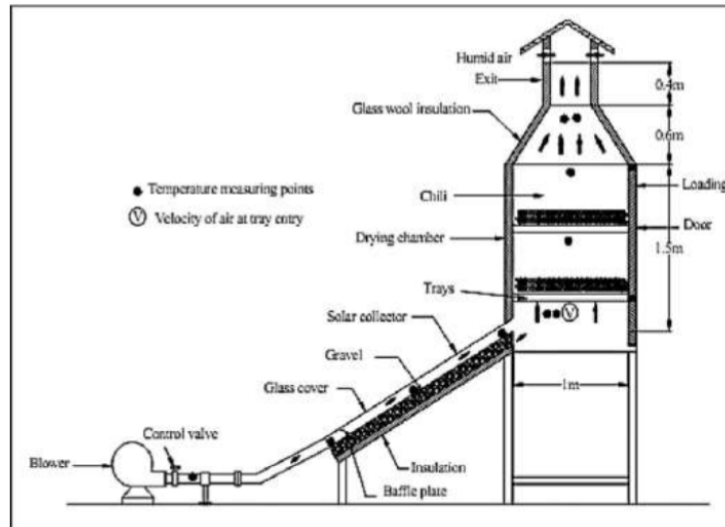
Fig. 4. Schematic view of the experimental setup [23]

Ayyappan et al. (2015) conducted an experiment to improve the thermal performance of a natural convection solar greenhouse dryer using concrete, sand and rock as sensible heat storage materials. Various experimental trials were run for different materials and they found that for both sand and rock a 4-inch thickness layer was the optimum solution to provide better drying during the day and night. Coconut was used as the drying product during the experiment. When concrete was used to store heat energy, the dryer system was able to lower the moisture content of coconut from 52 % (wet basis) to 7 % (wet basis) in 78 hours in comparison to open sun drying which takes 174 hours. This indicated a saving of drying time by about 55 %. When heat energy was stored using sand, the drying time of coconut was reduced to 66 hours with a saving

of 62 % of drying time as compared to open sun drying. If rock was used, the drying time was further reduced to 53 hours, saving the drying time by about 69 %. According to their results, rock provided the highest thermal efficiency of 11.65 % while sand yielded the least thermal efficiency of 9.5 %. An experimental study conducted by Hailu et al. (2017) on storage of solar thermal energy using sand-bed storage for seasonal space heating applications as shown by the schematic in Fig. 5. Their main idea was to address cold winter climate issues by ensuring solar energy is stored as heat during summer and recovered for house heating during the long freezing temperatures of winter. Water is heated inside a solar collector.
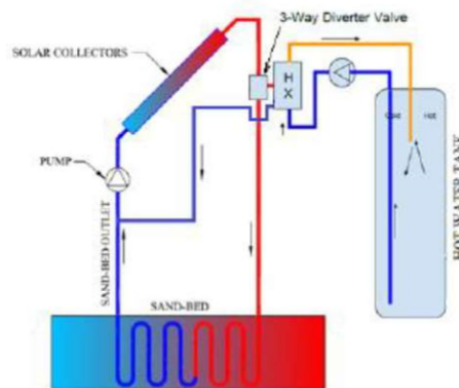

Fig. 5. Schematic diagram of a seasonal pace heater using solar thermal energy sand-bed storage [21]

2809

106

III. CONCEPTUAL DESIGNS

In order to improve drying efficiency of a solar dryer, one needs to look into ways of increasing its drying capacity and minimizing thermal energy loses. One of the cheapest and yet most effective way to increase drying capacity of a solar dryer is to incorporate a TES system which can be used during low or off-peak sunshine hours. As discussed in the preceding section, thermal energy can be stored in many ways. Considering various factors of selecting a suitable TES material as discussed in section IIA, two conceptual designs are proposed and considered to be economically effective in aiding solar drying. The first concept is based on the use of rocks to store solar thermal energy while the second one relies on the use of heated water to store solar thermal energy

A. Concept 1: Rock Bed Solar Thermal Energy Storage

The use of rocks as a thermal storage material has many advantages such as low cost to implement and maintain. Depending on the application, various types of rocks can be used to store thermal energy; granite, gravel or limestone are frequently used as thermal storage materials in food dryers [26]. Rocks have poor thermal conductivity, allowing them to store heat for relatively longer periods. However, they have a fairly low specific heat capacity which makes them suitable only for storing heat for low temperature applications such as food drying in solar dryer systems. Fig. 6 shows the design layout of the proposed rock bed TES system that harvests and stores solar energy. This system is designed as a standby unit for a solar dryer system which will supply hot air to the drying chamber for drying during off-peak periods such as cloudy hours or nighttime.
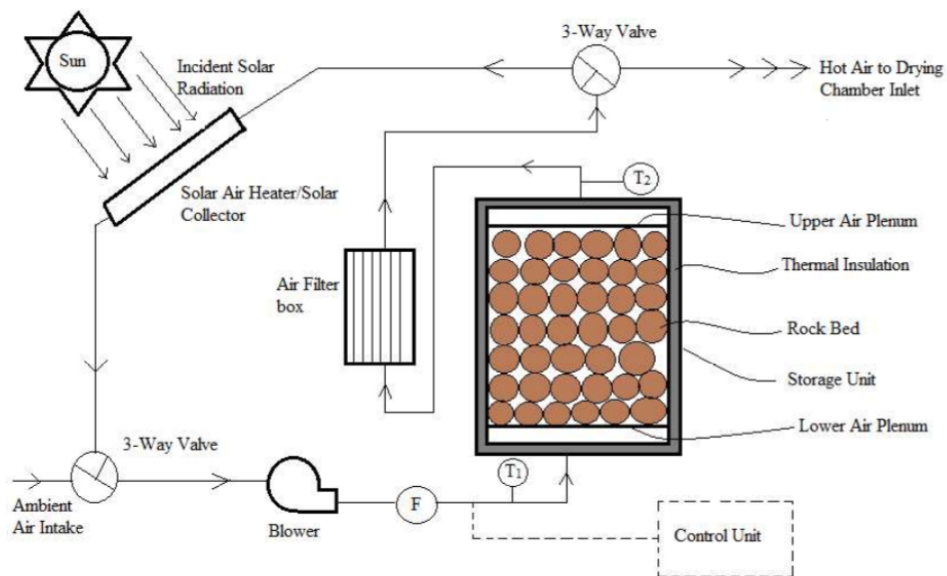

Fig. 6. Conceptual design layout for the rock bed solar thermal energy storage system

The working fluid of the system is air, which is heated in the solar collector as a results of the incident solar radiation. The system can work on its own independent solar collector or hot air can be channeled from the outlet(s) of the solar collector for the solar dryer system. Hot air is sucked and blown by the blower into the storage unit where heat is absorbed and stored in the rock bed due to the heat transfer process. The storage unit is covered with a thermal insulation layer to prevent any heat loss. The system is designed with an air filter box to ensure that small rock particles or debris do not clog the control valves or enter the drying chamber where food products are dried. Three-way control valves are positioned within the system flow network to control the air flow during the processes of charging and discharging of the TES system.

It is also proposed that such a system can have a flow control meter (denoted "F") to monitor the air flow rate. Temperature sensors "T1" and "T2" are also essential in the system to monitor the temperature across the storage unit. The entire TES system can be electronically controlled to ensure the working fluid is optimally circulated during charging and discharging phases. Magdalena et al. [26] conducted an experiment using granite spheres of three different sizes as materials to fill the bed storage. Based on their findings, the drying process was prolonged by two hours which indicates in improvement in the drying process. It is however noted that

efficiency of such thermal storage systems is affected by the sizes of materials, inlet air temperature and air flow rate.

B. Concept 2: Hot water tank for Solar Thermal Energy Storage

Water is one of the cheapest heat storage materials used in low temperature (not more than 100 °C) applications such house space heating, car interior heating and hot water supply for various applications [10]. It has many favorable advantages such as easy availability and high specific heat capacity in comparison with other sensible heat materials such as rocks,

sands, mineral oil, etc. Apart from many favorable advantages as discussed section IIB1a, storing thermal energy using water also possesses disadvantages such as corrosiveness and high vapor pressure which one could possibly control. A schematic of the design layout of the proposed solar TES system that uses a hot water tank for thermal storage is shown in Fig. 7. This conceptual design represents a standby thermal storage system which can be coupled to a food drying system such a solar grain dryer to provide intermittent thermal energy support to the drying process.
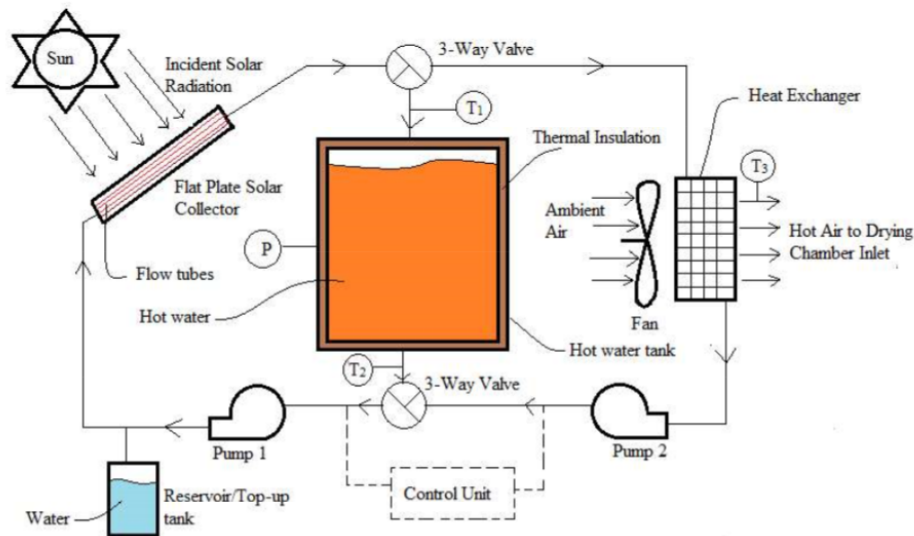
Fig. 7. Conceptual design layout for the hot water tank solar thermal energy storage system

This system is designed similarly to the one with the rock bed TES system as discussed in section IIIA. During peak hours of the day, the working fluid (water) is heated (charging phase) to a high temperature inside the flat plate solar collector as a result of the heat transfer process between the cool water and heated flow tubes. The hot water is pumped (by pump 1) and circulated between the flat plate solar collector and a thermally insulated hot water tank where it is stored. During off-peak hours, hot water from the tank can be pumped (by pump 2) and circulated between the tank and a heat exchanger where heat is transferred from the water to air (discharging phase). A fan can be incorporated in the system to induce forced convection over the heat exchanger which enhances the heat transfer process. The hot air exiting the heat exchanger can be channeled to the drying chamber where products such as foods can be dried. The flow of the working fluid in the entire system can be electronically controlled through control valves and feedback sensors. As a safety precaution, a pressure relief valve (denoted "P") can be included to control the pressure inside the hot water tank. While the temperature sensors denoted "T1", "T2" and "T3" are crucial in monitoring the temperatures across the hot water tank and that of the hot air, respectively.

C. Conclusion

A study was conducted on the utilization of thermal energy storage materials with an emphasis on the optimization of solar dryer systems for drying food products. Different materials aimed at storing thermal energy were discussed and suitable materials for solar drying applications were considered. Two conceptual design layouts were considered as economically viable solutions to improve thermal efficiency of solar dryer systems and prolong the drying process, namely, concept 1 which uses a bed of rocks to store solar thermal energy, and concept 2 that uses water to store solar thermal energy. Both energy storage materials are charged during peak hours of the day and discharged during off-peak hours when it is necessary. These were considered as viable concepts for the intended application, and further research can be put in place to determine the best of two. In conclusion, for low temperature applications, a well-designed thermal energy storage unit that utilizes an energy storage media such as water or rocks can be used for the optimization of food solar dryers.

D. Recommendations

This paper gives preliminary indications that solar dryer systems can be optimized with suitable thermal energy storage materials. Due to the limit of the scope of this study, it is recommended that further research be conducted with experimental studies of the two conceptual designs discussed in the paper.

REFERENCES

[1] A. Saxena, Varun, and A.A. El-Sebaii. "A thermodynamic review of solar air heaters," Renewable Sustainable Energy Rev., vol. 43, pp. 863-890, 2015. https://doi.org/10.1016/j.rser.2014.11.059.

[2] K. Kant, A. Shukla, A. Sharma, A. Kumar, and A. Jain. "Thermal energy storage based solar drying systems: A review," Innovative Food Sci. Emerg. Technol., vol. 34, pp. 86-99, 2016,. https://doi.org/10.1016/j.ifset.2016.01.007.

[3] M.L. Bal, S. Satya, and N.S. Naik. "Solar dryer with thermal energy storage systems for drying agricultural food products: A review," Renewable Sustainable Energy Rev., vol. 14, no. 8, pp. 2298-2314, 2010. https://doi.org/10.1016/j.rser.2010.04.014.

[4] South Africa. Department of Energy. Renewable Energy – Solar Power, 2017. http://www.energy.gov.za/files/esources/renewables/r_solar.html.

[5] I. Sarbu and C. Sebarchievici. "A comprehensive review of thermal energy storage," Sustainability, vol. 10, no. 1, p. 191, 2018. https://doi.org/10.3390/su10010191.

[6] L. Vikramjose. "A review on solar drying process with thermal energy storage system," Int. Res. J. Eng. Technol., vol. 5, no. 6, pp. 1859-1862, 2018. https://www.irjet.net/volume5-issue6.

[7] Flood, M. Solar Prospects: The Potential for Renewable Energy. London: Wildwood House, 1983.

[8] G.N. Tiwari and S. Suneja. Solar Thermal Engineering Systems. London: Narosa Publishing House, 1997.

[9] D. Lefebvre. and F.H. Tezel. "A review of energy storage technologies with a focus on adsorption thermal energy storage processes for heating applications" Renewable Sustainable Energy Rev. vol. 67, pp. 116-125, 2017. DOI: 10.1016/j.rser.2016.08.019.

[10] G. Alva, L. Liu, X. Huang, and G. Fang. "Thermal energy storage materials and systems for solar energy applications," Renewable Sustainable Energy Rev., 68, 2017, pp. 693-706. https://doi.org/10.1016/j.rser.2016.10.021.

[11] C.J. Chen. Physics of Solar Energy. New York: John Wiley & Sons, 2011.

[12] A. Sharma, V.V. Tyagi, R.C. Chen, and D. Buddhi. "Review on thermal energy storage with phase change materials and applications," Renewable Sustainable Energy Rev., vol. 13, no. 2, pp. 318-345, 2009. https://doi.org/10.1016/j.rser.2007.10.005.

[13] T. Bauer, W. Steinmann, D. Laing, and R. Tamme. Chapter 5: Thermal Energy Storage Materials and Systems. In: Annual Review of Heat Transfer, 15, pp. 131-177, 2012. DOI: 10.1615/AnnualRevHeatTransfer.2012004651.

[14] A. Abhat. "Low temperature latent heat thermal energy storage: Heat storage materials," Solar Energy, vol. 30, no. 4, pp. 313-332, 1983. https://doi.org/10.1016/0038-092X(83)90186-X.

[15] M.S. Hasnain. "Review on sustainable thermal energy storage technologies, Part I: heat storage materials and techniques," Energy Convers. Manage., vol. 39, no. 11, pp. 1127-1138, 1998. https://doi.org/10.1016/S0196-8904(98)00025-9.

[16] H.P. Garg, S.C. Mullik, and A.K. Bhargava, Solar Thermal Energy Storage. Dordricht: D. Reider Publishing Company, 1985.

[17] M.M. Farid, M.A. Khudhair, A.S Razack, and S Al-Hallaj. "A review on phase change energy storage: materials and applications," Energy Convers. Manage., vol. 45, no. 9, 1597-1615, 2004. https://doi.org/10.1016/j.enconman.2003.09.015.

[18] C. Bruno and L. Noel. "High temperature latent heat thermal energy storage: Phase change materials, design considerations and performance enhancement techniques," Renewable Sustainable Energy Rev., vol. 27, pp. 724-737, 2013. https://doi.org/10.1016/j.rser.2013.07.028.

[19] A. Reyes, D. Negrete, A. Mahn, and F. Sepulveda. "Design and evaluation of a heat exchanger that uses paraffin wax and recycled materials as solar energy accumulator," Energy Convers. Manage., vol. 88, pp. 391-398, 2014. https://doi.org/10.1016/j.enconman.2014.08.032.

[20] M. Sandali, A. Boubekri, D. Mennouche, and N. Gherraf. "Improvement of a direct solar dryer performance using a geothermal water heat exchanger as supplementary energetic supply. An experimental investigation and simulation study," Renewable Energy, vol. 135, , pp. 186-196, 2019. https://doi.org/10.1016/j.renene.2018.11.086.

[21] G. Hailu, P. Hayes, and M. Masteller. "Seasonal solar thermal energy sand-based storage in a region with extended freezing periods: Par I Experimental investigation," Energies, vol. 10, no. 11, p. 1873, 2017. https://doi.org/10.3390/en10111873.

[22] D.K. Rabha and P. Muthukumar. "Performance studies on a forced convection solar dryer integrated with a paraffin wax-based latent heat storage system," Solar Energy, vol. 149, pp. 214-226, 2017. DOI: 10.1016/j.solener.2017.04.012.

[23] M. Mohanraj, and P. Chandrasekar. "Performance of a

forced convection solar drier integrated with gravel as heat storage material for chili drying," J. Eng. Sci. Technol., vol. 4, no. 3, pp. 305-314, 2009. http://jestec.taylors.edu.my/V4Issue3.html.

[24] S. Ayyappan, K. Mayilsamy, and V.V. Sreenarayanan. "Performance improvement studies in a solar greenhouse drier using sensible heat storage materials," Heat Mass Transfer, vol. 52, no. 3, pp. 459–467, 2016. DOI: 10.1007/s00231-015-1568-5.

[25] S.F. Dina, H. Ambarita, F.H. Napitupulu, and H. Kawai. "Study on effectiveness of continuous solar dryer integrated with desiccant," Case Stud. Therm. Eng., vol. 5, pp. 32-40, 2015. https://doi.org/10.1016/j.csite.2014.11.003.

[26] N. Magdalena, N. Artur, and Pawel, P. A granite bed storage for a small solar dryer. Materials, vol. 11, no. 10, p. 1969, 2018. https://doi.org/10.3390/ma11101969G.

CHAPTER 8

8. COMPARISON OF RESULTS, OVERALL CONCLUSION, AND RECOMMENDATIONS FOR FUTURE WORKS

8.1 Comparisons of Results

There are several errors to consider when comparing the experimental results in Chapter 6 with those obtained through modeling and simulation as presented in Chapter 5. This is because during CFD simulation several assumptions were made to simplify the model and reduce computational cost. Some of the crucial assumptions that were made were:

- The analysis is considered under steady-state conditions for constant solar irradiation. This was to simplify the CFD analysis but, in reality, solar irradiation will vary with time throughout the day. Other factors such as weather conditions affect the amount of solar irradiation received by the solar dryer system.

- All maize ears inside the drying chamber are assumed to have the same initial moisture content. In reality, the initial moisture content will vary from one maize ear to another due to various factors such as time harvested, size of maize cobs, susceptibility to moisture reabsorption, etc. These factors will affect the evaporation rate of different maize ears.

- The initial temperature of grains on the maize ears is the same as the drying air temperature inside the chamber. In practice, different chamber components initially absorb heat as the drying chamber warms-up prior to insertion of the maize ears and the start of the experiment, leading to an initial increase in internal temperature.

- There is negligible heat loss across the dryer system. In practice, heat loss through the dryer wall can be significant depending on the ambient conditions.

- Simulation was conducted for a constant average solar irradiation of Durban. In actual fact, drying depends on the available incident solar irradiation, which varies with time throughout the day.

In this study, the inclusion of assumptions led to some errors and deviations in results. Nevertheless, a very good correlation between experimental and simulation results for the temperature distribution was achieved. Flow characteristics are also in good agreement with experimental results although small air leakages were experienced at some parts of the solar dryer during the experiment. The experiment was conducted at various input drying parameters as stipulated in the methodology section. Therefore, to draw a fair comparison for the entire range of results, the results for the highest temperature recorded at minimum drying and maximum drying conditions should be compared. At minimum drying condition, the drying airflow speed was set at 0.5 m/s and preheated to 30 ℃. At maximum drying condition, the drying airflow speed was set at 2 m/s and preheated to 40 ℃. Table 4 compares the highest temperature performance results at the minimum and maximum drying parameters between the experiment and simulation methods.

Table 8-1 Comparison of drying temperature between experimental and simulation results.

Solar Dryer component	Experiment		Simulation		Relative Errors	
	At Minimum Drying	At Maximum Drying	At Minimum Drying	At Maximum Drying	At Minimum Drying	At Maximum Drying
Solar collector outlet	60.51 ℃	78.29 ℃	59.7 ℃	70.5 ℃	1.3 %	10 %
Drying chamber inlet	62.54 ℃	74.95 ℃	54.8 ℃	64.1 ℃	12.4 %	14.5 %
Drying chamber outlet	43.12 ℃	45.19 ℃	36.1 ℃	47.4 ℃	16.3 %	-4.9 %

The margins between experimental and simulation results were not more than 20 % which indicated a correlation of results with a maximum relative error of 16.3 % at minimum drying and 14.5 % at maximum drying. This shows a good correlation therefore validating the experimental results, although some of the results were underpredicted. Another critical parameter that was not included in the comparison analysis was relative humidity across the solar dryer system. During simulation analysis, it was complicated to obtain accurate results of relative humidity at different solar dyer model points due to the complexity of the flow phenomena within the drying chamber. However, one could say a good correlation of temperature readings could indicate a good correlation of the results for relative humidity between experiment and simulation.

8.2 Overall Conclusion

A thorough study was conducted on the applications of a forced convection mixed-mode solar dryer integrated with a preheater in improving grain drying processes. The study was carried out in two phases whereby the first phase employed the use of SolidWorks and ANSYS Fluent codes in developing and simulating the CFD model of the solar dyer system, and the second phase was an experimental study that was conducted so that the simulation results could be validated against the experimental results. The experimental study led to sufficient information to be collected regarding the temperature distribution, airflow distribution, and drying air relative humidity across the dryer system. A strong correlation between experimental results and simulation results was achieved with a maximum relative error of 16.3 %. The dryer system's performance results indicated a maximum thermal efficiency of 58.8 % with a corresponding drying rate of 0.0438 kg/hr. The minimum thermal efficiency for the dryer system was 47.7 %, with a corresponding drying rate of 0.0356 kg/hr. The fastest drying time of maize ears was achieved in 4 hours and 34 minutes (on the same day of the start of drying) from an initial moisture content of 24.7 % wb to 12.5 % wb. In contrast, open-sun drying yielded the slowest drying time of 15 hours (on day three from the start of drying) from an initial moisture content of 27.3 % wb to 12.7 % wb.

The results obtained in this study indicated a significant improvement for the dryer system whose initial efficiency was 36 %. This was a clear indication that operating a dryer system in mixed mode operation using forced convection drying air with the assistance of a preheater or backup heater can significantly improve drying processes. The study has also proven that increasing both the drying air velocity and temperature at the inlet of the solar collector yielded improvement in the drying process. It further indicated that the performance of solar dryers is significantly affected by the amount of solar irradiation available. As presented in Chapter 6, this performance deficit was addressed with two design concepts that employed the use of thermal energy storage (TES) materials to allow solar dryer systems to be optimized. A combination of forced air convection, preheated air, and the possibility of incorporating TES units in solar dryer systems can improve and optimize drying processes. An efficient dryer system will lead to improved grain storage capacity.

8.3 Recommendations for Future Works

Recommendations for further research on this work to continue improving the performance of mixed-mode solar dryer systems are:

- Develop and test prototype thermal energy storage systems such as those presented in this study to analyze their effect on improving solar drying processes.

- Automate the solar collector to continuously track the sun's rays for maximum efficiency. This could be done through the use of a solar powered tracking mechanism.

- Use a more powerful computer to model the drying process under transient conditions for varying solar irradiation. This is because in reality solar irradiation varies with time and weather conditions throughout the day.

- Replace the electric heater used in this study as a preheater with a biomass heater to cut operational costs.

- Improve the design of the drying chamber to prevent condensation of moisture inside the chamber during the drying process.

APPENDICES

APPENDIX A: SAMPLE CALCULATIONS OF TEMPERATURE AND RELATIVE HUMIDITY

This appendix provides sample calculations for estimating the temperature and relative humidity of drying air across the preheater during the CFD simulation analysis.

a) Ambient air temperature and relative humidity at inlet of the Preheater (*using Table A-2 data)*

$$Temperature = \frac{\sum Avg.Min\,Temp(T_{2017}+T_{2018}+T_{2019})}{3}$$

$$= \frac{14.6\,°C+15.8\,°C+15.1\,°C}{3} = \mathbf{15.2}\,°C\ (1\ d.\ p)$$

$$Relative\ humidity = \frac{\sum Avg.Max\,RH(RH_{2017}+RH_{2018}+RH_{2019})}{3}$$

$$= \frac{92\%+89\%+88\%}{3} = \mathbf{90}\%$$

b) Relative Humidity of air at outlet of the Preheater

By interpolation method and using Table A-1:

$\rightarrow$ *moisture content of saturated air at* $15.2\,°C = 0.0131\ kg/m^3$

$$at\ 90\%\ Relative\ Humidity, moisture\ content = 0.0131 \times \frac{90}{100} = 0.01179\ kg/m^3$$

$\rightarrow$ *moisture content of saturated air at* $30\,°C = 0.0303\ kg/m^3$

$\therefore$ ***Output 1****: at* $30\,°C, Relative\ Humidity = 100\% \times \frac{0.01179}{0.0303} = 38.9\% = \mathbf{39}\%$

$\rightarrow$ *moisture content of saturated air at* $33\,°C = 0.0356\ kg/m^3$

$\therefore$ ***Output 2****: at* $33\,°C, Relative\ Humidity = 100\% \times \frac{0.01179}{0.0356} = 33.1\% = \mathbf{33}\%$

$\rightarrow$ *moisture content of saturated air at* $36\,°C = 0.0416\ kg/m^3$

$\therefore$ ***Output 3****: at* $36\,°C, Relative\ Humidity = 100\% \times \frac{0.01179}{0.0416} = 28.3\% = \mathbf{28}\%$

$\rightarrow$ *moisture content of saturated air at* $40\,°C = 0.0510\ kg/m^3$

$\therefore$ **_Output_ 4**: $at\ 40\ °C, Relative\ Humidity = 100\% \times \dfrac{0.01179}{0.0510} = 23.1\% = \mathbf{23\%}$

Table A-1. Water content of air at 100% Relative Humidity.

°C	kg/cu.m	°C	kg/cu.m	°C	kg/cu.m	°C	kg/cu.m	°C	kg/cu.m
-30	0.000578	-10	0.00218	10	0.00943	30	0.0303	50	0.0828
-29	0.000553	-9	0.00238	11	0.0100	31	0.0320	51	0.0867
-28	0.000540	-8	0.00259	12	0.0107	32	0.0337	52	0.0908
-27	0.000540	-7	0.00281	13	0.0114	33	0.0356	53	0.0951
-26	0.000551	-6	0.00305	14	0.0121	34	0.0375	54	0.0995
-25	0.000573	-5	0.00330	15	0.0129	35	0.0395	55	0.104
-24	0.000606	-4	0.00357	16	0.0137	36	0.0416	56	0.109
-23	0.000650	-3	0.00385	17	0.0145	37	0.0438	57	0.114
-22	0.000704	-2	0.00415	18	0.0154	38	0.0461	58	0.119
-21	0.000769	-1	0.00447	19	0.0163	39	0.0485	59	0.124
-20	0.000845	0	0.00481	20	0.0173	40	0.0510	60	0.130
-19	0.000931	1	0.00516	21	0.0183	41	0.0536	61	0.136
-18	0.00103	2	0.00554	22	0.0194	42	0.0563	62	0.142
-17	0.00113	3	0.00594	23	0.0206	43	0.0592	63	0.148
-16	0.00125	4	0.00636	24	0.0218	44	0.0621	64	0.154
-15	0.00138	5	0.00680	25	0.0230	45	0.0652	65	0.161
-14	0.00152	6	0.00727	26	0.0243	46	0.0685	66	0.168
-13	0.00167	7	0.00777	27	0.0257	47	0.0718	67	0.175
-12	0.00183	8	0.00829	28	0.0272	48	0.0753	68	0.182
-11	0.00200	9	0.00884	29	0.0287	49	0.0790	69	0.190

Table A-2. Weekly average relative humidity and temperature data for Durban during October 2017 – 2019. (Sourced: Metrological data, Virginia Weather Station, Durban)

	Oct-17			
	Average Minimum		**Average Maximum**	
	Rel. humidity (%)	Temperature (°C)	Rel. humidity (%)	Temperature (°C)
Week 1	48	11,1	92	21,8
Week 2	61	13,3	93	21,4
Week 3	55	16,1	90	26,3
Week 4	69	17,7	93	24,7
	Oct-18			
	Average Minimum		**Average Maximum**	
	Rel. humidity (%)	Temperature (°C)	Rel. humidity (%)	Temperature (°C)
Week 1	63	17,3	89	26
Week 2	55	14,5	90	23,8
Week 3	48	14,9	87	26,3
Week 4	54	16,4	89	26,3
	Oct-19			
	Average Minimum		**Average Maximum**	
	Rel. humidity (%)	Temperature (°C)	Rel. humidity (%)	Temperature (°C)
Week 1	47	13,3	90	26
Week 2	53	16,4	87	25,5
Week 3	55	14,5	90	23
Week 4	48	16	87	27,8

APPENDIX B: CALCULATIONS FOR SOLAR DRYER PERFORMANCE

This appendix provides calculations pertaining to the solar dryer performance based on the experimental results. Calculations were made to obtain the thermal efficiency and drying rate for the solar dryer system.

Thermal efficiency

a) <u>Maximum Efficiency for the solar dryer system</u> *(with reference to results in Fig.9 and Fig.12 of Chapter 6)*

$$\eta_{sys} = \frac{(M_w \times L_v) + (M_g \times C_{pg} \times \Delta T)}{M_a C_{pa}(T_{dc} - T_{amb})}$$

$$M_w = M_p \left(\frac{M_i - M_f}{100 - M_f}\right) = (6 \times 0.235 \ kg)\left(\frac{24.7 - 12.5}{100 - 12.5}\right) = 0.197 \ kg$$

$C_{pg} = 1.3066 + 1.2045 M_d + 0.0198T = 1.3066 + (1.2045 \times 0.125) + (0.0198 \times 25)$
 $= 1.952$ kJ/kg.K

$M_g = M_p - M_w = 1.41$ kg $- 0.197$ kg $= 1.213$ kg

ΔT = Temperature at Drying chamber Outlet - T_{amb} = 45.19 °C - 25 °C = 20.19 °C

$M_a = density \times volume = 1.184$ kg/m³ $\times 14.076$ m³ $= 16.666$ kg

$$\therefore \ \boldsymbol{\eta_{sys}}(maximum) = \frac{(0.197 \times 2257) + (1.213 \times 1.952 \times 20.19)}{(16.666 \times 1.006 \times (74.95 - 25)} = 0.588 \ (\boldsymbol{58.8} \ \%)$$

b) <u>Minimum Efficiency for the solar dryer system</u> *(with reference to results in Fig.5 and Fig.10 of chapter 6)*

$$\eta_{sys} = \frac{(M_w \times L_v) + (M_g \times C_{pg} \times \Delta T)}{M_a C_{pa}(T_{dc} - T_{amb})}$$

$$M_w = M_p \left(\frac{M_i - M_f}{100 - M_f}\right) = (6 \times 0.235 \ kg)\left(\frac{27.3 - 12.8}{100 - 12.8}\right) = 0.234 \ kg$$

$C_{pg} = 1.3066 + 1.2045 M_d + 0.0198T = 1.3066 + (1.2045 \times 0.128) + (0.0198 \times 25)$
 $= 1.956$ kJ/kg.K

$M_g = M_p - M_w = 1.41$ kg $- 0.234$ kg $= 1.176$ kg

ΔT = Temperature at Drying chamber Outlet - T_{amb} = 43.12 °C - 25 °C = 18.12 °C

$M_a = density \times volume = 1.184 \text{ kg/m}^3 \times 26.721 \text{ m}^3 = 31.638 \text{ kg}$

$$\therefore \boldsymbol{\eta_{sys}} \ (minimum) = \frac{(0.234 \times 2257) + (1.176 \times 1.956 \times 18.12)}{(31.638 \times 1.006 \times (62.54 - 25)} = 0.477 \ (\boldsymbol{47.7} \%)$$

Drying rate

a) <u>Maximum drying rate, DR_{max}</u>

$$\mathbf{DR_{max}} = \frac{M_w}{t_d} = \frac{0.197 \ kg}{4.5 \ hr} = \mathbf{0.0438} \text{ kg/hr}$$

b) <u>Minimum drying rate, DR_{min}</u>

$$\mathbf{DR_{min}} = \frac{M_w}{t_d} = \frac{0.234 \ kg}{6.5667 \ hr} = \mathbf{0.0356} \text{ kg/hr}$$

APPENDIX C: SOLAR IRRADIANCE AND MEASURING INSTRUMENTS

This appendix provides the information on solar energy in Durban during the period of experiment. It also provides pictures for some of the instruments used during the experiment.
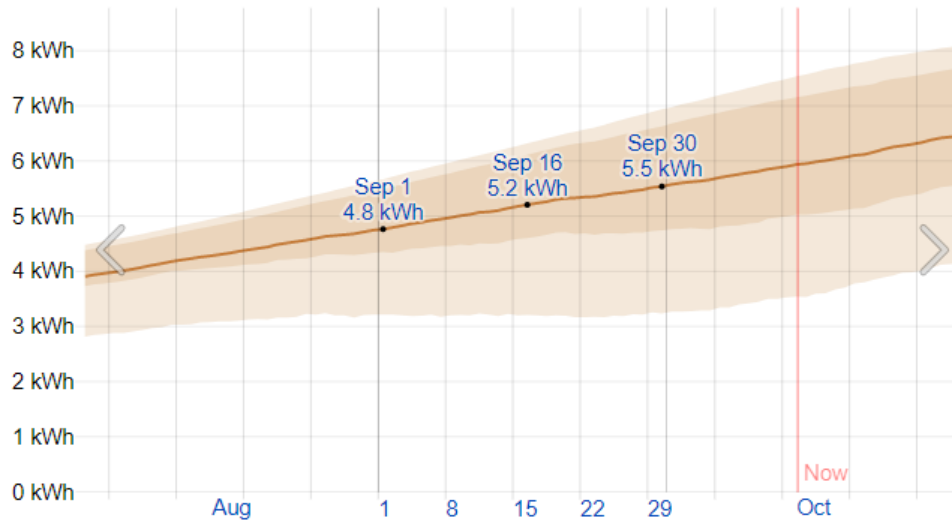
Figure C-1. Average daily solar irradiance In September for Durban (Sourced: https://weatherspark.com/m/96783/10/Average-Weather-in-October-in-Durban-South-Africa#Sections-SolarEnergy)
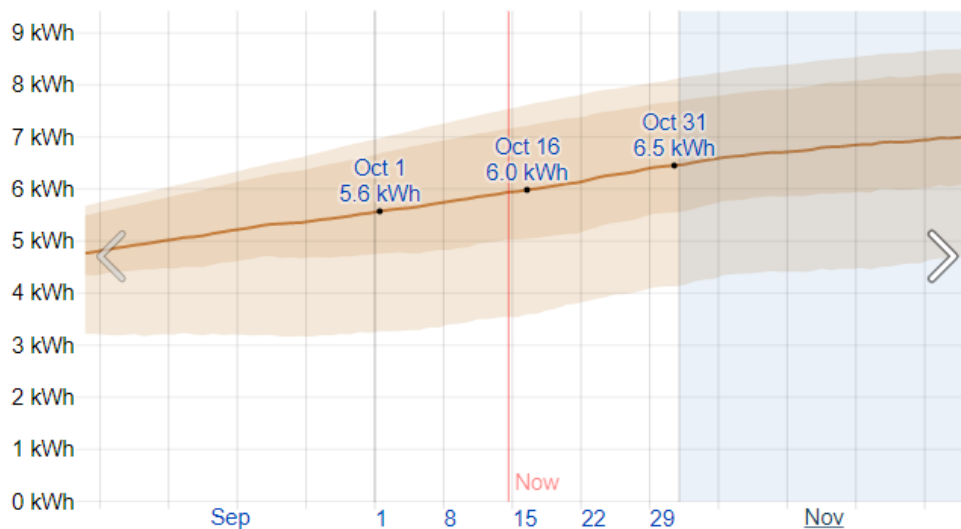
Figure C-2. Average daily solar irradiance In October for Durban (Sourced: https://weatherspark.com/m/96783/10/Average-Weather-in-October-in-Durban-South-Africa#Sections-SolarEnergy)

Figure C-3. Solid State Relay (top left), Lutron HT315 Humidity/Temperature meter (top right), Temperature controller (bottom left), and an RTD temperature sensor (bottom right)
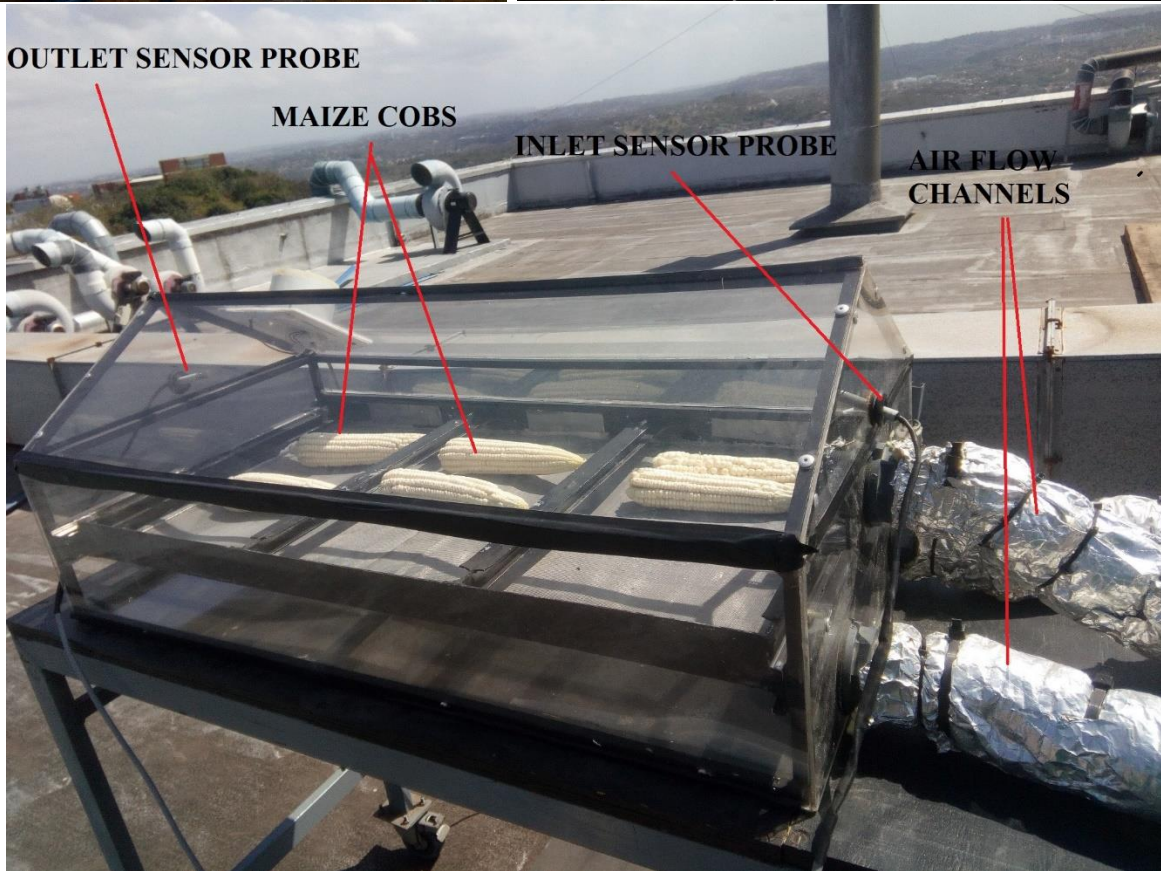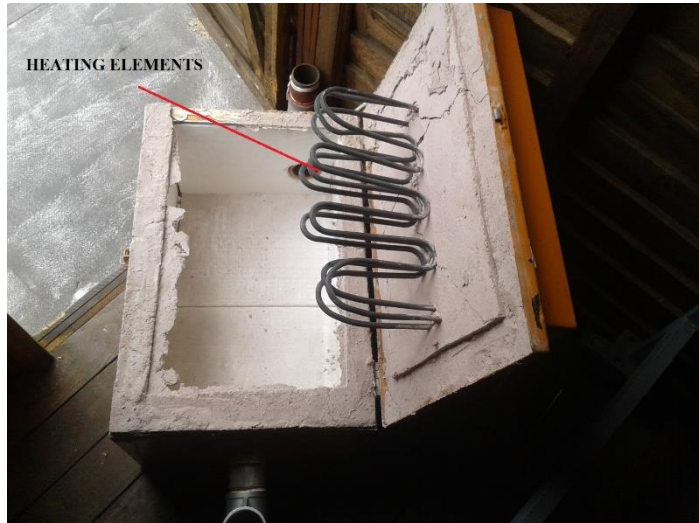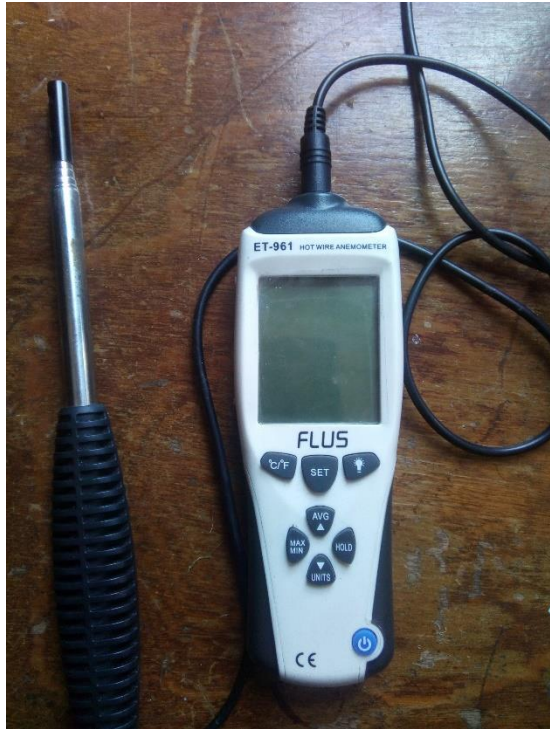
Figure C-4. ET961 Hot Wire Anemometer (top left), Preheater/air heater box (top right), and Drying chamber (bottom)
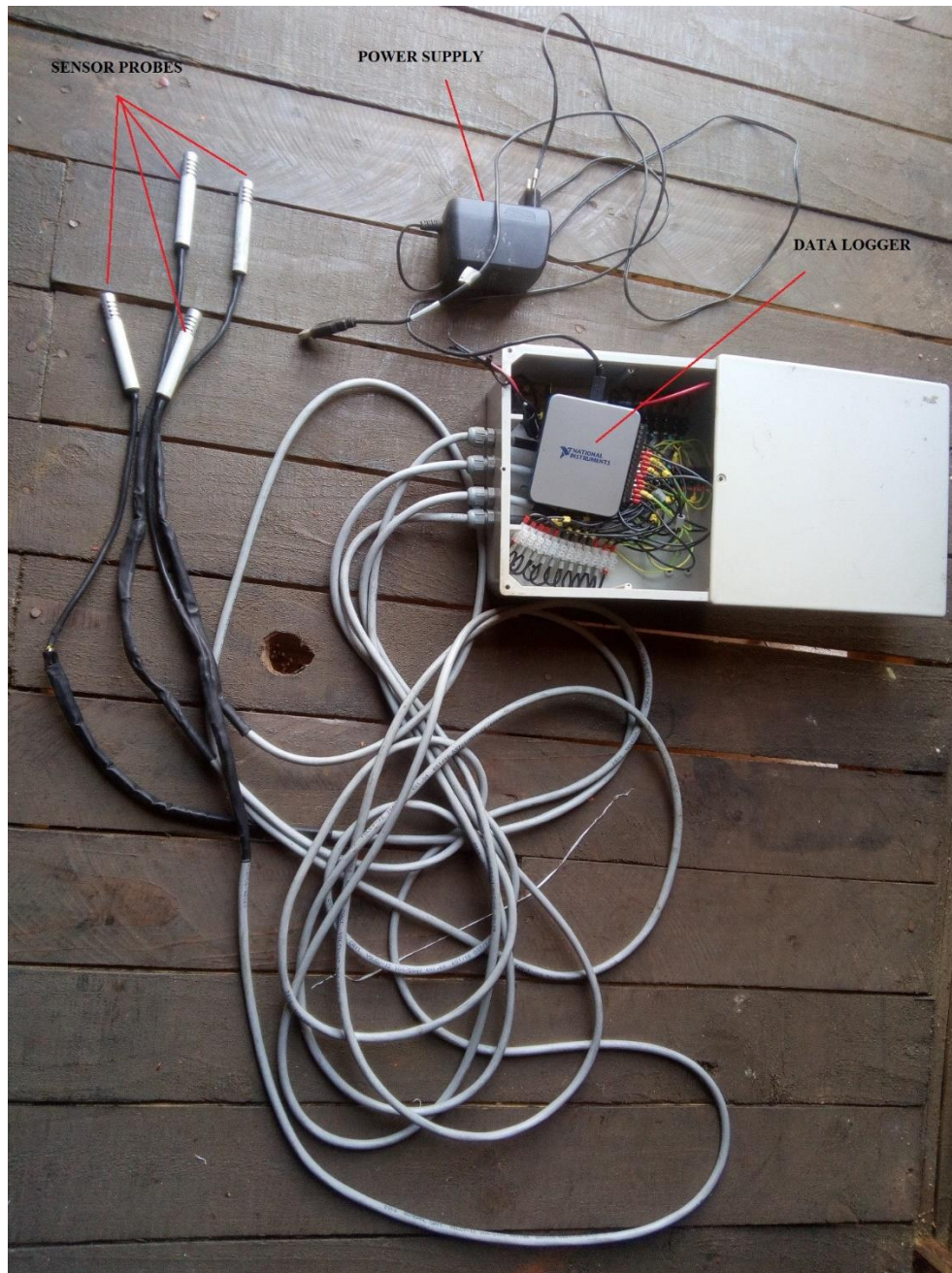
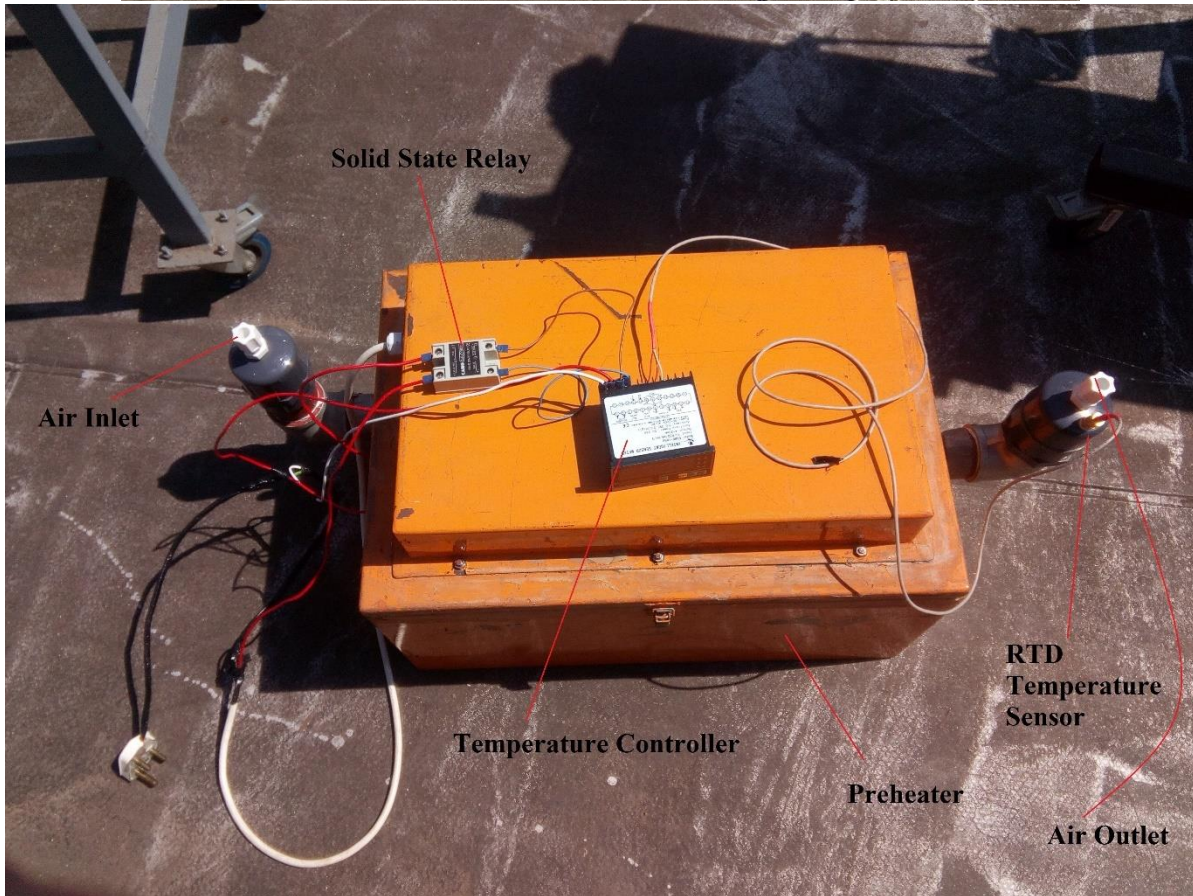Figure C-5. NI USB-6000 Data logger with HTM2500LF sensor probes

Figure C-6. Side view of the experimental setup (top) and preheater with temperature control circuit (bottom)

APPENDIX D: SPECIFICATIONS OF THE HTM2500LF SENSOR PROBES

Specifications of the HTM2500LF sensor probes used during the experiment are provided in this appendix.

HTM2500LF
Temperature and Relative Humidity Module

APPLICATIONSPERFORMANCE SPECS

MAXIMUM RATINGS

Ratings	Symbol	Value	Unit
Storage Temperature	Tstg	-40 to	°C
Storage Humidity	RHstg	0 to 100	%
Supply Voltage (Peak)	Vs	12	Vdc
Humidity Operating Range	RH	0 to 100	%
Temperature Operating	Ta	-40 to	°C

Peak conditions: less than 10% of the operating time

OPERATING RANGE
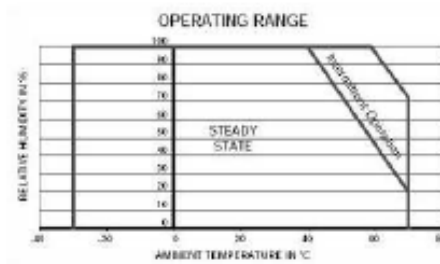
ELECTRICAL CHARACTERISTICS

(Ta=23°C, Vs=5Vdc +/-5%, R$_L$>1MΩ unless otherwise stated)

Humidity Characteristics	Symbol	Min	Typ	Max	Unit
Humidity Measuring Range	RH	1		99	%RH
Relative Humidity Accuracy (10 to 95% RH)	RH		+/-3	+/-5	%RH
Supply Voltage	Vs	4.75	5.00	5.25	Vdc
Nominal Output @55%RH (at 5Vdc)	Vout	2.42	2.48	2.54	V
Current consumption	Ic		1.0	1.2	mA
Temperature Coefficient (10 to 50°C)	Tcc		+0.1		%RH/°C
Average Sensitivity from 33% to 75%RH	ΔVout/ΔRH		+26		mV/%RH
Sink Current Capability (RL=15kΩ)	Is			300	µA
Recovery time after 150 hours of condensation	tr		10		s
Humidity Hysteresis			+/-1.5		%RH
Long term stability	T		+/-0.5		%RH/yr
Time Constant (at 63% of signal, static) 33% to 76%RH [1]	τ		5		s
Output Impedance	Z		70		Ω

(1) At 1m/s air flow

(Ta=25°C)

Temperature Characteristics	Symbol	Min	Typ	Max	Unit
Nominal Resistance @25°C	R		10		kΩ
Beta value: B25/50	β	3347	3380	3413	K
Temperature Measuring Range*	Ta	-40		85	°C
Nominal Resistance Tolerance @25°C	R$_N$			1	%
Beta Value Tolerance	β		1		%
Response Time	τ		10		s

*For temperature upper than 60°C, specific high temperature cable is required: HTM2500LFL products*

TYPICAL PERFORMANCE CURVES

HUMIDITY SENSOR

Typical response look-up table (Vs = 5V)

RH (%)	Vout (mV)	RH (%)	Vout (mV)
10	1235	55	2480
15	1390	60	2605
20	1540	65	2730
25	1685	70	2860
30	1825	75	2990
35	1960	80	3125
40	2090	85	3260
45	2220	90	3405
50	2350	95	3555

Modeled linear voltage output (Vs = 5V)
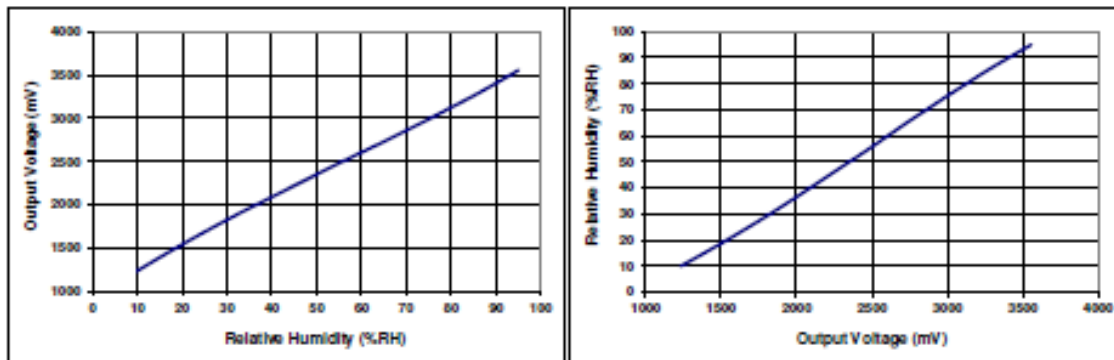
Linear Equations

$$Vout = 26.65 * RH + 1006$$
$$RH = 0.0375 * Vout - 37.7$$
with Vout in mV and RH in %

Polynomial Equations

$$Vout = 1.05E^{-3} * RH^3 - 1.76E^{-1} * RH^2 + 35.2 * RH + 898.6$$
$$RH = -1.92E^{-9} * Vout^3 + 1.44E^{-5} * Vout^2 + 3.4E^{-3} * Vout - 12.4$$
with Vout in mV and RH in %

Measurement Conditions

HTM2500LF is specified for accurate measurements within 10 to 95% RH.

Excursion out of this range (<10% or >95% RH, including condensation) does not affect the reliability of HTM2500LF characteristics.

HTM2500LF TEMPERATURE SENSOR: DIRECT NTC OUTPUT

- **Typical temperature output**

Depending on the needed temperature measurement range and associated accuracy, we suggest two methods to access to the NTC resistance values.

$$R_T = R_N \times e^{\beta\left(\frac{1}{T} - \frac{1}{T_N}\right)}$$

R_T	NTC resistance in Ω at temperature T in K
R_N	NTC resistance in Ω at rated temperature T in K
T, T_N	Temperature in K
β	Beta value, material specific constant of NTC
e	Base of natural logarithm (e=2.71828)

① The exponential relation only roughly describes the actual characteristic of an NTC thermistor can, however, as the material parameter β in reality also depend on temperature. So this approach is suitable for describing a restricted range around the rated temperature or resistance with sufficient accuracy.
② For practical applications, a more precise description of the real R/T curve may be required. Either more complicated approaches (e.g. the Steinhart-Hart equation) are used or the resistance/temperature relation as given in tabulation form. The below table has been experimentally determined with utmost accuracy for temperature increments of 1 degree.

Actual values may also be influenced by inherent self-heating properties of NTCs. Please refer to MEAS-France Application Note HPC106 "Low power NTC measurement".

- **Temperature look-up table**

Temp (°C)	R (Ω)	Temp (°C)	R (Ω)
-40	195652	25	10000
-35	148171	30	8315
-30	113347	35	6948
-25	87559	40	5834
-20	68237	45	4917
-15	53650	50	4161
-10	42506	55	3535
-5	33892	60	3014
0	27219	65	2586
5	22021	70	2228
10	17926	75	1925
15	14674	80	1669
20	12081	85	1452

- **Steinhart-Hart coefficients**

According to the equation below, the Steinhart-Hart coefficients for the operating temperature range for HTM2500LF thermistor are:

$$\frac{1}{T} = a + b * \ln(R) + C * \ln(R) * \ln(R) * \ln(R)$$

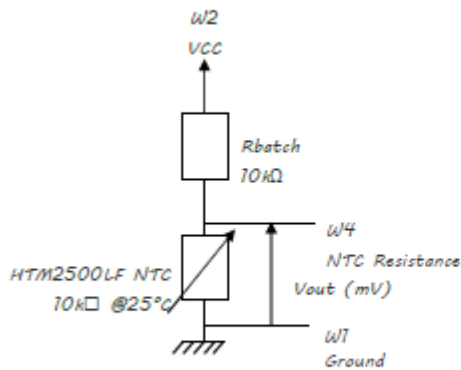|	
R	NTC resistance in Ω at temperature T in K
T	Temperature in K
a	Constant value (a = 8.54942E-04)
b	Constant value (b = 2.57305E-04)
c	Constant value (c = 1.65368E-07)

- **Temperature Interface Circuit**

Concerning the temperature sensor of the HTM2500LF, the following measuring method described below is based on a voltage bridge divider circuit. It uses only one resistor component (Rbatch) at 1% to design HTM2500LF temperature sensor interfacing circuit.
Rbatch is chosen to be equal to NTC @25°C to get: Vout = Vcc/2 @25°C.
The proposal method connects Rbatch to Vcc (5Vdc) and NTC to Ground. It leads to a negative slope characteristic (Pull-Up Configuration).

$$V_{OUT}(mV) = \frac{Vcc(mV) * NTC_{HTM2500LF}(\Omega)}{R_{batch}(\Omega) + NTC_{HTM2500LF}(\Omega)}$$

W2
VCC

Rbatch
10 kΩ

W4
NTC Resistance
Vout (mV)

HTM2500LF NTC
10kΩ @25°C

W1
Ground

Temp (°C)	R (Ω)	Pull-up Configuration Vout (mV)
-40	195652	4757
-30	113347	4595
-20	68237	4361
-10	42506	4048
0	27219	3657
10	17926	3210
20	12081	2736
25	10000	2500
30	8315	2270
40	5834	1842
50	4161	1469
60	3014	1158
70	2228	911
80	1669	715

APPENDIX E: SPECIFICATIONS OF THE DATA LOGGER

Specifications of the data logger used during the experiment are provided in this appendix.

SPECIFICATIONS

USB-6000

8 AI (10 kS/s), 4 DIO USB Multifunction I/O Device

Definitions

Warranted specifications describe the performance of a model under stated operating conditions and are covered by the model warranty.

The following characteristic specifications describe values that are relevant to the use of the model under stated operating conditions but are not covered by the model warranty.

- *Typical* specifications describe the performance met by a majority of models.
- *Nominal* specifications describe an attribute that is based on design, conformance testing, or supplemental testing.

Specifications are *Typical* unless otherwise noted.

Conditions

Specifications are valid at 25 °C unless otherwise noted.

Analog Input

Number of analog inputs	8, single-ended
Input resolution	12 bits
Maximum sample rate (aggregate), system-dependent	10 kS/s
Converter type	Successive approximation
AI FIFO	2,047 samples
Timing resolution	125 ns (8 MHz timebase)
Timing accuracy	100 ppm of actual sample rate
Input range	±10 V
Working voltage	±10 V
Input impedance	>1 MΩ

NATIONAL INSTRUMENTS

Figure 1. USB-6000 Dimensions

If you need to clean the module, wipe it with a dry towel.
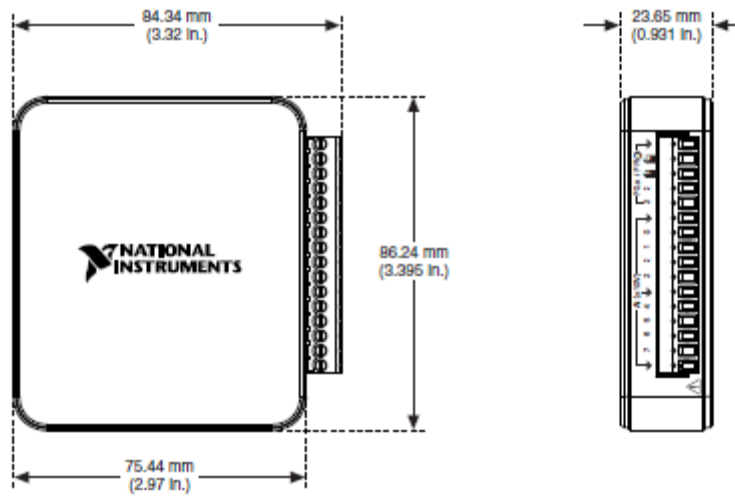
Weight	
Without screw terminal connector plug	73 g (2.58 oz)
With screw terminal connector plug	84 g (3 oz)
USB connector	USB Micro-B receptacle (1)
I/O connector	
Type	16-position screw terminal plug (1)
Screw-terminal wiring	1.31 mm² to 0.08 mm² (16 AWG to 28 AWG)
Torque for screw terminals	0.22 N · m to 0.25 N · m (2.0 lb. · in. to 2.2 lb. · in.)

If you need to clean the module, wipe it with a dry towel.

Safety Voltages

Connect only voltages that are within these limits.

Channel-to-GND	±30 V max, Measurement Category I

Measurement Category I is for measurements performed on circuits not directly connected to the electrical distribution system referred to as MAINS voltage. MAINS is a hazardous live electrical supply system that powers equipment. This category is for measurements of voltages

from specially protected secondary circuits. Such voltage measurements include signal levels, special equipment, limited-energy parts of equipment, circuits powered by regulated low-voltage sources, and electronics

⚠ **Caution** Do not use this module for connection to signals or for measurements within Measurement Categories II, III, or IV

📝 **Note** Measurement Categories CAT I and CAT O (Other) are equivalent. These test and measurement circuits are not intended for direct connection to the MAINS building installations of Measurement Categories CAT II, CAT III, or CAT IV.

Environmental

Temperature (IEC 60068-2-1 and IEC 60068-2-2)

Operating	0 °C to 40 °C
Storage	-40 °C to 85 °C

Humidity (IEC 60068-2-56)

Operating	5% to 90% RH, noncondensing
Storage	5% to 95% RH, noncondensing
Pollution Degree (IEC 60664)	2
Maximum altitude	2,000 m

Indoor use only.

Safety

This product is designed to meet the requirements of the following electrical equipment safety standards for measurement, control, and laboratory use:

- IEC 61010-1, EN 61010-1
- UL 61010-1, CSA C22.2 No. 61010-1

📝 **Note** For UL and other safety certifications, refer to the product label or the *Online Product Certification* section.

Electromagnetic Compatibility

This product meets the requirements of the following EMC standards for electrical equipment for measurement, control, and laboratory use:

- EN 61326-1 (IEC 61326-1): Class A emissions; Basic immunity
- EN 55011 (CISPR 11): Group 1, Class A emissions
- EN 55022 (CISPR 22): Class A emissions
- EN 55024 (CISPR 24): Immunity

APPENDIX F: EDITING CERTIFICATES

Editing certificates for all published articles and the entire dissertation are included in this appendix.

DR RICHARD STEELE
BA, HDE, MTech(Hom)
HOMEOPATH
Registration No. A07309 HM
Practice No. 0807524
Freelance academic editor
Associate member: Professional Editors'
Guild, South Africa

110 Cato Road
Glenwood, Durban 4001
031-201-6508/082-928-6208
Fax 031-201-4989
Postal: P.O. Box 30043, Mayville 4058
Email: rsteele@vodamail.co.za

EDITING CERTIFICATE

Re: **Johannes P. Angula**
Journal article: **REVIEW OF SOLAR GRAIN DRYING**

I confirm that I have edited this article and the references for clarity, language and layout. I returned the document to the author with track changes so correct implementation of the changes and clarifications requested in the text and references is the responsibility of the author. I am a freelance editor specialising in proofreading and editing academic documents. My original tertiary degree which I obtained at the University of Cape Town was a B.A. with English as a major and I went on to complete an H.D.E. (P.G.) Sec. with English as my teaching subject. I obtained a distinction for my M.Tech. dissertation in the Department of Homeopathy at Technikon Natal in 1999 (now the Durban University of Technology). During my 13 years as a part-time lecturer in the Department of Homoeopathy at the Durban University of Technology I supervised numerous Master's degree dissertations.

Dr Richard Steele
29 July 2019
per email

Chapter 2 Editing certificate

EDITING CERTIFICATE

Re: Johannes P. Angula
Journal article: **COMPUTATIONAL FLUID DYNAMICS IN SOLAR DRYING**

I confirm that I have edited this article and the references for clarity, language and layout. I returned the document to the author with track changes so correct implementation of the changes and clarifications requested in the text and references is the responsibility of the author. I am a freelance editor specialising in proofreading and editing academic documents. My original tertiary degree which I obtained at the University of Cape Town was a B.A. with English as a major and I went on to complete an H.D.E. (P.G.) Sec. with English as my teaching subject. I obtained a distinction for my M.Tech. dissertation in the Department of Homeopathy at Technikon Natal in 1999 (now the Durban University of Technology). During my 13 years as a part-time lecturer in the Department of Homoeopathy at the Durban University of Technology I supervised numerous Master's degree dissertations.

Dr Richard Steele
01 September 2019
per email

Chapter 3 Editing certificate

EDITING CERTIFICATE

Re: Johannes P. Angula
Journal article: **Modelling and CFD Simulation of Temperature and Airflow distribution inside a Forced convection Mixed-mode Solar Grain Dryer with a Preheater**

I confirm that I have edited this article and the references for clarity, language and layout. I returned the document to the author with track changes so correct implementation of the changes and clarifications requested in the text and references is the responsibility of the author. I am a freelance editor specialising in proofreading and editing academic documents. My original tertiary degree which I obtained at the University of Cape Town was a B.A. with English as a major and I went on to complete an H.D.E. (P.G.) Sec. with English as my teaching subject. I obtained a distinction for my M.Tech. dissertation in the Department of Homoeopathy at Technikon Natal in 1999 (now the Durban University of Technology). I was a part-time lecturer in the Department of Homoeopathy at the Durban University of Technology for 13 years and supervised many Masters degree dissertations during that period.

Dr Richard Steele
12 November 2020
per email

Chapter 5 Editing certificate

EDITING CERTIFICATE

Re: **Johannes P. Angula**
Journal article: **Performance Evaluation of a Forced Convection Mixed-Mode Solar Grain Dryer with a Preheater**

I confirm that I have edited this article and the references for clarity, language and layout. I returned the document to the author with track changes so correct implementation of the changes and clarifications requested in the text and references is the responsibility of the author. I am a freelance editor specialising in proofreading and editing academic documents. My original tertiary degree which I obtained at the University of Cape Town was a B.A. with English as a major and I went on to complete an H.D.E. (P.G.) Sec. with English as my teaching subject. I obtained a distinction for my M.Tech. dissertation in the Department of Homoeopathy at Technikon Natal in 1999 (now the Durban University of Technology). I was a part-time lecturer in the Department of Homoeopathy at the Durban University of Technology for 13 years and supervised many Masters degree dissertations during that period.

Dr Richard Steele
16 November 2020
per email

Chapter 6 Editing certificate

EDITING CERTIFICATE

Re: **Johannes. P Angula**
For editing journal article: **Optimization of Solar Dryers through Thermal Energy Storage: Two Concepts**

I confirm that I have edited this article and the references for clarity, language and layout. I returned the document to the author with track changes so correct implementation of the changes and clarifications requested in the text and references is the responsibility of the author. I am a freelance editor specialising in proofreading and editing academic documents. My original tertiary degree which I obtained at the University of Cape Town was a B.A. with English as a major and I went on to complete an H.D.E. (P.G.) Sec. with English as my teaching subject. I obtained a distinction for my M.Tech. dissertation in the Department of Homeopathy at Technikon Natal in 1999 (now the Durban University of Technology). I was a part-time lecturer in the Department of Homoeopathy at the Durban University of Technology for 13 years.

Dr Richard Steele
07 March 2020
per email

Chapter 7 Editing certificate

EDITING CERTIFICATE

Re: Johannes Penda Angula
Master's dissertation: **CFD MODELING, PERFORMANCE EVALUATION, AND OPTIMIZATION OF A FORCED CONVECTION MIXED-MODE SOLAR GRAIN DRYER WITH A PREHEATER**

I confirm that I have edited Chapter 1, Chapter 4, and Chapter 8 of this dissertation and the references for clarity, language and layout. I returned the document to the author with track changes so correct implementation of the changes and clarifications requested in the text and references is the responsibility of the author. I am a freelance editor specialising in proofreading and editing academic documents. My original tertiary degree which I obtained at the University of Cape Town was a B.A. with English as a major and I went on to complete an H.D.E. (P.G.) Sec. with English as my teaching subject. I obtained a distinction for my M.Tech. dissertation in the Department of Homoeopathy at Technikon Natal in 1999 (now the Durban University of Technology). I was a part-time lecturer in the Department of Homoeopathy at the Durban University of Technology for 13 years.

Dr Richard Steele
07 February 2021
per email

Thesis editing certificate

APPENDIX G: JOURNAL PUBLISHING CERTIFICATES AND ACCEPTANCE LETTERS

Some of the journal's acceptance letter and publishing certificates for the published article are included in this appendix.

IAEME Publication

www.iaeme.com
editor@iaeme.com
iaemedu@gmail.com

(Publishers of High Quality Peer Reviewed Refereed Scientific, Engineering & Technology, Medicine and Management International Journals)

INTERNATIONAL JOURNAL OF MECHANICAL ENGINEERING & TECHNOLOGY (IJMET)

www.iaeme.com/ijmet/index.asp

Paper ID: IJMET_10_11_024

Date: 06-December-2019

Certificate of Publication

This is to certify that the research paper entitled "REVIEW OF SOLAR GRAIN DRYING" authored by "Johannes P. Angula and Freddie Inambao" had been reviewed by the Editorial Board and published in "International Journal of Mechanical Engineering & Technology (IJMET), Volume 10, Issue 11, November 2019, pp. 275-296; ISSN Print: 0976-6340 and ISSN Online: 0976-6359; Journal Impact Factor (2019): 10.6879 Calculated by GISI (www.jifactor.com)".

Chief Editor

Plot: 03, Flat- S 1, Poomalai Santosh Pearls Apartment, Plot No. 10, Vaiko Salai 6th Street, Jai Shankar Nagar, Palavakkam, Chennai - 600 041, Tamilnadu, India.
E-mail: editor@iaeme.com

Certificate of Publication

This is to certify that the research paper entitled "COMPUTATIONAL FLUID DYNAMICS IN SOLAR DRYING" authored by "Johannes P. Angula and Freddie Inambao" had been reviewed by the Editorial Board and published in "International Journal of Mechanical Engineering & Technology (IJMET), Volume 10, Issue 11, November 2019, pp. 259-274; ISSN Print: 0976-6340 and ISSN Online: 0976-6359; Journal Impact Factor (2019): 10.6879 Calculated by GISI (www.jifactor.com)".

Chief Editor

Chapter 3 Certificate of Publication

Acceptance Letter

Lattice Science
Bibliographic Database

Dear Author(s): Johannes P. Angula, Freddie Inambao

Paper ID:	B82821210220
Paper Title	Modelling and CFD Simulation of Temperature and Airflow Distribution Inside a Forced Convection Mixed-mode Solar Grain Dryer with a Preheater

This is to enlighten you that above manuscript appraised by the proficient and it is accepted by the Board of Referees (BoR) of 'Blue Eyes Intelligence Engineering and Sciences Publication (BEIESP)' for publication in the 'International Journal of Innovative Technology and Exploring Engineering' that will publish at **Volume-10 Issue-2, December 2020** in Regular Issue on **10 December 2020**. It will be available live at https://www.ijitee.org/download/volume-10-issue-2/

It is advised you to provide us **following supporting documents in a single email** before 03 December 2020 at submit2@ijitee.org

1. **Final Paper | Ms Word doc. | docx. file**

    camera ready paper should be prepared as per journal template which is available at http://www.ijitee.org/download/

2. **Copyright Transfer Form | Submit Online only | do not send it through email**

    https://www.blueeyesintelligence.org/copyright/

3. **Proof of Registration | Scanned | Online Received Email**

    please visit in this URL. All details available at https://www.blueeyesintelligence.org/registration/

INFORMATION FOR AUTHOR(S)- Please read very carefully.

1. Each author (s) profile of minimum of 100 words along with a photo should be available in the final paper. The final paper should be prepared as per the journal template. The Paper should have a minimum of 03 pages and a maximum of 10 pages. Maximum 05 authors can be seated in a paper. In the case of more than 05 authors, the paper (s) to be rejected. Final paper should not have more than 30% plagiarism including reference section.

2. If the above three supporting documents (Final Paper, Copyright and Registration) does not submit to the journal by the author in the given date (s), then paper will automatically suspend from publication for particular volume/issue. During the final email, you have to attach Final Paper, Copyright and Proof of Registration in a single email. Final paper should be result oriented and should be prepared as per the reviewer (s) comment (s). In the case of failure, it to be suspended for correction. Please read review report carefully. It is compulsory to write the Paper ID of the paper in place of Subject Area in the email during the final paper submission. Header and footer of the paper template will be edited by journal staff only.

3. Author (s) can make rectification/updation in the final paper but after the signing the copyright and final paper submission to the journal, any rectification/updation is not possible. Published paper to be available online from 10 December to 15 December 2020. Paper can not withdraw after submitting the copyright to the journal. Author(s) will receive publication certificate within 01 to 02 weeks after the date of publication of respective volume/issue.

4. The DOI can be checked and verified within 02 to 04 weeks after the date of publication of volume/issue. https://www.doi.org/

5. The published article (s) to be enlisted in the Lattice Science Database within 06 to 08 weeks. https://www.latticescience.com/bibliographic-search/

6. The whole process for including any article (s) in the indexing database/ bibliographic database (for example Lattice Science, crossref, kudos, wos, mendeley, etc) is done by their internal team only. Neither Journal nor 'Blue Eyes Intelligence Engineering and Sciences Publication' does not have any involvement in the decision whether to accept or reject a paper either from any database or enlisting database (for example crossref, kudos, wos, mendeley, etc) and can not influence the processing time of paper.

Jitendra Kumar Sen
(Manager)

BHOPAL

Dr. Shiv Kumar
(Editor-In-Chief)

Chapter 5 Acceptance letter

Acceptance Letter

Lattice Science
Bibliographic Database

Dear Author(s): Johannes P. Angula, Freddie Inambao

Paper ID:	B82831210220
Paper Title	Performance Evaluation of a Forced Convection Mixed-Mode Solar Grain Dryer with a Preheater

This is to enlighten you that above manuscript appraised by the proficient and it is accepted by the Board of Referees (BoR) of 'Blue Eyes Intelligence Engineering and Sciences Publication (BEIESP)' for publication in the 'International Journal of Innovative Technology and Exploring Engineering' that will publish at Volume-10 Issue-2, December 2020 in Regular Issue on 10 December 2020. It will be available live at https://www.ijitee.org/download/volume-10-issue-2/

It is advised you to provide us following supporting documents in a single email before 03 December 2020 at submit2@ijitee.org

1. **Final Paper | Ms Word doc. | docx. file**

   camera ready paper should be prepared as per journal template which is available at http://www.ijitee.org/download/

2. **Copyright Transfer Form | Submit Online only | do not send it through email**

   https://www.blueeyesintelligence.org/copyright/

3. **Proof of Registration | Scanned | Online Received Email**

   please visit in this URL. All details available at https://www.blueeyesintelligence.org/registration/

INFORMATION FOR AUTHOR(S)- Please read very carefully.

1. Each author (s) profile of minimum of 100 words along with a photo should be available in the final paper. The final paper should be prepared as per the journal template. The Paper should have a minimum of 03 pages and a maximum of 10 pages. Maximum 05 authors can be seated in a paper. In the case of more than 05 authors, the paper (s) to be rejected. Final paper should not have more than 30% plagiarism including reference section.

2. If the above three supporting documents (Final Paper, Copyright and Registration) does not submit to the journal by the author in the given date (s), then paper will automatically suspend from publication for particular volume/issue. During the final email, you have to attach Final Paper, Copyright and Proof of Registration in a single email. Final paper should be result oriented and should be prepared as per the reviewer (s) comment (s). In the case of failure, it to be suspended for correction. Please read review report carefully. It is compulsory to write the Paper ID of the paper in place of Subject Area in the email during the final paper submission. Header and footer of the paper template will be edited by journal staff only.

3. Author (s) can make rectification/updation in the final paper but after the signing the copyright and final paper submission to the journal, any rectification/updation is not possible. Published paper to be available online from 10 December to 15 December 2020. Paper can not withdraw after submitting the copyright to the journal. Author(s) will receive publication certificate within 01 to 02 weeks after the date of publication of respective volume/issue.

4. The DOI can be checked and verified within 02 to 04 weeks after the date of publication of volume/issue: https://www.doi.org/

5. The published article (s) to be enlisted in the Lattice Science Database within 06 to 08 weeks: https://www.latticescience.com/bibliographic-search/

6. The whole process for including any article (s) in the indexing database/ bibliographic database (for example Lattice Science, crossref, kudos, wos, mendeley, etc) is done by their internal team only. Neither Journal nor 'Blue Eyes Intelligence Engineering and Sciences Publication' does not have any involvement in the decision whether to accept or reject a paper either from any database or enlisting database (for example crossref, kudos, wos, mendeley, etc) and can not influence the processing time of paper.

Jitendra Kumar Sen
(Manager)

BHOPAL

Dr. Shiv Kumar
(Editor-In-Chief)

Chapter 8 Acceptance letter